SOME PRE-BREAKDOWN STUDIES IN NITROGEN AND AIR

Thesis presented for the degree of

Doctor of Philosophy in Engineering

of the University of Glasgow

September, 1962

D.T.A. Blair, B.Sc.,A.R.C.S.T.,Graduate I.E.E.

ProQuest LLC.
789 East Eisenhower Parkway
P.O. Box 1346
Ann Arbor, MI 48106 – 1346

CONTENTS

INDEX

GENERAL INTRODUCTION

The work reported in this thesis was carried out in the Electrical Engineering Department of the Royal College of Science and Technology, Glasgow, and developed out of an investigation carried out in that department into pre-breakdown phenomena in room air, using uniform-field electrodes at spacings of the order of 1 cm., with static voltage applied.

In the course of static voltage breakdown studies in room air[1], it had been noted that, in radium-irradiated gaps, when the voltage was within a few per cent of the breakdown value, a faint glow, observable in a darkened room, appeared in the region of the anode, and that a hissing sound was produced at the same time. Both effects became more pronounced as the breakdown voltage was approached, or the radium quantity increased. It was concluded that a considerable pre-breakdown discharge must occur under these conditions.

By connecting a galvanometer in series with such gaps, Tedford[1] measured currents of the order of 10^{-6}A. when the applied voltage approached breakdown value in the case of radium-irradiated gaps, but no detectable current for non-irradiated gaps. When an oscillographic technique was used to measure the variation of pre-breakdown current with gap voltage as the latter increased from 98% to 100% of breakdown value, discrete pulses

of current were observed, and pulses of light were also detected by a photomultiplier under these conditions. Irradiation of the gap resulted in a marked increase in the frequency of occurrence of the pulses.

In a continuation of this work, Kapoor[2] used a recording circuit of lower time-constant in order to resolve the shapes of individual current pulses in irradiated gaps, and at the same time a photomultiplier was used to detect the light emission accompanying the pre-breakdown discharge. Using a double-beam oscillograph to record current and light simultaneously, it was found that rapid increases in current were accompanied by light pulses of short duration (of the order of 10^{-6} sec.). This occurred at the start of each current pulse, and sometimes once or twice within its duration. The mean length of the current pulses (of the order of 10^{-5} sec.) increased as the gap length was increased from 0.5 to 2.0 cm.

The present author repeated[3] some of Kapoor's experiments. It was possible to define a "fundamental" current pulse shape, of constant duration for each gap length, such that current pulses of other shapes were made up of two or more fundamental pulses overlapping on the time scale: each fundamental current pulse was associated with one light pulse. The fundamental current pulse, with its attendant light pulse, could

be interpreted as the result of an individual electron avalanche[3],[4].

All of the above experiments were carried out in room air.

It was against this background that the author began the investigation reported in Part I of the present thesis, with the object of obtaining from the recorded pulses quantitative data on the physical processes involved in the pre-breakdown discharge.

Shortly after this investigation was begun, it was realized that somewhat similar research on individual electron avalanches was being carried out by Raether's group at Hamburg[5]. The relevant parts of this German work are discussed in relation to other investigations of the pre-breakdown discharge, in Section 1 of Part I of the present thesis.

One important part of this German work is Schmidt's theory of the current pulse shape[6]. In Section 2 of Part I, below, this theory is discussed in detail, and has been extended to cover the case of avalanches starting part-way across the gap, as may occur with radium irradiation, and to take account of circuit inductance, which may become significant in the systems of large physical size which will be required for experiments using higher voltages.

Section 3 of Part I describes the author's experiments in room air, which are a direct development from previous work in the department where the investigation was carried out. As this work progressed, the limitations imposed by the use of room air as the experimental gas became increasingly evident. Also during this time, a number of German papers were translated, and these indicated that a significant amount of work had already been carried out in the avalanche field, including investigations in nitrogen, oxygen, and dry air using a 2 cm gap at pressures of up to 500 mm Hg[7][8]. It was decided to extend the present investigation using an enclosed system, to cover the cases of nitrogen, dry air, and humid air with gaps of 1, 2 and 3 cm, and gas pressures up to nearly atmospheric; this part of the work is reported in Section 4 of Part I.

Part II of the present thesis reports an investigation of the factors affecting the intensity of ionization produced in a uniform-field discharge gap by a capsule of radium bromide enclosed in the anode. This method of irradiation has been used in some of the experiments described in Part I, and in much of the other work of the department in which these experiments were carried out.

PART I

OBSERVATION OF INDIVIDUAL ELECTRON AVALANCHES

1. INTRODUCTION

This introduction gives an account of experimental and theoretical work relating to the occurrence of electron avalanches in discharge gaps.

Firstly, a brief description is given of the well-known Townsend theory of breakdown, and of the experiments based upon it, involving measurements of the average (d.c.) pre-breakdown current resulting from the formation of electron avalanches. This is followed by a discussion of the experimental methods available for detecting individual electron avalanches, leading naturally to a consideration of the statistical nature of the pre-breakdown processes. Discussion of the streamer mechanism has been deferred until this point, since the most recent investigations of the mechanism developed out of experiments on individual avalanches. A summary is given of those investigations of individual avalanches which have been carried out in nitrogen and air, and a short concluding section briefly describes the present work.

1.1 Townsend Theory

Over a wide range of conditions, the observed growth of current that precedes breakdown of a discharge gap is explained satisfactorily by the well-known theory due to J. S. Townsend, or by a modified form of it. Townsend's work in this field has been reviewed by a number of authors; a recent account is by Llewellyn-Jones[9].

The brief description of Townsend theory that follows deals with those points which have a bearing on the present work. Only the case of a uniform electric field is considered.

1.1.1 Townsend theory in gases which do not form negative ions

According to this theory, electrons released at the cathode of the discharge gap by some external agency (e.g. by ultra-violet radiation causing photoemission), in travelling towards the anode under the action of the applied electric field, ionize the gas in the gap by collision, and in this way produce further free electrons according to the relation

$$d(n_-(x)) = \alpha\, n_-(x)\, dx \qquad . \quad . \quad . \quad (1)$$

Here $n_-(x)$ is the number of electrons at a distance x from the cathode, measured in the direction of the electron motion, and α is the "first Townsend coefficient", whose value depends upon the nature of the gas, the gas pressure, and the electric field strength.

In a uniform electric field, α is independent of x, and integration of (1) gives

$$n_-(x) = n_-(o)\, e^{\alpha x} \qquad . \quad . \quad . \quad (2)$$

If the gap length is d, then, at the anode,

$$n_-(d) = n_-(o)\, e^{\alpha d} \qquad . \quad . \quad . \quad (3)$$

Thus the number of electrons leaving the cathode is multiplied by $e^{\alpha d}$ in crossing the gap. This factor is called the "multiplication" or "gas amplification" of the process. Each individual electron leaving the cathode is said to produce an "avalanche" of $e^{\alpha d}$ electrons (as well as $(e^{\alpha d} - 1)$ positive ions); in considering such individual events, the quantity $e^{\alpha d}$ is called, particularly in the German literature, the "carrier-number" (die Trägerzahl) of the avalanche.

It follows from (3) that the current i flowing in the gap is

$$i = i_o e^{\alpha d} \quad . \quad . \quad . \quad (4)$$

where i_o is the current that would flow if the electrons released at the cathode were to cross the gap without ionizing.

If the gap length d is increased and α is kept constant, it is found that, with sufficiently large values of d, the current i increases more rapidly than is indicated by (4); this is ascribed to the production of "secondary" electrons, and, consequently, secondary avalanches. The distinguishing feature of a secondary avalanche is that its initiating electron is released as the result of a preceding avalanche. By way of distinction, initiating electrons released by an external agency are called "primary" electrons, and these give rise to "primary" avalanches.

Two mechanisms of secondary electron production which are usually considered to be active in the range of conditions covered by the present work, are (a) the production of photo-electrons at the cathode by radiation from molecules excited by electron collision, and (b) the release of electrons at the cathode by positive ion bombardment.

All of the known mechanisms of secondary electron production, acting either separately or together, lead to practically the same form of expression for gap current, so that the secondary effects may all be represented by a single coefficient γ, defined as the number of secondary electrons produced per ionizing collision in the gap; this leads to

$$i = i_o \frac{e^{\alpha d}}{1 - \gamma(e^{\alpha d} - 1)} \quad . \quad . \quad . \quad (5)$$

and i becomes infinite when

$$\gamma(e^{\alpha d} - 1) = 1 \quad . \quad . \quad . \quad (6)$$

This is often written in the approximate form

$$\gamma\, e^{\alpha d} = 1 \quad . \quad . \quad . \quad (7)$$

and is interpreted as a breakdown criterion.

1.1.2 Townsend theory in electronegative gases

A process that is possible in electronegative gases is the formation of negative ions by the attachment of electrons to neutral molecules. Such a process will tend to suppress avalanche formation, since the negative ions are not capable of being accelerated by the applied electric field between collisions to such an extent that they can ionize further molecules.

The effect of negative ion formation is allowed for in the theory by an "attachment coefficient" η defined by

$$d(n_n(x)) = \eta\, n_-(x)\, dx \qquad . \quad . \quad . \quad (8)$$

where $n_n(x)$ is the number of negative ions formed when an avalanche travels a distance x from the cathode.

The rate of positive ion formation is now taken to be governed by

$$d(n_+(x)) = \alpha\, n_-(x)\, dx \qquad . \quad . \quad . \quad (9)$$

where $n_+(x)$ is the number of positive ions formed when the avalanche travels a distance x from the cathode.

The equation for the rate of production of free electrons therefore becomes

$$d(n_-(x)) = (\alpha - \eta)\, n_-(x)\, dx \quad . \quad . \quad . \quad (10)$$

In the case of a uniform electric field, the gas-amplified pre-breakdown current in the absence of secondary processes is

$$i = \frac{i_o}{\alpha - \eta} \left[\alpha \, e^{(\alpha - \eta)d} - \eta \right] \quad . \quad . \quad (11)$$

Allowing for secondary processes, represented by the coefficient γ, leads to

$$i = i_o \frac{\frac{\alpha}{\alpha - \eta} e^{(\alpha - \eta)d} - \frac{\eta}{\alpha - \eta}}{1 - \frac{\gamma\alpha}{\alpha - \eta}\left[e^{(\alpha - \eta)d} - 1 \right]} \quad . \quad (12)$$

and the corresponding breakdown criterion is

$$\frac{\gamma\alpha}{\alpha - \eta} \left[e^{(\alpha - \eta)d} - 1 \right] = 1 \quad . \quad . \quad (13)$$

The derivation of equation (11) is detailed by Loeb[10]. Equations (12) and (13) are derived in a similar manner to that used[9] for equations (5) and (6).

Schlumbohm[11] has considered the case where detachment of electrons from negative ions occurs, and introduces a quantity ζ, defined as the probability that a negative ion will lose its attached electron in travelling unit distance towards the anode.

(8) and (10) then become, respectively,

$$d(n_n(x)) = \left[\eta n_-(x) - \zeta n_n(x)\right] dx$$

and

$$d(n_-(x)) = \left[(\alpha - \eta)\, n_-(x) + \zeta n_n(x)\right] dx$$

These lead to an expression for current

$$\left.\begin{aligned} i &= \frac{i_o}{\Theta_+ - \Theta_-}\left[(\Theta_+ + \zeta + \eta)\, e^{\Theta_+ d} - (\Theta_- + \zeta + \eta)\, e^{\Theta_- d}\right] \\ \text{where} \quad \Theta_{\pm} &= \tfrac{1}{2}(\alpha - \eta - \zeta) \pm \tfrac{1}{2}\sqrt{(\alpha - \eta + \zeta)^2 + 4\eta\zeta} \end{aligned}\right\} \quad (14)$$

The effect of secondary processes is not considered for this case.

1.1.3 Experimental work on Townsend theory

Experiments based on the theory outlined above involve measurement of the pre-breakdown current i in a discharge gap with different values of electrode spacing d, at constant field strength and gas pressure. Under these conditions, α, γ, and η (if it exists) are constant.

In the case of a gas which does not form negative ions, it is easily seen from (4) that, in the absence of secondary processes, a plot of $\log_e i$ against d will yield a straight line of slope α, which can thus be measured. If the spacing d is increased until secondary processes become significant, the $\log_e i$,d plot will curve upwards, according to (5); measurements on this part of the curve yield the value of γ. The values of α and γ thus found can then be used in (6) to determine the value of d at which the gap would be expected to break down under the given conditions of field strength and gas pressure - agreement with the measured value substantiates the validity of the theory.

Numerous experiments of this kind have verified the theory in many different gases. Of particular interest in the present context are the results of Dutton et al[12] in nitrogen, which indicate that breakdown in that gas takes place by the Townsend

mechanism in the range $41 \leqslant \frac{E}{p} \leqslant 45$ V cm^{-1} (mm Hg)$^{-1}$ for values of pd up to 810 mm Hg cm and breakdown voltages up to 38 kV. (E = electric field strength, p = gas pressure, d = gap length).

The case of electron-attaching gases is less simple: it is again usual to plot $\log_e i$ against d, the values of α and η being found by a process of curve-fitting, using equation (11). In this way, Prasad and Craggs[13] have measured η and α in dry air over the range $25 \leqslant \frac{E}{p} \leqslant 45$ V cm^{-1} (mm Hg)$^{-1}$ with pd-values up to ~1200 mm Hg cm. Dutton et al[14] report similar measurements, extending the range to cover the case of breakdown at pd values of up to 2020 mm Hg cm (and sparking potentials of up to 71 kV); in these latter measurements, the occurrence of a secondary mechanism was apparent (equation (12)).

Prasad and Craggs have carried out measurements of this kind in humid air[15] in the range $30 \leqslant \frac{E}{p} \leqslant 40$ V cm^{-1} (mm Hg)$^{-1}$ with water vapour partial pressures of 2.5 to 15 mm Hg and total pressures of 150 to 300 mm Hg. α and η were measured from $\log_e i$, d plots and values of γ were estimated by measuring sparking potentials and applying the breakdown criterion, equation (13). The attachment coefficient η showed a marked increase over the values obtained in dry air, while γ was much smaller. Meek suggests[16] that the latter effect may be due to the absorption of photons by the water vapour.

Schlumbohm[11] has calculated $\log_e i$, d curves on the basis of equation (14) and finds that these bear a strong resemblence to curves calculated from equation (11). He concludes that experiments of the kind just described fail to indicate whether or not electron detachment occurs, and that the application of equation (11) in the curve-fitting is justified only if other experiments show conclusively that detachment does not occur. Some experimental results obtained in air[17][18] (see below, Section 1.4) have been interpreted as indicating that detachment does in fact take place in that gas.

1.2 Experimental Observation of Individual Avalanches

While a great deal has been learned from experiments of the kind described in the preceding section, involving measurement of the average currents resulting from the occurrence of large numbers of avalanches, it is clearly desirable to carry out experimental studies of individual avalanches, where possible. Such experiments can yield quantitative data, as well as demonstrating graphically the soundness of the ideas on which the Townsend theory is based.

1.2.1 The cloud-chamber method

A cloud-chamber may be used to observe the ion clouds formed in individual avalanches. The method was first used by Raether; a useful critical survey of the early work is given by Loeb[19]. More recently, experiments of a similar nature have been carried out by Allen and Philips[20].

The technique involves the addition of condensable vapours (water and alcohol) to the experimental gas, and so precludes the use of pure gases.

1.2.2 The electrical method

This method consists in detecting the current pulse produced in the external circuit by the passage of an avalanche across the discharge gap. In a gas which does not form negative ions, the current pulse has two components: an electron component, being a rising current of perhaps 10^{-7} sec. duration, due to the electrons crossing the gap to form the avalanche, and a positive ion component of perhaps 10^{-5} sec. duration, due to the positive ions drifting towards the cathode, where they are neutralized. (The figures given here are of the order of magnitude to be expected in a 1 cm gap in most gases). In electronegative gases, a negative ion component may also be detected.

Pulses of this nature, occurring in the radial electric field between two coaxial conductors, form the basis of proportional counter action[21], but the interpretation of current pulse shape is greatly simplified by the use of uniform electric fields. Schmidt[6] has calculated theoretical current pulse shapes for the latter case, and gives experimental results in support of these calculations. The theory of current pulse shape for uniform electric fields is discussed in Section 2, below.

Working on parallel-plate counters, Pidd and Madansky[22] observed pulses with amplitudes of the order of millivolts which were

presumably the result of uniform-field avalanche current pulses; in those experiments, however, they were spurious pulses, and were not studied in detail. Later, Schmidt used a parallel-plate counter to study these pulses in organic vapours[6] and in vapour-gas mixtures[23]. The reason for the use of organic vapours is that they give a low value of secondary coefficient γ as a result of their capacity for pre-dissociation[24] - too high a value of γ causes the gap to break down before the avalanche carrier-number has become sufficiently large for the current pulses of individual avalanches to be detectable.

An important feature of this kind of experiment is that secondary effects can be distinguished: a secondary avalanche brought about by positive ion bombardment of the cathode gives rise to a current pulse whose front occurs near the end of the preceding pulse, since the rate at which positive ions fall on the cathode is greatest at the end of the positive ion transit-time; a secondary avalanche due to a photo-electric process, on the other hand, starts before the positive ions of the preceding avalanche have moved appreciably from their position of formation, and this secondary process is revealed as a "step" on the pulse front.

1.2.3 The optical method

During the occurrence of an electron avalanche, a number of the gas molecules will be raised to an excited state by electron collision, and will radiate their excess energy after a very short time (~0.01 μsec) - this radiation has already been mentioned as a source of secondary electrons. Detection of such radiation by means of a photomultiplier provides a third method of investigating individual avalanches.

Irradiation of the discharge gap with ultra-violet light is impracticable in such experiments, due to the large amount of light reflected from the cathode surface, and other surfaces, on to the photomultiplier; a radioactive agent provides a useful source of primary electrons in this case.

Legler[25] has investigated the radiation from avalanches, using air as the experimental gas, and Dibbern[26] has applied this method in experiments in methane and nitrogen, as well as a nitrogen/carbon dioxide mixture. Their results are discussed further, below.

1.3 Statistical Effects and the Streamer Theory

When pre-breakdown processes are to be viewed in terms of individual avalanches, it becomes useful to regard the coefficients (α, γ, η, ζ) introduced in Section 1.1 as probability values.

Consider first the secondary coefficient γ, defined above as the number of secondary electrons released per ionizing collision in the gap; it is less than unity, and must be an average value taken over a large number of collisions (and, of course, over an integral number of secondary electrons) - in terms of individual events, γ is to be interpreted as the probability that a secondary electron will be produced as the result of an ionizing collision. It is useful to define a quantity $\Gamma = \gamma e^{\alpha d}$, which is the probability that a secondary electron will be produced as the result of an avalanche of $e^{\alpha d}$ electrons. (A similar argument applies in the case of electronegative gases). When Γ is unity, the discharge is self-sustaining, and the breakdown criterion (equation (7)) is satisfied. Thus, in the pre-breakdown region, Γ must be fractional, while the number of secondary electrons resulting from an individual primary avalanche may have any of the values 0, 1, 2, 3..... Since a secondary avalanche has itself a finite probability of producing a further avalanche, "chains" of avalanches may be formed,

the chain breaking off whenever one of its component avalanches chances to produce no secondary electron. These chains have been observed experimentally - for example, in the work of Schmidt[23] and Legler[25], already mentioned - at voltages below the breakdown value.

Regarding the process of avalanche formation in terms of individual collisions, one may define α (see equation (1)) as the probability that an electron will suffer an ionizing collision in travelling unit distance towards the anode; it follows[27] from this definition that the avalanche carrier-number is not constant under fixed conditions, but varies statistically from one avalanche to another. Since the amplitude of the current pulse of an avalanche is proportional to its carrier-number, it is possible to investigate this statistical effect, such experiments having been carried out in a proportional counter by Curran, Cockroft and Angus[28]. In the case of a uniform electric field, for gases in which negative ions are not formed, Wijsman[27] has calculated the probability $p(n,d)$ that a single electron starting at the cathode will produce an avalanche of n electrons in travelling a distance d to the anode. The result is

$$p(n,d) = \frac{1}{\bar{n}} e^{-n/\bar{n}} \quad . \quad . \quad . \quad (15)$$

for $\bar{n} \gg 1$

and $\frac{E}{\alpha} \gg V_i$

Here $\bar{n}$ is the average carrier-number $e^{\alpha d}$, as calculated from α measured according to Section 1.1.3, above. E is again the electric field strength, and V_i the minimum ionization potential of the gas; the latter inequality results from the condition that an electron's probability of ionizing must be independent of the distance travelled since its last ionizing collision, in order for the theory to be valid[29]. If a large number of avalanches are measured, equation (15) expresses the theoretical frequency distribution of carrier-numbers.

This distribution has been verified by Frommhold, in experiments in ethyl alcohol[30] and methane[31] over the range $\frac{\bar{n}}{10} \leq n \leq 10\bar{n}$, with $\bar{n}$ of the order of 10^5. Frommhold also found[31] that the same distribution applies in the electronegative gases oxygen and dry air with

$$\bar{n} = \left(\frac{\alpha}{\alpha - \eta}\right)^2 e^{(\alpha-\eta)d}$$

A theoretical derivation of this relation has since been given by Legler[32]. In Frommhold's experiments in dry air, the distribution was modified, for $n \gtrsim 8 \times 10^4$, by the occurrence of a secondary process ($\gamma e^{(\alpha-\eta)d} \gtrsim 0.2$).

Experiments of a similar nature have been carried out in methylal by Schlumbohm[33], with a view to investigating avalanches

of large carrier-number. It was found that the above distribution, equation (15), obtained for values of n up to about 5×10^6 - for larger values of n, a greater number of small pulses occurred at the expense of the larger pulses, up to the maximum value of n, which was about 1.2×10^8. This tendency towards smaller pulses was attributed to distortion of the electric field by the space-charge of the avalanche, leading to a smaller effective value of α.

In experiments in methane, Frommhold[34] found a significant increase in the time-constant of growth of the electron component of the current pulses for $n \gtrsim 10^6$, indicating a reduction in the effective value of α; this was again attributed to space-charge distortion of the electric field.

A similar increase in electron component time-constant, for $n \gtrsim 10^6$, was recorded by Dibbern, using an optical method, with methane as the experimental gas[26].

Deviations from the normal for avalanches of more than 10^6 electrons have been found also by Richter[35] in experiments in ether, where the effects were detected as changes in the shape (effective value of ψ; see Section 2.1.1.3) of the observed current pulses. A reduction in the effective value of α was indicated for $10^6 \leq n \leq 10^8$, in accord with the other results mentioned above, while for $n > 10^8$, α effectively increased, and

the distribution of carrier-numbers showed a preponderance of avalanches with large carrier-number. This tendency for large avalanches to grow more rapidly than smaller ones may again be due to space-charge distortion, as Raether points out[36], although Richter originally suggested that it might result from the production of free electrons by photoionization of the gas, with the consequent formation of additional (small) avalanches as the photoelectrons travelled towards the head of the main avalanche, under the influence of the space-charge-distorted electric field.

The latter mechanism is that of the "streamer" or "kanal" theory[37], which was originally put forward before any uniform-field current pulse experiments had been reported, in an attempt to explain breakdown where no secondary coefficient had been detected in experiments of the kind indicated in Section 1.1.3, above. In this latter case, it was assumed that the process resulted in the rapid formation of a conducting channel across the gap, along which large currents could pass, i.e. along which the spark occurred.

In observations of the current pulses of avalanches with $n > 10^8$, in ether and in methylal, Pfaue and Raether[38] found that the electron component was sometimes followed by a rapid rise of current, and breakdown. This rising current did not show

the "steps" characteristic of a series of avalanches produced by a photoelectric secondary process, and its time-constant of increase was different from that of the electron components; it was interpreted as a streamer breakdown.

Richter[39] has carried out an experimental investigation of the probability of this so-called streamer formation in ether: the probability is zero for avalanches of carrier-number less than a critical value, and increases with carrier-number for values above the critical; this critical value is decreased by increasing the applied electric field. These results are in qualitative agreement with the original streamer theory.

1.4 Pulse Experiments in Nitrogen and Air

As previously mentioned, Legler has applied the optical method to dry air[25]. A 2 cm gap was used, over the pressure range 10 to 60 mm Hg: the apparatus was not sufficiently sensitive to detect individual avalanches without the intervention of a secondary process, but "chains" of avalanches, produced by a photoelectric secondary mechanism, were recorded when the gap voltage was close to breakdown value.

Observations of avalanche current pulses in nitrogen and dry air, as well as oxygen, have been reported by Vogel and Raether[7] and by Vogel[8]. Carrier-numbers were of the order of 10^6, with gas pressures of 100 to 500 mm Hg. Two of their results will be noted here: firstly, that the production of secondary electrons in nitrogen was due mainly to a photoelectric effect, some positive ion effect also being observed, while in air only the photoelectric effect was observed; secondly, that the rise-time of the current pulses in both nitrogen and dry air was anomalously great, although consistent from one pulse to the next ($\pm 5\%$), and was reduced to the expected order of magnitude by the addition of a small quantity of methane to the experimental gas.

Frommhold has carried out somewhat similar experiments[40] with avalanches of carrier-numbers of the order of 10^2, using the radiation from a spark in an auxiliary gap to release about 10^4

electrons practically simultaneously at the cathode of the main gap. (The method is therefore similar to that used by Hornbeck at low pressures[41]). The rise-time of the current pulses in nitrogen, in the pressure range 10 to 500 mm Hg, was in agreement with the value indicated by theory, while the extended rise-time was again found in dry air, over the pressure range 10 to 200 mm Hg. Frommhold suggests that Vogel's pulses in nitrogen were not the results of individual avalanches, but of chains of avalanches produced by a photo-electric secondary mechanism; this suggestion is supported by the fact that, in nitrogen, Frommhold found a mean gas amplification of only 10^3 at breakdown, under the same conditions as obtained in Vogel's experiments, and indeed in the same apparatus.

Dibbern[26], using the optical method to measure the rate of avalanche growth in nitrogen, with carrier-numbers of the order of 10^3, also found the "normal" growth in that gas.

Schröder[17] has applied the optical method to the case of room air, using gaps of 2.5 to 9 cm. He found that the rate of avalanche growth was not anomalously low, as in the case of dry air, and that an avalanche was sometimes followed by one or more photo-electric secondaries at regular intervals of the order of 10^{-7} sec. In addition, he found that, after the occurrence of a sufficiently large avalanche, an "after-current" was detected by the photo-

multiplier: it could not be due simply to ion motion, as this is not detected by the optical method, and Schröder suggests that it was brought about by the occurrence of further avalanches initiated by electrons detached from unstable negative ions; the form of the after-current was clearly distinguishable from that of the current produced by a secondary process. In some cases, the after-current fell to zero after a number of microseconds, while in others it rose to a high value, and breakdown ensued. The latter phenomenon was interpreted as a modified streamer breakdown, in which the high space-charge concentration required for this mechanism was not provided by the primary avalanche itself, but by the avalanches constituting the after-current. This was found to be the normal breakdown mechanism in non-irradiated gaps longer than 5 cm, while a Townsend mechanism, involving a photo-electric secondary process, was operative in shorter gaps.

In experiments carried out by Schlumbohm[18], a small central portion of the anode was insulated from the remainder. (Diameter of inner portion 0.64 cm, maximum diameter of anode 12 cm, electrode spacing 2 cm). α-particles from a polonium source entered the discharge gap through a small hole drilled axially in the central portion of the anode, producing a large number of primary electrons along the axis of the gap. The currents

flowing to the two separate parts of the anode were recorded simultaneously on a double-beam oscillograph. In nitrogen, as expected, photo-electric secondary avalanches were recorded, occurring at an interval corresponding with the electron transit time, and the current produced by these secondary avalanches was not confined to the central region of the gap. In dry air, the anomalously long rise-time of the current pulses was again recorded, and it was found that the current flow during this time was confined to the central region of the gap. After-currents were also detected in dry air, similar in nature to those reported by Schröder[17] in room air, and these too flowed entirely within the central region of the gap; this latter result is in accord with the suggestion that the after-current results from the detachment of electrons from negative ions produced in the initial avalanche.

1.5 The Present Work

The experiments reported in the present thesis were carried out during the period 1957-1960. They were therefore preceded by the work of Legler[25], of Vogel and Raether[7], and of Vogel[8], and were approximately simultaneous with Frommhold's[40] experiments, the results of which were published towards the end of 1960. The other experimental work described in Section 1.4 was carried out later than the experiments reported here.

The present experimental work falls into two parts:

(i) Simultaneous application of the electrical and optical methods (Sections 1.2.2 and 1.2.3, above) to observe the current and light pulses produced by electron avalanches in room air, in uniform-field gaps of 1 cm to 4 cm, and (in less detail) under non-uniform field conditions.

(ii) A more detailed study of current pulses only, in nitrogen, dry air, and humid air, at pressures of approximately 100 mm Hg to 700 mm Hg and with gap lengths of 1 cm, 2 cm and 3 cm (uniform field only).

2. THEORY OF CURRENT PULSE SHAPE

This section presents the theory relating the shape of the observed current pulses (see p.18, above) to the avalanche processes, and indicates how measurements from the observed pulses can yield quantitative data on these processes. In Section 2.1, the circuit containing the discharge gap is assumed to have zero inductance, and the theory is developed separately for gases in which negative ions are not formed and for gases in which negative ions are formed by electron attachment. The theory of these sections is similar to previous work by Schmidt[6] and Vogel[8], with the differences that the work has been extended to cover the case of avalanches initiated part-way across the gap, as may occur with some types of irradiation, and that it has not been assumed here that the positive and negative ions have equal drift velocities. Section 2.2 considers the effect of inductance in the circuit containing the discharge gap; this might be expected to become important in systems of large physical size, for example in experiments using very high voltages.

The contents of this section, with slight modification, have been submitted for publication.

A discharge gap inevitably has some capacitance C, and in avalanche pulse experiments is placed in series with a resistance R, across which an oscillograph is connected to detect the pulses. Figure 1 shows the equivalent circuit of the arrangement, with the inductance of the circuit represented by a lumped element L.

In Figure 1, i is the current that would be induced in the external circuit by movement of charge across the gap if C, R and L were all negligibly small. i_1 is the gap capacitance current, and i_2 is the current indicated by the oscillograph. V is the static supply voltage, assumed to be constant at all times, and v is the instantaneous voltage across the discharge gap.

To obtain a physical picture of the effect of the circuit elements on the measured current, suppose that initially no current is flowing, i.e. $i = i_1 = i_2 = 0$ and, consequently, $V = v$. Now let i increase from zero to some finite value in the direction of the arrow: this implies that electrons must be travelling from cathode to anode and/or positive ions in the reverse direction. The effect of the moving charges is to discharge the gap capacitance partially, causing v to fall below its initial value V. The difference voltage $(V - v)$ causes current i_2 to flow, recharging the gap capacitance through L and R, and it is this recharging current i_2 that is measured. When R, L and C are such that i_2

is able to vary as rapidly as i, then (V - v) never becomes significant, and $i_2 \approx i$.

In the following, the relationship between i_2 and i is considered for different cases. It is assumed throughout that: (a) the electric field in the discharge gap is uniform, and is not appreciably altered by the presence of the free charge carriers; and (b) that the voltage v is so close to V that quantities such as Townsend's first coefficient, electron drift velocity, etc. are constant.

A similar calculation for the cylindrical geometry of the proportional counting tube has been given by Thomas[42].

2.1 Current Pulse Shape with Zero Circuit Inductance

In this case, the equivalent circuit is as shown in Figure 1, but with the inductance L = 0.

Clearly,

$$i_1 = -C\frac{dv}{dt}$$

$$= -C\frac{d}{dt}(V - i_2R)$$

$$= +CR\frac{di_2}{dt}$$

since V is assumed to be constant.

Also

$$i_1 + i_2 = i$$

i.e. $$CR\frac{di_2}{dt} + i_2 = i \qquad . \quad . \quad . \quad (16)$$

The solution is simplified in two particular cases[36]:

(a) CR large, so that

$$CR\frac{di_2}{dt} \gg i_2$$

and

$$CR\frac{di_2}{dt} \approx i$$

i.e. $$i_2 \approx \frac{1}{CR}\int i.\, dt$$

(b) CR small, so that

$$CR \frac{di_2}{dt} \ll i_2$$

and

$$i_2 \approx i$$

These particular cases are not discussed in detail here.

2.1.1 Gases which do not form negative ions

2.1.1.1 Current during the electron transit time

Consider an avalanche produced by a single electron leaving the cathode. When the avalanche has progressed a distance x towards the anode, the number $n_-(x)$ of electrons in the avalanche is given by equation (2) with $n_-(o) = 1$, i.e.

$$n_-(x) = e^{\alpha x} \quad . \quad . \quad . \quad (17)$$

If the avalanche is initiated at time t = 0, and if the electrons travel with a constant drift velocity v_-, then (17) may be written

$$n_-(t) = e^{\alpha v_- t} \quad . \quad . \quad . \quad (18)$$

It can readily be shown[43] that a number of charged particles moving in a uniform-field gap at constant velocity will induce in the external circuit a current i given by

$$i = \frac{qu}{d} \quad . \quad . \quad . \quad (19)$$

where q is the total charge moving, u is its velocity, and d the gap length.

In the present case, $q = \varepsilon n_-(t) = \varepsilon e^{\alpha v_- t}$, where ε is the charge on an electron; and $u = v_-$. Thus the current due to

the motion of electrons only, is

$$i_- = \frac{v_-}{d} \varepsilon e^{\alpha v_- t} \quad . \quad . \quad . \quad (20)$$

or

$$i_- = \frac{\varepsilon}{\tau_-} e^{\alpha v_- t} \quad . \quad . \quad . \quad (21)$$

where $\tau_- = \frac{d}{v_-}$ is the electron transit time.

The number $n_+(t)$ of positive ions in the gap at time t is the number formed up to that time, less the number that have reached the cathode. The latter quantity is $e^{\alpha s}$ where s is given by

$$\frac{s}{v_+} + \frac{s}{v_-} = t$$

and v_+ is the positive ion drift velocity. This is because a time $\frac{s}{v_-}$ elapses from t = 0 until the formation of an ion at s, and a further time $\frac{s}{v_+}$ before that ion arrives at the cathode. Thus,

$$n_+(t) = e^{\alpha v_- t} - e^{\alpha v_* t} \quad . \quad . \quad . \quad (22)$$

where

$$v_* = \left(\frac{1}{v_+} + \frac{1}{v_-} \right)^{-1}$$

Since $v_- \gg v_+$, equation (22) may be written

$$n_+(t) = e^{\alpha v_- t} - e^{\alpha v_+ t}$$

or, to a close approximation,

$$n_+(t) = e^{\alpha v_- t}$$

This last equation is obtained directly by neglecting loss of positive ions from the gap during the electron transit time, i.e. by assuming that the number of positive ions is equal to the number of electrons, given by equation (18).

The current i_+ induced in the external circuit by the motion of the positive ions is then

$$i_+ = \frac{\varepsilon}{\tau_+} e^{\alpha v_- t} \qquad . \quad . \quad . \quad (23)$$

where τ_+ is the positive ion transit time.

The total induced current i is given by

$$i = i_- + i_+$$

i.e. from (20) and (23)

$$i = \left(\frac{1}{\tau_-} + \frac{1}{\tau_+} \right) \varepsilon \, e^{\alpha v_- t} \qquad . \quad . \quad . \quad (24)$$

Substituting this value in (16), and solving for i_2 with the condition $i_2 = 0$ at $t = 0$, gives

$$i_2 = \left(\frac{1}{\tau_-} + \frac{1}{\tau_+} \right) \varepsilon \frac{1}{1 + CR\alpha v_-} \left(e^{\alpha v_- t} - e^{-\frac{t}{CR}} \right)$$

or, to a close approximation,

$$i_2 = \left(\frac{1}{\tau_-} + \frac{1}{\tau_+}\right) \varepsilon \frac{1}{1 + CR\alpha v_-} e^{\alpha v_- t} \quad . \quad . \quad . \quad (25)$$

Comparison with (24) shows that i_2 has in this case the same waveform as i, but is reduced in magnitude by a factor

$$\frac{1}{1 + CR\alpha v_-} \quad . \quad . \quad . \quad (26)$$

For the typical values C = 10 pF, R = 50 kΩ, α = 15 cm^{-1}, v_- = 10^7 cm sec^{-1}, this factor has the value $\frac{1}{76}$.

For later reference, the value of i_2 at time $t = \tau_-$ will be defined as I_{2-}. From (25)

$$I_{2-} = \left(\frac{1}{\tau_-} + \frac{1}{\tau_+}\right) \varepsilon \frac{1}{1 + CR\alpha v_-} e^{\alpha d} \quad . \quad . \quad . \quad (27)$$

2.1.1.2 Current during the positive ion transit time

In this section, τ_- is considered to be negligibly short in comparison with τ_+, so that at time t = 0, $e^{\alpha d}$ positive ions are assumed to appear simultaneously in the gap and to begin to move towards the cathode with velocity v_+. The number $n_+(t)$ of positive ions remaining in the gap at time t is then given by

$$n_+(t) = e^{\alpha d} - e^{\alpha v_+ t} \quad . \quad . \quad . \quad (28)$$

The corresponding value of i, designated i_+, is

$$i_+ = \frac{\varepsilon}{\tau_+}\left(e^{\alpha d} - e^{\alpha v_+ t}\right)$$

For convenience, this will be written

$$i_+ = i_a + i_b$$

where
$$i_a = \frac{\varepsilon}{\tau_+} e^{\alpha d} \quad . \quad . \quad . \quad (29)$$

and
$$i_b = -\frac{\varepsilon}{\tau_+} e^{\alpha v_+ t} \quad . \quad . \quad . \quad (30)$$

i_a may be considered as the component of current due to the motion of the $e^{\alpha d}$ positive ions which suddenly appear in the gap, and i_b as the decrease in current caused by the diminution with time in the number of positive ions in the gap, in accordance with their original exponential distribution along the avalanche path.

Since equation (16) is linear, it can be solved with $i = i_a$ and with $i = i_b$ separately. For $i_{2a} = i_{2b} = 0$ at $t = 0$, the two solutions are

$$i_{2a} = \frac{\varepsilon}{\tau_+} e^{\alpha d}\left(1 - e^{-\frac{t}{CR}}\right) \quad . \quad . \quad . \quad (31)$$

and

$$i_{2b} = -\frac{\varepsilon}{\tau_+}\frac{1}{1 + CR\alpha v_+}\left(e^{\alpha v_+ t} - e^{-\frac{t}{CR}}\right)$$

or, with negligible error,

$$i_{2b} = -\frac{\varepsilon}{\tau_+}\frac{1}{1 + CR\alpha v_+}e^{\alpha v_+ t} \quad . \quad . \quad (32)$$

At time $t = 0$, however, i_2 has the value I_{2-} given by (27), and, in the absence of positive ion motion would decay exponentially to zero with time-constant CR. This initial value may be thought of as adding a further component i_{2c} to the measured current, where

$$i_{2c} = I_{2-} e^{-\frac{t}{CR}} \quad . \quad . \quad . \quad (33)$$

The total measured current i_2 is then

$$i_2 = i_{2a} + i_{2b} + i_{2c}$$

At time $t = \tau_+$, i.e. at the end of the positive ion transit time, i_2 has a finite value, and for $t > \tau_+$ will decrease exponentially to zero, with time constant CR.

2.1.1.3 The "balanced" pulse shape

Equation (31) shows that i_{2a} increases from zero to a final value I_{2+} given by

$$I_{2_+} = \frac{\varepsilon}{\tau_+} e^{\alpha d} \qquad . \quad . \quad . \quad (34)$$

The component i_{2b} is negligible for small values of t, but becomes appreciable for $t \geqslant 0.8\tau_+$. Thus, when t is small,

$$i_2 \approx i_{2a} + i_{2c}$$

$$= I_{2_+}\left(1 - e^{-\frac{t}{CR}}\right) + I_{2_-} e^{-\frac{t}{CR}}$$

and, if conditions are such that I_{2_+} and I_{2_-} are equal, then $i_2 = I_{2_+} = I_{2_-}$ = constant.

In this case, then, the measured current rises in a negligible time (τ_-), to a value I_{2_-} ($= I_{2_+}$), and remains at this 'plateau' value for a considerable fraction of the positive ion transit time. This leads to a pulse of the form described in the German literature as 'balanced' or 'compensated' ('abgeglichen'[6]).

A parameter ψ is now introduced, defined by

$$I_{2_+} = \psi I_{2_-} \qquad . \quad . \quad . \quad (35)$$

Substitution for I_{2_+} from (34) and for I_{2_-} from (27) leads to

$$\psi = \frac{v_+ + (CR\alpha v_+)v_-}{v_+ + v_-} \qquad . \quad . \quad . \quad (36)$$

Clearly, $\psi = 1$ if $CR\alpha v_+ = 1$, and the pulse is of the balanced form ($I_{2_+} = I_{2_-}$).

Schmidt[6] defines a quantity $\rho = CR\alpha v_+$; thus

$$\psi = \frac{v_+ + \rho v_-}{v_+ + v_-} \qquad . \quad . \quad . \quad (37)$$

or

$$\psi = \frac{1 + \frac{v_+}{\rho v_-}}{1 + \frac{v_+}{v_-}} \cdot \rho$$

Since $\frac{v_+}{v_-}$ is generally of the order of 10^{-2}, the factor $\frac{1 + \frac{v_+}{\rho v_-}}{1 + \frac{v_+}{v_-}}$ varies from unity by less than 1% for $0.5 \leq \rho \leq \infty$. Thus, ψ and ρ are, for practical purposes, identical, and the distinction between them makes no difference to the results of the theory.

Further, since $\psi \approx \rho = CR\alpha v_+$, variation of R provides a method of adjusting the pulse shape to the balanced form required for the measurement of some of the physical quantities, as outlined in Section 2.1.1.5.

At time $t = \tau_-$, the voltage across R, which forms the input to the oscillograph, has a value equal to

$$RI_{2_-} = R\left(\frac{1}{\tau_-} + \frac{1}{\tau_+}\right) \varepsilon \frac{1}{1 + CR\alpha v_-} e^{\alpha d}$$

from equation (27). If the conditions are such that $CR\alpha v_+ \approx 1$, then $CR\alpha v_- \gg 1$, since normally $v_- \gg v_+$. This leads to

$$RI_{2_-} \approx \left(\frac{1}{\tau_-} + \frac{1}{\tau_+}\right) \varepsilon \frac{1}{C\alpha v_-} e^{\alpha d} \quad . \quad . \quad (38)$$

and this voltage is independent of R. When i_2 has reached the value I_{2_+}, the voltage input to the oscillograph is

$$RI_{2_+} = R \frac{\varepsilon}{\tau_+} e^{\alpha d},$$

which is proportional to R. Variation of the value of R, therefore, causes the amplitude of the 'plateau' of the observed pulse to vary in proportion, but the initial amplitude remains practically constant. Increasing R does not, as might be expected, increase pulse amplitude without changing pulse shape, unless the gap capacitance C is reduced in the same proportion. In the interests of sensitivity, therefore, it is desirable to keep C small. Further, since the power supply of Figure 1 is to maintain a constant static voltage, it must have negligible a.c. impedance, so that the gap capacitance C is effectively in parallel with R; it follows that stray capacitance across R will give the same result as an increase in C; that is, it will effectively reduce sensitivity.

2.1.1.4 Normalized expressions for measured current

If ψ is set equal to $CR\alpha v_+$ in equations (31), (32) and (33), the result is

$$\left.\begin{aligned} i_{2a} &= \psi I_{2-}\left(1 - e^{-\frac{\alpha d}{\psi}\frac{t}{\tau_+}}\right) \\ i_{2b} &= -\frac{\psi}{1+\psi} I_{2-}\left[e^{\alpha d\,(\frac{t}{\tau_+} - 1)}\right] \\ i_{2c} &= I_{2-}\, e^{-\frac{\alpha d}{\psi}\frac{t}{\tau_+}} \end{aligned}\right\} \quad (39)$$

Current is now expressed in terms of I_{2-} and time in terms of τ_+, with ψ and αd as parameters.

Figure 2 shows the pulse shape indicated by (39), for $\psi = 1$ and $\alpha d = 15$.

In Figures 3 and 4, ψ has the values 0.9 and 1.1 respectively, and again $\alpha d = 15$.

The effect of varying αd from 10 to 20 is shown in Figure 5, for the case $\psi = 1$.

2.1.1.5 Measurements from the observed current pulses.

Positive ion drift velocity (v_+) can be determined from current pulses recorded experimentally, by measurement of positive ion transit time τ_+, on the following basis.

Summing the values of i_{2a}, i_{2b}, i_{2c} from (39), neglecting all negative exponential terms, and replacing ψI_{2-} by I_{2+}, gives

$$i_2 = I_{2+}\left[1 - \frac{1}{1+\psi} e^{\alpha d \left(\frac{t}{\tau_+} - 1\right)}\right] \quad . \quad (40)$$

If the value of i_2 at $t = \tau_+$ is $I_{2\tau_+}$, then

$$I_{2\tau_+} = I_{2+}\left(1 - \frac{1}{1+\psi}\right)$$

and, if $\psi = 1$,

$$I_{2\tau_+} = \tfrac{1}{2} I_{2+}$$

Thus, when the pulse is of the balanced form ($\psi = 1$), the time from the start of the pulse to the point where the recorded current has fallen to one half of its maximum (plateau)value, is the positive ion transit time.

Since it may be difficult to determine ψ accurately in the presence of noise, it is necessary to examine the degree of error introduced by applying this method of measurement to a pulse where ψ differs slightly from unity. To estimate the error, i_2 is set equal to $\frac{1}{2}I_{2_+}$ in (40), so that

$$\frac{1}{1+\psi}\, e^{\alpha d\left(\frac{\tau'_+}{\tau_+} - 1\right)} = \frac{1}{2}$$

where τ'_+ is the value of t making $i_2 = \frac{1}{2}I_{2_+}$, and is the measured positive ion transit time. The percentage error introduced in this way is then

$$100\left(\frac{\tau'_+}{\tau_+} - 1\right) = \frac{100}{\alpha d}\log_e \frac{1+\psi}{2} \quad . \quad . \quad (41)$$

The error is greatest for small αd, and in Figure 6 is plotted against ψ for $\alpha d = 10$. For values of $\psi = 1 \pm 0.1$, this error is only of the order of 0.5%.

Townsend's first coefficient (α) may be determined from the current pulse using two different methods:

(a) For a rectangular pulse,

$$CR\alpha v_+ = 1$$

so that

$$\alpha = \frac{1}{CRv_+} .$$

v_+ may be measured by the method described above, and C and R by any of the normal methods. Since C is effectively in parallel with R, due to the negligible a.c. impedance of the d.c. supply, the value of C used in this kind of measurement must include the stray capacitance across R, as well as that of the gap itself.

(b) An alternative method depends on the shape of the pulse when time t is a considerable fraction of τ_+. The current i_2 is then given by (40), which may be written in the form

$$\frac{I_{2_+} - i_2}{I_{2_+}} = \frac{1}{1 + \psi} e^{\alpha v_+ t} \cdot \frac{1}{e^{\alpha d}}$$

or

$$\log_e \frac{I_{2_+} - i_2}{I_{2_+}} = \left[\log_e \frac{1}{1 + \psi} - \alpha d \right] + \alpha v_+ t$$

Thus, a semilogarithmic plot of the fractional decrease of measured current against time will yield a straight line of slope αv_+. If v_+ is known, α can be found.

Electron drift velocity (v_-) may also be determined by two methods:

(a) Equation (25) shows that the current measured during the electron transit time increases exponentially with time-constant $\frac{1}{\alpha v_-}$. Thus, a semilogarithmic plot of measured current against time gives a straight line of slope αv_-, and v_- can be found in this way, provided α is known.

(b) Where secondary avalanches are produced by a photo-electric effect at the cathode, the time interval between the start of one avalanche and that of its secondary avalanche may be identified with the electron transit time. This can be measured directly from the oscillogram, to give v_-.

2.1.2 Gases which form negative ions

2.1.2.1 Current during the electron transit time

Let the coefficient for negative ion formation be η, and consider an avalanche produced by a single electron leaving the cathode at time t = 0. Then, by analogy with equation (18)

$$n_-(t) = e^{(\alpha-\eta)v_-t}$$

This follows readily from equation (10).

The motion of these $n_-(t)$ electrons produces a component of induced current

$$i_- = \frac{\varepsilon}{\tau_-} e^{(\alpha-\eta)v_-t} \quad . \quad . \quad . \quad (42)$$

The number $n_+(x)$ of positive ions formed in the avalanche, when it has travelled a distance x from the cathode, is obtained by integration of equation (9), i.e.

$$n_+(x) = \int_0^x \alpha\, n_-(x)\, dx$$

In this case,

$$n_+(x) = \alpha \int_0^x e^{(\alpha-\eta)x}\, dx$$

i.e.

$$n_+(x) \approx \frac{\alpha}{\alpha - \eta} \, e^{(\alpha-\eta)x}$$

or

$$n_+(t) = \frac{\alpha}{\alpha - \eta} \, e^{(\alpha-\eta)v_-t}$$

The motion of the positive ions, assuming that a negligible number reach the cathode during the electron transit time, gives rise to a component of induced current

$$i_+ = \frac{\varepsilon}{\tau_+} \, \frac{\alpha}{\alpha - \eta} \, e^{(\alpha-\eta)v_-t}$$

It is convenient to write $f = \frac{\eta}{\alpha}$, so that

$$i_+ = \frac{\varepsilon}{\tau_+} \, \frac{1}{1 - f} \, e^{(\alpha-\eta)v_-t} \quad . \quad . \quad . \quad (43)$$

The number $n_n(t)$ of negative ions formed after time t follows by a similar argument:

$$n_n(t) = \frac{\eta}{\alpha - \eta} \, e^{(\alpha-\eta)v_-t} \quad . \quad . \quad . \quad (44)$$

and the motion of the negative ions yields a component of induced current

$$i_n = \frac{\varepsilon}{\tau_n} \frac{f}{1-f} e^{(\alpha-\eta)v_- t} \quad . \quad . \quad . \quad (45)$$

since no negative ions reach the anode during the electron transit time. τ_n is the negative ion transit time.

The total induced current i is then

$$i = i_- + i_+ + i_n$$

$$= \left(\frac{1}{\tau_-} + \frac{1}{\tau_+} \frac{1}{1-f} + \frac{1}{\tau_n} \frac{f}{1-f}\right) \varepsilon e^{(\alpha-\eta)v_- t}$$

i.e.

$$i = \left[\frac{1}{\tau_-} + \frac{1}{\tau_+}\left(\frac{1+\kappa f}{1-f}\right)\right] \varepsilon e^{(\alpha-\eta)v_- t} \quad . \quad . \quad . \quad (46)$$

Here $\kappa = \frac{\tau_+}{\tau_n} = \frac{v_n}{v_+}$, where v_+ and v_n are the drift velocities of the positive and negative ions respectively. Substitution of (46) in (16) gives, for $i_2 = 0$ at $t = 0$,

$$i = \left[\frac{1}{\tau_-} + \frac{1}{\tau_+}\left(\frac{1+\kappa f}{1-f}\right)\right] \varepsilon \frac{1}{1 + CR(\alpha-\eta)v_-} \left(e^{(\alpha-\eta)v_- t} - e^{-\frac{t}{CR}}\right)$$

or, to a close approximation,

$$i_2 = \left[\frac{1}{\tau_-} + \frac{1}{\tau_+}\left(\frac{1 + \kappa f}{1 - f}\right)\right] \varepsilon \frac{1}{1 + CR(\alpha-\eta)v_-} e^{(\alpha-\eta)v_- t} \quad . \quad . \quad . \quad (47)$$

At $t = \tau_-$, i_2 has the value

$$I_{2-} = \left[\frac{1}{\tau_-} + \frac{1}{\tau_+}\left(\frac{1 + \kappa f}{1 - f}\right)\right] \varepsilon \frac{1}{1 + CR(\alpha-\eta)v_-} e^{(\alpha-\eta)d} \quad . \quad . \quad . \quad (48)$$

2.1.2.2 Current during the positive ion transit time

The current will be the sum of the separate components, as in Section 2.1.1.2, but with the addition of a fourth component due to negative ion motion.

The number $n_+(t)$ of positive ions in the gap at time t is

$$n_+(t) = \frac{1}{1 - f}\left(e^{(\alpha-\eta)d} - e^{(\alpha-\eta)v_+ t}\right)$$

This is of the same form as (28) and, using the same terminology as before, the corresponding components of measured current i_2 are:

$$i_{2a} = \frac{\varepsilon}{\tau_+} \frac{1}{1 - f} e^{(\alpha-\eta)d}\left(1 - e^{-\frac{t}{CR}}\right) \quad . \quad . \quad . \quad (49)$$

$$i_{2b} = -\frac{\varepsilon}{\tau_+}\ \frac{1}{(1-f)}\ \frac{1}{1+(\alpha-\eta)v_+CR}\left[e^{(\alpha-\eta)v_+t} - e^{-\frac{t}{CR}}\right]$$

The latter equation may be written, without significant loss of accuracy,

$$i_{2b} = -\frac{\varepsilon}{\tau_+}\ \frac{1}{1-f}\ \frac{1}{1+(\alpha-\eta)v_+CR}\ e^{(\alpha-\eta)v_+t} \quad . \quad (50)$$

The component of current i_{2c} due to the initial condition is again

$$i_{2c} = I_{2-}\ e^{-\frac{t}{CR}} \quad . \quad . \quad . \quad (33)$$

The total number of negative ions formed in the avalanche follows from (44) with $t = \tau_-$:

$$n_n(\text{total}) = \frac{f}{1-f}\ e^{(\alpha-\eta)d}$$

and the number remaining in the gap after time $t = \tau_-$ decreases exponentially with time-constant $\frac{1}{(\alpha-\eta)v_n}$ as a result of the initial exponential distribution of ion density along the avalanche path. Thus the number remaining at time $t > \tau_-$ is

$$n_n = \frac{f}{1-f}\ e^{(\alpha-\eta)d}\ .\ e^{-(\alpha-\eta)v_nt}$$

The motion of these ions induces a component of current i_d given by

$$i_d = \frac{\varepsilon}{\tau_n} \frac{f}{1-f} e^{(\alpha-\eta)d} e^{-(\alpha-\eta)v_n t} ,$$

and substitution of this value in (16) gives the solution

$$i_{2d} = \frac{\varepsilon}{\tau_n} \frac{f}{1-f} e^{(\alpha-\eta)d} \cdot \frac{1}{1 - CR(\alpha-\eta)v_n} \left[e^{-(\alpha-\eta)v_n t} - e^{-\frac{t}{CR}} \right] \quad . \quad . \quad . \quad (51)$$

for $i_{2d} = 0$ at $t = 0$.

The actual measured current is then

$$i_2 = i_{2a} + i_{2b} + i_{2c} + i_{2d}$$

for values of t up to τ_+, after which i_2 falls exponentially to zero, with time-constant CR.

2.1.2.3 The balanced pulse shape

The final value which i_{2a} attains is, from (49),

$$I_{2_+} = \frac{\varepsilon}{\tau_+} \frac{1}{1-f} e^{(\alpha-\eta)d} \quad . \quad . \quad . \quad (52)$$

If $I_{2_+} = I_{2_-}$, then the observed pulse will have the appearance of a pulse of balanced form as in Figure 2, but with the negative ion component superposed and easily distinguishable.

Substitution of the value for I_{2_+} from (52) and I_{2_-} from (48) in

$$I_{2_+} = \psi I_{2_-} \qquad . \quad . \quad . \quad (35)$$

gives, after rearrangement,

$$\psi = \frac{v_+ + \rho(1 - f)v_-}{(1 + \kappa f)v_+ + (1 - f)v_-} , \qquad . \quad . \quad . \quad (53)$$

where $\rho = CR\alpha v_+$ as before.

The condition for $\psi = 1$ is now

$$\rho = 1 + \frac{\kappa f}{1 - f} \frac{v_+}{v_-} \qquad . \quad . \quad . \quad (54)$$

which is the same as the previous condition ($\rho = 1$) if

$$\frac{\kappa f}{1 - f} \frac{v_+}{v_-} \ll 1 \qquad . \quad . \quad . \quad (55)$$

Since $\frac{v_+}{v_-}$ is normally of the order of 10^{-2}, and κ of the order of unity, this condition is fulfilled unless f is close to unity. The method used by Vogel[8] will therefore be followed, i.e. the condition for the balanced pulse shape will be written as

$$\rho = CR\alpha v_+ = 1$$

Further, (55) may be written

$$\kappa f v_+ \ll (1 - f)v_-$$

and, since κf is of the order of unity,

$$(1 + \kappa f)v_+ \ll (1 - f)v_-$$

and

$$v_+ \ll (1 - f)v_-$$

Applying these last two inequalities in equation (53) gives $\psi \approx \rho$, and these two quantities will now be treated as identical.

2.1.2.4 Normalized expressions for measured current

Setting $\psi = CR\alpha v_+$ in (49), (50), (33) and (51), the result is

$$\left.\begin{aligned} i_{2a} &= \psi I_{2-}\left(1 - e^{-\frac{\alpha d}{\psi}\frac{t}{\tau_+}}\right) \\ i_{2b} &= \frac{-\psi I_{2-}}{1 + (1 - f)\psi} e^{(1-f)\alpha d\left(\frac{t}{\tau_+} - 1\right)} \\ i_{2c} &= I_{2-} e^{-\frac{\alpha d}{\psi}\frac{t}{\tau_+}} \\ i_{2d} &= \frac{f\kappa\psi I_{2-}}{1 - (1 - f)\psi\kappa}\left[e^{-(1-f)\kappa\alpha d\frac{t}{\tau_+}} - e^{-\frac{\alpha d}{\psi}\frac{t}{\tau_+}}\right] \end{aligned}\right\} \quad (56)$$

Current is now expressed in terms of I_{2_-}, and time in terms of τ_+, with αd, f, ψ and κ as parameters.

Figure 7 shows the current pulse shape indicated by (56) for $\alpha d = 30$, $f = 0.5$, $\psi = 1$, $\kappa = 1.5$, and for the same conditions but with $\kappa = 1.0$.

2.1.2.5 Measurements from the observed current pulses

Positive ion drift velocity (v_+). Following the method of Section 2.1.1.5, it is required to find the value $I_{2\tau_+}$ of i_2 at $t = \tau_+$.

Summing equations (56), neglecting all negative exponential terms, and replacing ψI_{2_-} by I_{2_+}, gives

$$i_2 = I_{2_+}\left[1 - \frac{1}{1 + (1-f)\psi}\, e^{(1-f)\alpha d\left(\frac{t}{\tau_+} - 1\right)}\right] \quad . \quad (57)$$

When $t = \tau_+$, and $\psi = 1$

$$i_2 = I_{2\tau_+} = I_{2_+}\left(1 - \frac{1}{1 + (1-f)}\right)$$

or

$$I_{2\tau_+} = \frac{I_{2_+}}{1 + \frac{1}{1 - f}} \quad . \quad . \quad . \quad (58)$$

as given by Vàgel[8].

Thus, measurement of τ_+, and hence v_+, in this case involves a knowledge of f. Measurement of this latter parameter from the current pulse is discussed below.

Townsend's first coefficient (α) may be found by adjusting R to give the balanced pulse shape of Figure 7, and applying the relation $CR\alpha v_+ = 1$; C, R and v_+ can be measured independently.

Measurement of $(\alpha - \eta)$. From equation (57), a plot of $\log_e \frac{(I_{2_+} - i_2)}{I_{2_+}}$ against t, for $0.8\tau_+ \lesssim t \leq \tau_+$, will yield a straight line of slope $(\alpha - \eta)v_+$. If v_+ is known, $(\alpha - \eta)$ can be determined.

Measurement of $f(= \eta/\alpha)$. To demonstrate the method of estimating f from the pulse shape, it is necessary to examine that portion of the pulse which results from negative ion motion. With $\psi = 1$, the component of current i_2 produced by negative ion motion is, from equation (56),

$$i_{2d} = \frac{f\kappa I_{2_-}}{1 - (1-f)\kappa} \left[e^{-(1-f)\kappa\alpha d \frac{t}{\tau_+}} - e^{-\alpha d \frac{t}{\tau_+}} \right]$$

This has a maximum value $i_{2d_{max}}$ when

$$\frac{t}{\tau_+} = \frac{1}{\alpha d\left[(1-f)\kappa - 1\right]} \log_e \left[(1-f)\kappa\right],$$

given by

$$i_{2d_{max}} = \frac{f\kappa\, I_{2\_}}{1 - (1-f)\kappa} \left\{ \left[(1-f)\kappa\right]^{\frac{(1-f)\kappa}{1-(1-f)\kappa}} - \left[(1-f)\kappa\right]^{\frac{1}{1-(1-f)\kappa}} \right\}$$

If the maximum value of measured current is $\hat{I}_2$, then for $\psi = 1$, i.e. for $I_{2\_} = I_{2_+}$,

$$\hat{I}_2 = I_{2\_} + i_{2d_{max}}$$

and if a ratio δ is defined by

$$\delta = \frac{\hat{I}_2}{I_{2_+}} = \frac{\hat{I}_2}{I_{2\_}}$$

then $$\delta = 1 + \frac{i_{2d_{max}}}{I_{2\_}}$$

$$= 1 + \frac{f\kappa}{1 - (1-f)\kappa} \left\{ \left[(1-f)\kappa\right]^{\frac{(1-f)\kappa}{1-(1-f)\kappa}} - \left[(1-f)\kappa\right]^{\frac{1}{1-(1-f)\kappa}} \right\}$$

For $\kappa = 1$, i.e. $v_n = v_+$,

$$\delta = 1 + \frac{f}{1-f}(1-f)^{\frac{1}{f}} \quad . \quad . \quad . \quad (59)$$

as obtained by Vogel[8] for this condition.

δ can be measured from the observed current pulse, and f may then be found using curves of f against δ, as shown in Figure 8 for the cases $\kappa = 1.0$ and $\kappa = 1.5$. When κ is not known accurately, curves of this type would be useful in estimating the probable error in f.

Electron drift velocity (v_-) can again be measured by two methods:

(a) The time-constant of increase of measured current during the electron transit time is $\frac{1}{(\alpha-\eta)v_-}$, from equation (31), so a plot of $\log_e i_2$ against time will yield a value of v_-, provided $(\alpha-\eta)$ is known.

(b) Where secondary avalanches occur as a result of a photo-electric process at the cathode, the electron transit time (and hence v_-) can be measured from the oscillogram as previously discussed in Section 2.1.1.5.

2.1.3 Avalanches starting part-way across the gap

When the primary electrons are produced by ionizing radiations from a radioactive substance, or by ambient irradiation, it is conceivable that at least some of the observed avalanches will start within the gap and not at the cathode surface. On account of the statistical variations in avalanche carrier-number[27], such avalanches will not be immediately distinguishable by their reduced size, although their presence might be detected by measurement of the statistical distribution of pulse heights. It is of interest to enquire whether the observed current pulse shape is affected as a result of the avalanche's starting at a point not on the cathode surface. This case has not been considered by previous authors. For simplicity, only the case of a gas which does not form negative ions will be considered.

Suppose that, at time t = 0, an initiating electron is released within the gap at x = a. The induced current i_- is, as before,

$$i_- = \frac{v_-}{d} \varepsilon e^{\alpha v_- t} \quad . \quad . \quad . \quad (20)$$

Here, however, $\frac{d}{v_-}$ is not the transit time of the initiating electron.

It is assumed that the number of positive ions in the gap during the electron transit time is equal to the number of

electrons, so that

$$i_+ = \frac{v_+}{d}\,\varepsilon\, e^{\alpha v_- t}$$

(compare equation (23)).

For $0 \leq t \leq \tau_-$, there results an induced current

$$i = \left(\frac{v_-}{d} + \frac{v_+}{d}\right) \varepsilon\, e^{\alpha v_- t},$$

and, at the end of the electron transit time,

$$i_2 = I_{2_-} = \left(\frac{v_-}{d} + \frac{v_+}{d}\right) \varepsilon \frac{1}{1 + CR\alpha v_-} e^{\alpha(d-a)} \quad . \quad (60)$$

For the "final" (plateau) value I_{2_+} of the positive ion current, there results

$$I_{2_+} = \frac{v_+}{d}\,\varepsilon\, e^{\alpha(d-a)} \quad . \quad . \quad . \quad (61)$$

and if, as before,

$$I_{2_+} = \psi\, I_{2_-} \quad . \quad . \quad . \quad (35)$$

then precisely the same result is obtained for ψ. Thus the value of ψ is not affected by variations in the starting position of the avalanche.

The observed pulse shape during the positive ion transit time is calculated from the following expressions for the number of positive ions in the gap during the interval $\tau_- \leq t \leq \tau_+$:

$$n_+(t) = e^{\alpha(d-a)} \qquad \text{for } 0 \leq t \leq \frac{a}{v_+}$$

$$n_+(t) = e^{\alpha(d-a)} - e^{\alpha(v_+t-a)} \qquad \text{for } \frac{a}{v_+} \leq t \leq \tau_+.$$

In a practical case, the term $e^{\alpha(v_+t-a)}$ will be negligible in comparison with $e^{\alpha(d-a)}$ for $t \lesssim 0.8\tau_+$, so that

$$n_+(t) \approx e^{\alpha(d-a)} - e^{\alpha(v_+t-a)} \qquad \text{for } 0 \leq t \leq \tau_+$$

provided that $\frac{a}{v_+} \lesssim 0.8\tau_+$, i.e. $a \lesssim 0.8d$.

This leads to

$$i_a = \varepsilon \frac{v_+}{d} e^{\alpha(d-a)}$$

$$i_b = -\varepsilon \frac{v_+}{d} \frac{1}{e^{\alpha a}} e^{\alpha v_+ t}$$

and consequently

$$i_{2a} = \frac{v_+}{d} e^{\alpha(d-a)} \left(1 - e^{-\frac{t}{CR}}\right)$$

$$i_{2b} = -\varepsilon \frac{v_+}{d} \frac{1}{e^{\alpha a}} \frac{1}{1 + CR\alpha v_+} \left(e^{\alpha v_+ t} - e^{-\frac{t}{CR}}\right)$$

Using the values of I_{2_-} and I_{2_+} from (60) and (61), and setting $CR\alpha v_+ = \psi$ in the above, results in a relationship identical with (39).

Thus the observed current pulse shape does not depend on the starting-point of the initiating electron. This result would be expected on purely physical grounds, since, provided a is not a very large fraction of d, the number of electrons (and ions) produced in the space $0 \leqslant x \leqslant a$ by an electron leaving the cathode would be only a small fraction of the total number for the avalanche, and failing to allow for an avalanche's starting at $x = a$ instead of $x = 0$ is equivalent to neglecting this small fraction of the total. These remarks, clearly, apply equally well to gases which form negative ions, and this latter case will not be discussed in detail.

2.2 The Effect of Circuit Inductance

This section considers the effect of a finite inductance L (see Figure 1) on the shape of the observed current pulses and on the accuracy of measurements made from them. It is reasonable to interpret L as the inductance of the 'single turn' formed by the final smoothing capacitor of the d.c. supply in series with the discharge gap and resistor R; the order of magnitude of L is then most conveniently estimated from the relation given by Astbury[44], namely, $L \approx$ (mean diameter of turn in metres) $\times 10^{-6}$ H. In most practical cases, this mean diameter will be of the order of 1 metre or less, so it will be sufficient to consider values of L up to about 10μH.

The theory will be developed only for gases which do not form negative ions.

From Figure 1,

$$i_1 = -C \frac{dv}{dt}$$

$$= -C \frac{d}{dt}\left(V - i_2 R - L \frac{di_2}{dt} \right)$$

$$= CR \frac{di_2}{dt} + LC \frac{d^2 i_2}{dt^2}$$

since V is assumed to be constant.

Also,

$$i_1 + i_2 = i$$

i.e. $$LC \frac{d^2 i_2}{dt^2} + CR \frac{di_2}{dt} + i_2 = i \quad . \quad . \quad (62)$$

2.2.1 Current during the electron transit time

The value of i is unaffected by the external circuit, and is therefore the same as in Section 2.1.1.1 above, i.e.

$$i = \left(\frac{1}{\tau_-} + \frac{1}{\tau_+}\right) \varepsilon \, e^{\alpha v_- t} \qquad . \qquad . \qquad . \qquad (24)$$

Substituting this value in (62), and solving for i_2 with the initial conditions $i_2 = 0$ and $\frac{di_2}{dt} = 0$ at $t = 0$, gives the result

$$\left.\begin{aligned} i_2 &= a \frac{A^2 - B^2}{2B}\left[\frac{2B\, e^{\alpha v_- t}}{(A + \alpha v_-)^2 - B^2} + \frac{e^{-(A+B)t}}{(A + \alpha v_-) + B} - \frac{e^{-(A-B)t}}{(A + \alpha v_-) - B}\right] \\ \text{where} \quad a &= \left(\frac{1}{\tau_-} + \frac{1}{\tau_+}\right)\varepsilon \\ A &= \frac{R}{2L} \\ B &= +\sqrt{\frac{R^2}{4L^2} - \frac{1}{LC}} \end{aligned}\right\} \quad (63)$$

In general, solutions of (62) are oscillatory when B is imaginary, i.e. when $R < \sqrt{\frac{4L}{C}}$. Since this condition is unlikely to be

fulfilled in a practical experiment, only non-oscillatory solutions will be considered.

The negative exponential terms in (63) may be neglected; substituting for a, A and B then gives

$$i_2 = \left(\frac{1}{\tau_-} + \frac{1}{\tau_+}\right)\varepsilon \frac{1}{1 + CR\alpha v_- + LC\alpha^2 v_-^2} e^{\alpha v_- t}$$

Setting L = 0 reduces this to equation (25): in the present case, i_2 has again the same waveform as i, but is reduced in magnitude by a factor

$$\frac{1}{1 + CR\alpha v_- + LC\alpha^2 v_-^2} \quad . \quad . \quad . \quad (64)$$

For the typical values C = 10 pF, R = 50 kΩ, $\alpha = 15$ cm^{-1}, $v_- = 10^7$ cm sec^{-1}, the value of (64) varies from $\frac{1}{76}$ for L = 0 to $\frac{1}{78.25}$ for L = 10 μH.

At $t = \tau_-$, i_{2-} has the value

$$I_{2-} = \left(\frac{1}{\tau_-} + \frac{1}{\tau_+}\right)\varepsilon \frac{1}{1 + CR\alpha v_- + LC\alpha^2 v_-^2} e^{\alpha d} \quad . \quad . \quad (65)$$

and is changing at the rate

$$\left(\frac{di_{2-}}{dt}\right)_{\tau_-} = \alpha v_- I_{2-} \quad . \quad . \quad . \quad (66)$$

2.2.2 Current during the positive ion transit time

As in Section 2.1.1.2, τ_- is neglected in comparison with τ_+, and the solution is again divided into three parts. i_a and i_b are given by (29) and (30) respectively, and the corresponding solutions of (62) with $i_2 = \frac{di_2}{dt} = 0$ at $t = 0$ are

$$i_{2_a} = \frac{\varepsilon}{\tau_+} e^{\alpha d} \left[1 + \frac{A-B}{2B} e^{-(A+B)t} - \frac{A+B}{2B} e^{-(A-B)t} \right] \quad . \quad . \quad (67)$$

where A and B are defined in (63); and

$$i_{2_b} = - \frac{\varepsilon}{\tau_+} \frac{A^2 - B^2}{2B} \left[\frac{2B\, e^{\alpha v_+ t}}{(A+\alpha v_+)^2 - B^2} + \frac{e^{-(A+B)t}}{(A+\alpha v_+) + B} - \frac{e^{-(A-B)t}}{(A+\alpha v_+) - B} \right]$$

or, very nearly,

$$i_{2_b} = - \frac{\varepsilon}{\tau_+} \frac{A^2 - B^2}{(A+\alpha v_+)^2 - B^2} e^{\alpha v_+ t} \quad . \quad . \quad . \quad (68)$$

To take into account the initial condition, the third component i_{2_c} is introduced, obtained by solving equation (62) with the right-hand side equal to zero, under the initial condition given by (65) and (66). The result is

$$i_{2_c} = I_{2_-} \left[\frac{A+B+\alpha v_-}{2B} e^{-(A-B)t} - \frac{A-B+\alpha v_-}{2B} e^{-(A+B)t} \right] \quad . \quad . \quad (69)$$

The measured current i_2 is obtained by summing (67), (68) and (69), for values of t up to τ_+.

2.2.3 The balanced pulse shape

Following the method of Section 2.1.1.3, $\frac{\varepsilon}{\tau_+} e^{\alpha d}$ is set equal to I_{2_+} in (67) so that,

$$i_{2_a} = I_{2_+}\left[1 + \frac{A-B}{2B} e^{-(A+B)t} - \frac{A+B}{2B} e^{-(A-B)t}\right] \quad . \quad . \quad . \quad (70)$$

As in the case of zero inductance, the contribution of i_{2_b} to the total measured current is negligible for small values of t, so that

$$i_2 \approx i_{2_a} + i_{2_c}$$

for t small.

Substituting for i_{2_a} from (70), and for i_{2_c} from (69), with $I_{2_-} = I_{2_+}$, leads to

$$i_2 \approx I_{2_-}\left\{1 + \frac{\alpha v_-}{2B}\left[e^{-(A-B)t} - e^{-(A+B)t}\right]\right\} \quad . \quad . \quad . \quad (71)$$

The term inside the square brackets has a maximum value

$$\left[\left(\frac{A-B}{A+B}\right)^{\frac{A-B}{2B}} - \left(\frac{A-B}{A+B}\right)^{\frac{A+B}{2B}}\right]$$

at time

$$t_m = \frac{1}{2B} \log_e\left(\frac{A+B}{A-B}\right) .$$

At this point, it is convenient to make the simplifying assumption that the circuit is heavily damped, i.e. $R \gg \sqrt{\frac{4L}{C}}$. This leads to

$$B \approx A = \frac{R}{2L}$$

$$A + B \approx 2A = \frac{R}{L}$$

and $$A - B \approx \frac{A^2 - B^2}{2A} = \frac{1}{CR}$$

Under these conditions, the term inside the square brackets of (71) has a maximum value of approximately unity, occurring at time

$$t_m \approx \frac{L}{R} \log_e \frac{CR^2}{L} \quad . \quad . \quad . \quad (72)$$

It would be most useful to express t_m in terms of τ_+ only, but this is not possible: it is possible, however, to make a numerical calculation of some generality, on the following basis. Equation (72) can be written

$$t_m = \frac{L}{R} \log_e \frac{CR}{\left(\frac{L}{R}\right)}$$

and t_m is now expressed in terms of two time-constants, CR and $\frac{L}{R}$. Since the case of interest is that of the balanced pulse, it will

be taken that $CR\alpha V_+ = 1$. (This is shown below to be the condition for the balanced pulse with finite inductance, if the circuit is heavily damped). In most practical cases, α will be of the order of 10 cm^{-1}, and v_+ of the order of 10^5 cm sec^{-1}, making αv_+ of the order of 10^6 sec^{-1}. It is, therefore, sufficient to consider values of CR in the range 10^{-7} to 10^{-5} sec. Since the circuit is heavily damped,

$$R \gg \sqrt{\frac{4L}{C}}$$

i.e. $$CR \gg \frac{4L}{R}$$

so that $$CR \gg \frac{L}{R}$$

Thus, only values of $\frac{L}{R}$ up to $\frac{CR}{100}$ will be considered. The resulting values of t_m are plotted in Figure 9 to a base of $\frac{L}{R}$, and it is seen that t_m is, at greatest, of the order of 10^{-7} sec, and therefore unlikely to be more than a few per cent of the positive ion transit time, for a gap length of the order of 1 cm. On this basis, t_m will be neglected in comparison with τ_+, so that, at the start of a current pulse, i_2 rises from zero to a value

$$I_{2-}' = \left(1 + \frac{\alpha v_-}{2B}\right) I_{2-} \qquad . \quad . \quad . \quad (73)$$

in a negligible time, and then must fall to a plateau value of I_{2_+} ($= I_{2_-}$): the pulse would have the general appearance of that shown in Figure 3.

Now consider the case

$$I_{2_+} = I'_{2_-} = \left(1 + \frac{\alpha v_-}{2B}\right) I_{2_-}.$$

In place of equation (71), there results

$$i_2 \approx I_{2_-} \left\{1 + \frac{\alpha v_-}{2B}\left[1 - \frac{3B-A}{2B} e^{-(A+B)t} - \frac{A-B}{2B} e^{-(A-B)t}\right]\right\}$$

for small values of t.

Using the approximation $A \approx B$, this becomes

$$i_2 \approx I_{2_-} \left\{1 + \frac{\alpha v_-}{2B}\left[1 - e^{-(A+B)t}\right]\right\}$$

In a practical case, the time-constant $\frac{1}{A+B}\left(\approx \frac{L}{R}\right)$ is likely to be negligible in comparison with τ_+, so that as far as the recorded pulse is concerned, at small values of t

$$i_2 = I_{2_-}\left(1 + \frac{\alpha v_-}{2B}\right) = I'_{2_-} = I_{2_+}$$

and a pulse of balanced form is observed.

If, as before,

$$I_{2_+} = \psi I_{2_-} \qquad . \quad . \quad . \quad (35)$$

and, additionally,

$$I_{2_+} = \psi' I'_{2_-}$$

then, substituting for I_{2_+}, I_{2_-}, and I'_{2_-} ,

$$\psi = \left(1 + \frac{\alpha v_-}{2B}\right) \psi' = \frac{v_+ + (CR\alpha v_+ + LC\alpha^2 v_+ v_-)v_-}{v_+ + v_-}$$

By analogy with (36), a new value of ρ can be defined by

$$\rho = CR\alpha v_+ + LC\alpha^2 v_+ v_-$$

The relation between ψ and ρ is given by (37), and, by the argument given in Section 2.1.1.3, ρ and ψ are usually indistinguishable.

Thus,

$$\rho \approx \left(1 + \frac{\alpha v_-}{2B}\right) \psi' \qquad . \quad . \quad . \quad (74)$$

and the condition for a pulse of rectangular appearance, i.e. for $\psi' = 1$ is

$$CR\alpha v_+ + LC\alpha^2 v_+ v_- = 1 + \frac{\alpha v_-}{2B} ,$$

or substituting

$$B \approx A = \frac{R}{2L} ,$$

$$CR\alpha v_+ + LC\alpha^2 v_+ v_- = 1 + \frac{\alpha v_- L}{R}$$

i.e.

$$CR\alpha v_+ = 1$$

The condition for the balanced pulse shape with L = 0 is therefore valid for finite values of L, provided only that the circuit is heavily damped..

It is also of interest (compare Section 2.1.1.3) to examine how the sensitivity of the system is affected by the presence of inductance in the circuit of the discharge gap. The voltage across R at the beginning of the pulse is effectively

$$RI_2'_- = R\left(1 + \frac{\alpha v_-}{2B}\right)\left(\frac{1}{\tau_-} + \frac{1}{\tau_+}\right)\varepsilon \frac{1}{1 + CR\alpha v_- + LC\alpha^2 v_-^2} e^{\alpha d}$$

from (65) and (73). Using again the approximation $B \approx A = \frac{R}{2L}$, and neglecting unity in comparison with $CR\alpha v_-$ (since $CR\alpha v_+ \approx 1$ for the case being considered, and $v_+ \ll v_-$), the value of $RI_2'_-$ becomes

$$RI_2'_- = \left(\frac{1}{\tau_-} + \frac{1}{\tau_+}\right)\varepsilon \frac{1}{C\alpha v_-} e^{\alpha d}$$

This is identical with the result obtained with zero inductance (equation (38)).

As in the case L = 0, the voltage across R on the 'plateau' of the pulse is

$$RI_{2_+} = R \frac{\varepsilon}{\tau_+} e^{\alpha d} ,$$

and the same argument applies as in Section 2.1.1.3. Thus, as far as sensitivity is concerned, the aim in designing the gap circuit should be to keep down the capacitance, and little or no attention need be paid to the circuit inductance.

So far, diffusion of the electrons has been neglected: its effect is to reduce the rate of change of i_2 at $t = \tau_-$. (This has been observed by Frommhold[34]).

Writing

$$\left(\frac{di_2}{dt}\right)_{\tau_-} = kI_{2_-} \text{ where } k < \alpha v_-$$

in place of (66), eqn. (73) becomes

$$I'_{2_-} = \left(1 + \frac{k}{2B}\right) I_{2_-}$$

and it is clear that the effect of electron diffusion will be to reduce I'_{2_-}, i.e. to make it more nearly equal to I_{2_-}.

2.2.4 Measurement from the observed current pulses - errors introduced by neglecting inductance

Positive ion drift velocity (v_+). The method of Section 2.1.1.5 will be applied to the case $L \neq 0$. Summing i_{2_a}, i_{2_b}, i_{2_c}, given by (67), (68) and (69), with $t = \tau_+$, and neglecting all negative exponential terms, gives

$$I_{2_{\tau_+}} = \frac{\varepsilon}{\tau_+} e^{\alpha d} - \frac{\varepsilon}{\tau_+} \frac{A^2 - B^2}{(A+\alpha v_+)^2 - B^2} e^{\alpha v_+ t_+}$$

$$= I_{2+} \left(1 - \frac{1}{1 + CR\alpha v_+ + LC\alpha^2 v_+^2} \right)$$

For the balanced pulse shape, if the circuit is heavily damped,

$$CR\alpha v_+ = 1$$

and

$$I_{2_{\tau_+}} = I_{2+} \left(1 - \frac{1}{2 + \frac{L}{CR^2}} \right)$$

but, since the circuit is heavily damped,

$$CR \gg \frac{L}{R}$$

i.e. $$\frac{L}{CR^2} \ll 1$$

so that, for practical purposes,

$$I_{2\tau_+} = \tfrac{1}{2} I_{2+}$$

as for the case of zero inductance (Section 2.1.1.5).

A possible source of error lies in the neglect of electron diffusion: as has been shown, this has the effect of reducing I_{2-}', making it more nearly equal to I_{2-}. Thus, in order to obtain a pulse of balanced form, it will be necessary to reduce the value of R below $\frac{1}{C\alpha v_+}$, so that $CR\alpha v_+$ will be less than unity. The error in the measured value of τ_+ will be comparable with the error introduced by having $\psi \neq 1$ in the case of zero inductance (see Figure 6 and the discussion of Section 2.1.1.5).

To take a numerical example: for R = 50 kΩ, α = 15 cm^{-1}, v_- = 10^7 cm sec^{-1}, and L = 10 μH, the difference between I_{2-}' and I_{2-} is only 3%. Figure 6 shows that if ψ varies from unity by this amount, a negligible error in τ_+ will result.

Townsend's first ionization coefficient (α). The first method of Section 2.1.1.5, using the condition $CR\alpha v_+ = 1$ for a rectangular pulse, has been shown above to be valid also for the case $L \neq 0$, provided that the circuit is heavily damped and that electron diffusion has negligible effect.

As has been shown earlier, the effect of electron diffusion is to effectively reduce I'_{2-}. To obtain a rectangular pulse, then, it would be necessary to reduce R below the value $\frac{1}{C\alpha v_+}$ and application of the relation $CR\alpha v_+ = 1$ would give too high a value of α. Taking again the numerical example R = 50 kΩ, $\alpha = 15\ cm^{-1}$, $v_- = 10^7\ cm\ sec^{-1}$, L = 10 μH, the difference between I'_{2-} and I_{2-} is 3%, and the resulting error in measured α must be less than this. Thus the error is likely to be small in most practical cases.

The second method of Section 2.1.1.5 is independent of circuit inductance, since the appropriate term (equation (68)) still has the exponent αv_+.

Electron drift velocity (v_-). Both methods of Section 2.1.1.5 are clearly independent of circuit inductance.

It may be said in conclusion that the inductance of the discharge circuit is unlikely to have a significant effect on the observed pulse shape. Any such effect will be most marked at the end of the electron transit time, and in practice might be masked by the effect of electron diffusion, which becomes apparent at this time, or by the finite rise-time of the oscillograph

amplifier. Where it is suspected that the presence of inductance may lead to errors in measurements from the current pulses, it will be useful to calculate the order of magnitude of $\frac{\alpha v_-}{2B}$.

Normally, $\frac{\alpha v_-}{2B} \approx \frac{\alpha v_-}{2A} = \frac{L\alpha v_-}{R}$ and if this quantity is not small compared with unity, the errors introduced may not be negligible, and should be estimated by the above methods.

3. EXPERIMENTS IN ROOM AIR

3.1 Simultaneous Records of Current and Light Pulses

The contents of Section 3.1.1 and part of 3.1.2 have previously been presented by the author in a thesis for A.R.C.S.T.[3]. It is felt that some repetition is desirable for the sake of completeness, since some of the other experiments described below used the same apparatus and techniques.

Some of the results of Section 3 have been published in reference (4).

3.1.1 Apparatus

The high-voltage supply

The circuit diagram of the high-voltage d.c. supply used throughout this work is shown in Figure 10: a voltage-doubling circuit was used, each of the rectifiers MR1, MR2 consisting of twenty K8/200 "Sen-Ter-Cel" rectifiers in series. The milliameter M1 indicated the rectifier current so that overloading could be avoided. The voltage on the discharge gap was indicated by microammeter M2, more accurate measurement being carried out by means of the calibrated potentiometer R6 and galvanometer G. R5, for which a Tinsley decade resistor was used, was adjusted to a suitable value depending on the voltage to be measured.

The parts operating at high potential were made free from corona at voltages up to the highest used, i.e. about 120 kV.

The discharge gap

100 kV uniform-field brass electrodes of the Stephenson profile[45] were used, with a bakelite gap structure. With these electrodes, breakdown occurs in the uniform-field region for gap lengths of up to about 3.8 cm. Telescopic gauges

were used to check the gap length and parallelism of the electrode surfaces. Before each experiment, the electrodes were cleaned with "Silvo" polish, polished with a soft cloth, then washed with ether and wiped with a piece of cotton bandage. After mounting in the gap structure, the electrodes were wiped with a piece of nylon.

The complete apparatus

Figure 11 shows a block diagram of the apparatus employed to record the current and light pulses simultaneously.

The gap enclosure was a light-tight box, six feet square and four feet high, made of "Celotex" softboard on a "Dexion" aluminium framework and covered with 1/32" thick aluminium. The softboard interior was painted matt black and provided a good non-reflecting surface; unfortunately, it also proved to be an inexhaustible source of dust. The high-voltage connection to the gap was made through a 200 kV oil-filled bushing in the top of the enclosure, and leads to the pulse recording apparatus were taken through a light-proof seal in the side.

Current pulses were detected by the series resistor $R(= 1\ k\Omega)$, and were displayed, after amplification, on one trace of a double-beam oscillograph. Light pulses were detected by a photomultiplier and displayed, after amplification, on the other

trace of the oscillograph. Cathode followers provided the low-impedance sources required to feed the few yards of coaxial cable leading to the amplifier inputs; each of these cables was terminated at the amplifier end in a 100Ω resistor.

Details of the electronic apparatus have been given in reference (3). The response of this apparatus was such as to produce no visible distortion of the pulses at the sweep speeds used.

A plentiful supply of primary electrons was ensured by inserting a capsule of radium bromide (~0.5 mg radium equivalent) in a hole drilled axially from the back of the upper electrode to within 1 mm of the sparking surface.

The time-base of the oscillograph was triggered at random while the voltage on the discharge gap was within 2% of the breakdown value, and the traces photographed. The use of higher sweep speeds than those reported below was precluded by, firstly, the limited writing speed of the oscillograph on single-shot operation, and, secondly, the reduced probability of recording a useful part of a pulse when triggering the time-base at random.

3.1.2 Results

Figure 12 shows a result typical of those obtained with the apparatus described above, under conditions where breakdown occurred in the region of uniform electric field. Current pulses in accord with the theory of Section 2 were recorded, with $\psi \approx 1$. (Compare the theoretical pulse shape of Figure 7; note that the total resistance in series with the gap comprised R3 of Figure 10 in series with R of Figure 11, i.e. a total of approximately 100 kΩ). Some of the recorded pulses overlap on the time scale on account of the strong irradiation employed. The start of each individual current pulse is accompanied by the occurrence of a light pulse, since it is at this instant (the electron transit) that excitation of the gas molecules occurs. The lengths of the individual current pulses are constant for a given gap length, while their heights vary statistically. Current pulses of large amplitude are accompanied by light pulses of large amplitude.

The order of magnitude of the avalanche carrier-numbers in Figure 12 can be estimated on the following basis. The positive ion transit time is ~12 μsec., and a current of the order of 1 μA flows for this period, so that the total charge carried by the positive ions is $\sim 12 \times 10^{-12}$ coulombs. If these

ions are singly charged, their number will be of the order of 10^8, and it is reasonable to take this as the order of magnitude of the carrier-number. (In an electronegative gas, the carrier-number of an avalanche is usually taken to mean the number of electrons, rather than the number of positive ions. The quantity calculated above is $\frac{\tau_+ I_{2+}}{\varepsilon}$, and, from equation (52)(page 56),

$$\frac{\tau_+ I_{2+}}{\varepsilon} = \frac{1}{1-f} e^{(\alpha-\eta)d}$$

$$= \frac{1}{1-f} n_-(d)$$

so it is necessary to multiply this quantity by (1-f) to obtain the correct carrier-number. This is not very significant if only the order of magnitude is required). In view of this large carrier-number, it may be that the pulses recorded here do not represent individual avalanches, but chains of avalanches produced by a photo-electric secondary mechanism, which would not be detected with the comparatively slow recording speeds used.

Using the same apparatus, the experiments described above were extended to gap lengths of up to 5 cm., i.e. into the region where breakdown no longer takes place between the flat surfaces of the electrodes, but between their curved edges, in

the region of non-uniform electric field. Figure 13 shows a result obtained under these conditions.

The current pulse shapes obtained in the experiments so far described are summarized in Figure 14. Type "a" is characteristic of uniform-field conditions; "b", non-uniform. In the 3 cm gap, less than 2% of the observed pulses were of the "b" type, and in the 4 cm gap a similar fraction of "a" type occurred - this last result, however, was later found to have been influenced by the proximity of the photomultiplier to the gap, the proportion of "a" type increasing when the photomultiplier was moved further away. The occurrence of pulses of type "b" in the 3 cm gap was probably also due to the proximity of the photomultiplier, since no pulses of this type were recorded in the experiments described in Section 4, below, where gaps of up to 3 cm were used.

The positive ion transit times indicated by the "a" type pulses are shown in Figure 14. The method of Section 2.1.1.5 was used, the time stated being that taken by the current to fall to one half of its "plateau" value - the effect of negative ion formation was, therefore, not taken into account, and this probably leads to an error of a few per cent. In Figure 15, these values are compared with transit times calculated on the arbitrary assumption of a positive ion mobility of 2.6 $cm^2\ sec^{-1}\ V^{-1}$,

i.e. of a positive ion drift velocity of 2.6 E cm sec^{-1} where E is the electric field strength in V cm^{-1}; the values of E were in the range $26 \leq E \leq 31$kV cm^{-1}.

The shape of the "b" type of pulse may be understood qualitatively if it is borne in mind that the vast majority of the positive ions are formed close to the anode, so that practically all cross the gap together; the instantaneous current which they produce in the external circuit will vary with their velocity, and hence with the field strength as they move across the gap. Since the field has a minimum value in the centre of the gap and is of maximum value at the electrodes, a current minimum would be expected to occur during the positive ion transit-time. This interpretation is supported by results obtained in the non-uniform electric field between spherical electrodes: Figure 16 shows results obtained with this geometry.

3.2 Records of Individual Current Pulses

The usefulness of the method described above, i.e. triggering the oscillograph time-base at random, is limited to the case of strongly irradiated gaps. In order to record current pulses in a discharge gap subject only to naturally occurring radiation, the apparatus of Figure 17 was set up. No arrangements were made to record light pulses in this case.

The high-voltage supply, discharge gap, and gap enclosure have been described in Section 3.1.1. Details of the electronic apparatus are as follows:

Cathode follower:	As in reference (3), of straightforward design, using the two halves of an ECC81 in parallel.
Trigger amplifier:	A1 amplifier of Cossor 1035 oscillograph, switched to a suitable range.
Delay line:	Approximately 400 yards of coaxial cable, with the ends of the braiding connected together by a short length of 16 swg copper wire.

Signal amplifier: A1 amplifier of Mullard L101 oscillograph, switched to a suitable range, cascaded with the pulse amplifier described in reference (3).

Oscillograph: Southern Instruments TR12 transient recorder.

The bandwidth of the signal amplifier was about 4 Mc/s so that the rise-time of the system was negligible for the sweep speeds used.

Results were obtained in 1, 2 and 3 cm gaps, a typical oscillogram being shown in Figure 18. As expected, individual current pulses were recorded, with none of the "overlapping" that was evident in the case of strongly irradiated gaps. The current pulse lengths observed in these experiments are in satisfactory agreement with those observed in the radium-irradiated gaps.

3.3 The Anode Glow

The rate of occurrence of light pulses in a highly stressed discharge gap may be increased by strong irradiation with radium, to such an extent that a faint glow in the region of the anode becomes visible to an observer in a suitably darkened room. This glow has been photographed by Tedford[1] in a 2 cm uniform-field gap in room air.

As part of the present work, the glow was photographed over a range of gap lengths, in order to observe any change as the gap length increased to values where breakdown occurred in the non-uniform field region. The gap was viewed obliquely, as shown in Figure 19.

The camera was fitted with a 4" silica lens of fixed aperture f/4.5; exposures of one minute were made on 5G91 film (Ilford), followed by development in ID11 (Ilford) for 10 minutes at 20°C.

The results obtained are shown in Figure 20, and indicate a disc-shaped region of luminosity at small gap lengths, giving way to a "halo" at 5 cm, with a transition region exemplified by the result obtained at 4 cm. These results are in accord with the view that the glow results from the passage of electron

avalanches, which occur only in the uniform-field region of the gap for spacings of 3 cm and less, and only in the non-uniform field region at 5 cm, but in both regions at 4 cm.

A further experiment indicated that the transition to a halo was complete at 4.2 cm. This last figure is not very meaningful, however, and would no doubt be changed slightly by different photographic processing.

3.4 Discussion

All of the above results are in accord with the view that the observed current and light pulses are produced by individual electron avalanches (or by groups of avalanches occurring practically simultaneously). The usefulness of any results obtained in room air is, however, necessarily limited by two factors: firstly, by the small range of experimental conditions that it is possible to cover; and secondly, by complete lack of control over the content of the experimental gas. In the present case, the usefulness of the results was also limited by the inability of the apparatus to record satisfactorily the rapidly rising electron components of the current pulses.

It was therefore decided to extend the work in an enclosed system, where different gases could be used, at pressures up to nearly atmospheric. To simplify the apparatus, only current pulses were recorded; and the pulse recording system was re-designed to allow detailed investigation of the electron components. Some of the results obtained in the enclosed system have been reported in references (46) and (47).

4. EXPERIMENTS IN AN ENCLOSED SYSTEM

4.1 Apparatus

4.1.1 The Experimental Vessel

The experiments described in this section were carried out with the discharge gap enclosed in the vessel shown in Figure 21. This consisted of a glass cylinder of approximately 30 cm diameter and 60 cm length, closed at the ends by a nickel-plated base plate and a Perspex top-piece. Neoprene L-gaskets formed the seals between the cylinder and its end-covers. A perforated metal screen, partly enclosing the vessel, served to reduce pick-up of electrical interference.

It was found necessary to treat all glass and Perspex surfaces with a water-repellant preparation; if this was not done, spurious pulses were observed. The preparation used was "Repelcoat", a 2% v/v solution of dichlorodimethylsilane in carbon tetrachloride.

The electrodes were of copper, of similar design to the brass electrodes used in the work described in Section 3, above. Electrode spacings of 1, 2 and 3 cm were used, and in all cases the pulse shapes observed were characteristic of uniform electric field conditions.

The lower electrode (the cathode in these experiments) was isolated from earth by a Perspex insulating support, and could be moved vertically by a micrometer arrangement operated through a simple vacuum seal; the micrometer scale was read through the perforations in the metal screen. A bare tinned copper wire connected the cathode to a lead-through terminal (not shown in Figure 21) on the base-plate, and thence to the series resistor, which was mounted in a screening enclosure on the lower side of the base-plate, together with a cathode follower (see Figure 24). The lower electrode assembly was fixed to the base-plate via over-size bolt holes, in order to allow sufficient horizontal movement for the electrodes to be aligned.

The upper electrode was supported by a Perspex structure screwed to the base-plate. This electrode could be tilted in order to make the sparking surfaces accurately parallel.

A telescopic gauge was used in initial adjustment of the electrodes, with the glass cylinder removed - subsequent changes in gap length were achieved by the micrometer arrangement mentioned, without disturbing the vessel.

4.1.2 The Vacuum System

Details of the apparatus used for evacuating the experimental vessel are given in Figure 22.

Using the rotary pump alone, the pressure (measured on the thermocouple gauge) could be reduced to below 10^{-2} mm Hg, while use of the diffusion pump brought the pressure in the vessel down to about 5×10^{-5} mm Hg (measured on the ion gauge).

To test the system, the pressure was reduced to about 10^{-2} mm Hg by means of the rotary pump, and the rate of rise of pressure measured after closing the tap "A". A rate of rise of less than 10^{-2} mm Hg per hour was achieved after running a glow discharge of 2 to 3 mA for about 30 minutes, at a pressure of a few mm Hg, with a dish containing phosphorous pentoxide inside the vessel. Removal of the Perspex parts from the vessel resulted in lower rates of pressure rise, suggesting that considerable outgassing of the Perspex was taking place. Outgassing by baking was not considered practicable.

In the majority of the experiments, the vessel was evacuated by means of the rotary pump alone, and in all cases the experimental work concluded within one hour of filling the vessel. Thus, the partial pressure of any impurities added to the

experimental gas as a result of the imperfections of the system would amount to less than 2×10^{-2} mm Hg; with the lowest gas pressures used, i.e. ~100 mm Hg, this represents an added impurity content of <0.02%. In some experiments with nitrogen where the diffusion pump was used in order to reduce the initial pressure to below 10^{-4} mm Hg, the results were indistinguishable from comparable results obtained using the rotary pump only.

4.1.3 The Gas System

The gas system is shown in Figure 23. Gas was admitted from a steel cylinder via a needle valve and about 30 inches of rubber vacuum tubing; the remainder of the system was constructed of glass, except for the metal stopcock S4. The glass tube was of 10 mm bore.

Flexible joints J1 to J5 were made with short pieces of rubber vacuum tubing pushed over the ends of the glass tube, and rendered vacuum-tight with Apiezon "Q" sealing compound. These joints enabled the humidifying solution to be changed or removed, and also protected the glassware from strain when adjustments were being carried out on the vessel. The remaining joints were of standard conical type, and were sealed with Apiezon "M" grease, as were the stopcocks S1 to S4.

The system could be evacuated back to the needle valve, which was made vacuum-tight by replacing the normal packing ring with a rubber O-ring.

The mercury manometer indicated the gas pressure to within $\pm$ 1 mm Hg. Since the lowest pressures used were not much less than 100 mm Hg, it is considered that the pressure measurement was accurate to better than $\pm$ 1% under all conditions. All pressure readings were reduced to equivalent values at 20°C.

The cold trap, containing solid carbon dioxide and alcohol, was maintained at a temperature below -65°C during pumping and experiments. Its purpose was to minimize the quantity of mercury vapour entering the vessel from the manometer. Pieces of zinc sheet were placed inside the cold trap for the purpose of trapping mercury which would otherwise vaporise when the trap became warm, as it did overnight. Stopcock S2 was closed when the apparatus was not in use.

The drying column was packed with Molecular Sieve, type 5A; this is a dehydrated crystalline zeolite which is claimed to have excellent water-absorbing properties.

In the experiments in nitrogen and dry air, no humidifying solution was used - the flask shown in Figure 23 was empty in those cases - and a dish containing phosphorous pentoxide was kept inside the vessel; it was found that this collected considerable amounts of water, presumably desorbed from the Perspex. It was necessary to change the phosphorous pentoxide once per week, and this, of course, involved letting atmospheric air into the vessel. After this had been done, the system was flushed at least four times with the experimental gas.

For the humid air experiments, the humidifying solution used was a saturated solution of potassium hydroxide with excess

solid present. This should maintain the relative humidity of the air entering the vessel at 86%. A further quantity of the same humidifying solution was placed in a dish inside the vessel itself. (The phosphorous pentoxide kept in the vessel during the experiments in dry gases was, of course, removed). The drying column, in this case, served to prevent migration of water vapour from the humidifying solution to the cold trap, where it would have frozen and blocked the system.

The cylinder nitrogen used was of the "oxygen-free" grade, and its composition was stated by the suppliers to be as follows:

Nitrogen	>99.9%
Oxygen	<10 V.P.M.
Carbon dioxide	<20 V.P.M.
Carbon monoxide	NIL
Other carbon compounds	<5 V.P.M.
Hydrogen	<20 V.P.M. (usually NIL)
Neon	~600 V.P.M.
Helium	~160 V.P.M.
Argon	probably <50 V.P.M.

The cylinder air used was stated to be free from carbon dioxide.

4.1.4 The Pulse Recording Apparatus

A block diagram of the apparatus used to record the pulses in these experiments is given in Figure 24.

The high-voltage supply was that shown in Figure 10. The purpose of the additional 0.5 MΩ resistor and 5000 pF capacitor was to minimize the effects of inadvertent breakdown of the experimental gas; such breakdown did occur occasionally in the present work, and appears to have had no effect on the measurements. The gap voltage was measured with an accuracy of better than $\pm$ 1%, so that, with an error in pressure measurement of $< \pm$ 1% (see Section 4.1.3, above), the total error in $\frac{E}{p}$ is considered to be less than $\pm$ 2% in all the measurements reported below.

The pulse recording system was essentially similar to that of Figure 17, but used different apparatus in order to achieve increased sensitivity and bandwidth.

Figure 25 shows the circuit diagram of the cathode follower and signal amplifier. The cathode follower was of simple design, using the two halves of an ECC81 in parallel. The delay line consisted of approximately 200 yards of coaxial cable, terminated in a 75Ω resistor at the pre-amplifier end - this

resistor provided a matched termination for the cable and was also the cathode follower load. The signal amplifier had two identical stages, each consisting of an amplifier (EF91) plus cathode follower (half of ECC81). The anode loads of the EF91's contained inductance, adjusted experimentally for minimum rise-time with no overshoot, using an input pulse with 1 mμsec rise-time. Two separate ECC81's were used in the amplifier to avoid the risk of instability resulting from the use of two valves in the same envelope. Power supplies to the cathode follower and signal amplifier were obtained from batteries, to avoid possible trouble with hum and smoothing. The measured voltage gain of cathode follower plus signal amplifier was approximately 8 times, and the measured rise-time about 25 mμsec.

For the trigger amplifier, the A1 amplifier of a Mullard L101 oscillograph was used.

The oscillograph was a Tektronix 541A, with plug-in pre-amplifier type 53/54L.

An overall sensitivity of 0.6 mV/cm was obtained, with a rise-time of 0.03 μsec. Pick-up of extraneous signals was found to set a limit to the sensitivity that could usefully be employed.

The value of the gap series resistor R was adjusted to give current pulses of balanced form. Carrier-numbers (designated "n" in the Figures showing oscillograms) were estimated as described in Section 3.1.2 (p.87).

A capsule of radium bromide (0.46 mg Ra equivalent) was mounted on the outside of the perforated metal screen shown in Figure 21, i.e. approximately 12 cm from the axis of the gap, in order to provide pulses of useful amplitude at intervals of the order of one second.

4.2 Results in Nitrogen

Figure 26 shows an oscillogram of a current pulse of "balanced" form, observed in nitrogen. (Compare Figure 2, showing calculated pulse shape).

The method of Section 2.1.1.5, above, was used to obtain values of positive ion transit time, and hence drift velocity: the values obtained in any one set of measurements at a given pressure and gap length were consistent to within $\pm$ 2% of the average, this difference being attributable to experimental inaccuracy. (This was also the case in dry and humid air). The values of drift velocity are plotted in Figure 27 as a function of $\frac{E}{p}$. A different curve was obtained for each gap length, that for 3 cm agreeing well with the results reported by Frommhold[40] using a 3 cm gap. The constant-pressure lines of Figure 27 illustrate how this dependence of measured drift velocity on gap length may be interpreted as a dependence on pressure as well as on $\frac{E}{p}$. (Since it was necessary to work at voltages close to breakdown value to obtain pulses of useful amplitude, it was not practical to change the pressure at a fixed value of $\frac{E}{p}$ without also altering gap length). Further data is required to ascertain whether the differences do in fact result from a pressure effect.

The electron components of some typical current pulses are shown in Figure 28: their duration is longer than would be expected on the basis of an electron drift velocity of the order of 10^7 cm sec^{-1}, and the individual pulses show variations in the waveform, as well as the duration, of the electron component. The rise-times of some of these pulses were measured (from 0 to 90% of final amplitude), and gave the distribution shown in Figure 29. Due to the rather high noise level, measurements on the electron components in nitrogen could be carried out accurately only at the highest pd values, where the largest pulses occur: it is for this reason that results are not given over a range of experimental conditions.

The above results were obtained using voltages 0.5% to 1% below the breakdown value. When the voltage was increased to within about 0.2% of breakdown value, current pulses of the form shown in Figure 30 were recorded. Vogel and Raether[7] have found similar pulses and interpret them as evidence of the occurrence of photo-electric secondary process - secondary avalanches are produced in a time interval short in comparison with the positive ion transit time and the summation of the resulting pulses of statistically varying amplitude causes the irregular pulse structure observed. No evidence was found in

the present work for the occurrence of a secondary process involving positive ions, although Vogel and Raether detected such a process in their experiments in nitrogen[7].

4.3 Results in Dry Air

Figure 31 shows a typical current pulse of balanced form recorded in dry air, where a negative ion component is in evidence. (Compare the theoretical current pulse shape, Figure 7). The beginning of the negative ion component is marked by an abrupt change of slope at the end of the electron component: this is seen more clearly in the oscillogram of Figure 32, where it will also be noted that the duration of the electron component is of the same order of magnitude as in the case of nitrogen.

Measurement of positive ion transit time, according to equation (58), requires a knowledge of $f = \eta/\alpha$. For the present measurements, the values of η and α given by Prasad and Craggs[13] were used, and the resulting positive ion drift velocities are plotted in Figure 33. The results obtained at different gap lengths are less clearly spaced than in the case of nitrogen, and again there is agreement with Frommhold's results[40].

Measurements of pulse rise-times (0 to 90% of final electron component amplitude) indicate considerable variations under fixed conditions of gas pressure and gap length (see Figures 34 and 35). Mean rise-time was found to be roughly proportional to gap length, and Figure 36 shows values of the ratio (mean rise-time)/(gap length) as a function of $\frac{E}{p}$.

The oscillograms of Figure 34 show how the presence of noise makes it difficult to estimate accurately the end of the electron transit time, and thus the value of $\psi = \frac{I_{2+}}{I_{2-}}$ which may therefore appear to vary from one pulse to another under fixed conditions. This difficulty is greater in the case of gases which form negative ions than in those which do not.

An attempt was made to measure $f = \eta/\alpha$ from the observed pulses, using equation (59), i.e. assuming that the drift velocities of the positive and negative ions are equal. At any one condition of gas pressure and gap length, the measured values showed large and apparently random variations from one pulse to the next: the results are shown in Figure 37, where the vertical lines represent the range of scatter, and the points indicate mean values. (Where the presence of noise on the oscillograms caused ψ to appear to vary randomly between pulses, it made no significant difference to this result whether $\frac{\hat{I}_2}{I_{2-}}$ or $\frac{\hat{I}_2}{I_{2+}}$ was measured).

The use of gap voltages within about 0.2% of breakdown value led to a distorted pulse shape, with considerable variations between individual pulses recorded under the same conditions; Figure 38 shows typical oscillograms. This behaviour is similar to that observed in nitrogen (Figure 30) and can again be

interpreted as the result of a photo-electric secondary process. As in nitrogen, no evidence was found for the occurrence of a secondary process involving positive ions.

4.4 Results in Humid Air

The current pulses recorded in humid air, when viewed on a slow time-base, are of the same general form as in dry air. (Figure 31).

In measurements of positive ion drift velocity (equation (58)), the α and η values of Prasad and Craggs[15] were used. Figure 39 shows the results, along with Frommhold's results in dry air, repeated here to facilitate comparison with Figure 33. The proportion of water vapour present varied from about 2% at the highest total pressures (lowest $\frac{E}{p}$ values) to about 20% at the lowest pressures (highest $\frac{E}{p}$ values): this variation may be expected to bring about a dependence of drift velocity on total pressure as well as on $\frac{E}{p}$, so that an apparent dependence on gap length would result, as in the case of nitrogen. Figure 39 shows that the measured drift velocities do in fact appear to be lower at longer gap lengths. Some of the scatter in the results may be due to the fact that the temperature varied between the limits of 18 to 22°C during the experiments, with consequent variation in water vapour pressure. The results for $\frac{E}{p} > 40$ V cm^{-1} (mm Hg)$^{-1}$ depend on the extrapolation of Prasad and Craggs' results for α and η beyond the range of their measurements.

The electron components of the pulses observed in humid air differ considerably from those in nitrogen and dry air: their duration is shorter, and they do not show marked variations from one pulse to the next. A typical oscillogram is shown in Figure 40. With increased gap voltage oscillograms of the type shown in Figure 41 occur, and can be interpreted as the result of secondary avalanche production by a photo-electric process. Using oscillograms of this form, it is possible to estimate the transit-time of electrons across the gap as the interval between the start of one avalanche and the start of the succeeding avalanche in the "chain". Values of electron drift velocity obtained from such measurements are shown in Figure 42, and are in good agreement with values extrapolated from the results of Nielsen and Bradbury[49], obtained in dry air for $\frac{E}{p} < 22$ V cm^{-1} (mm Hg)$^{-1}$. Variations in the measured transit time (see Figure 43) are attributable to experimental error.

As in dry air, an attempt was made to measure the ratio η/α from the observed pulses, but random variations were again found from one pulse to the next, and the range of measured values was approximately the same as in dry air.

When the voltage across the discharge gap was increased above the values used in the experiments just described, longer

chains of photo-electric secondary avalanches were recorded, the electron components of the pulses taking the form illustrated in Figure 44. These oscillograms are virtually free from noise, on account of the very much increased pulse amplitude (made possible by the low value of secondary coefficient that obtains in humid air[15]): the irregular structure of the current growth is entirely due to the statistical nature of the process. The effective rise-times of the pulses are now comparable with those measured in nitrogen and dry air, and the electron components show the same kind of random variations in form and duration (see Figure 45). Under these conditions, the pulses do not appear to be distorted when viewed on a time-base sufficiently slow to show the whole of the positive ion transit. As in nitrogen and dry air, severe distortion of the pulse shape occurs when the gap voltage is raised to within about 0.2% of breakdown value; this is shown in Figure 46. Pulses of this form were observed in all three gases at pd values up to the maximum of ~2100 mm Hg cm, indicating the occurrence of a considerable photo-electric secondary effect, while no other kind of secondary process was detected in any of the present experiments.

4.5 Discussion

The interpretation of the anomalously long rise-times of the current pulses observed here and in other work[8][40] requires comment.

In the present results, the extended rise-times in nitrogen and dry air were accompanied by variations in the form and duration of the electron components, and similar variations were observed in humid air when the pulses were clearly the results of chains of photo-electric secondary avalanches. On this basis, it is reasonable to suppose that the pulses here observed in nitrogen and dry air each represented many individual avalanches. In humid air, the reduced value of γ[15] would allow individual avalanches to grow to a detectable magnitude without the intervention of a secondary process.

As has been mentioned above (Section 1.4), experiments carried out by Frommhold[40] and Dibbern[26] indicate a normal rate of avalanche growth in nitrogen, and lend support to the suggestion that Vogel[8] did not observe individual avalanches in nitrogen, but chains of photo-electric secondaries. If this is so, it seems likely that the effect of adding methane to the experimental gas was in this case simply to reduce γ[24] and thus allow individual avalanches to be detected. On the other

hand, it seems unlikely that statistical variations in the number of secondary avalanches per pulse would allow a consistency of $\pm$ 5% in measured rise-time, as reported by Vogel.

In the case of dry air, both Vogel[8] and Frommhold[40] report an extended rise-time, but without the large variations recorded in the present work. This discrepancy may be explained if it is assumed that: (i) the nominally dry air used in the present experiments was not in fact completely dry, and (ii) that the processes resulting in the extended rise-time are in some way "quenched" by the addition of a very small quantity of water vapour, as they are by the addition of methane[8] - it would then be reasonable to interpret the pulses recorded here as the results of chains of avalanches, each individual avalanche having a "normal" electron component. The first of the above two assumptions is supported by the fact that the phosphorous pentoxide placed inside the vessel absorbed water over a period of a few days (Section 4.1.3, above). The second assumption is given some support by the fact that in humid air photo-electric secondary avalanches occur at an interval closely comparable with the expected electron transit time (Section 4.4 and reference (17)), indicating that the extended rise-time does not occur in the presence of comparatively large quantities of water vapour. Further experimental work is necessary to determine how small a quantity

of water vapour is effective in bringing about the reduced rise-time.

It is clear that in the interpretation of results of this kind, a knowledge of γ accurate to at least an order of magnitude is important, since this determines the mean size of individual avalanches. As γ is likely to be markedly dependent on the state of the cathode surface, and possibly on small quantities of impurities in the gas, it would be of advantage to measure γ, e.g. by the method of Section 1.1.3, in the same apparatus as used for the pulse experiments, under, as nearly as possible, the same conditions.

Attempts to measure η/α from the current pulses gave unsatisfactory results, in both dry and humid air. These measurements may have been affected by the occurrence of a detachment process[17][18], but this would not explain the large degree of scatter in the results. Some of this scatter - but certainly not all - is due to noise on the oscillograms, which will have to be reduced in future work.

5. CONCLUSIONS

It is clear from the results of the present work, and of other work, described above, that observation of the current and light pulses produced by electron avalanches provides a useful method of investigating the processes that occur in a discharge gap prior to breakdown, and can be useful in identifying the secondary mechanisms involved in the breakdown process itself, as well as yielding numerical data on such quantities as electron and positive ion drift velocities: such observations have here been made, using gas pressures up to nearly atmospheric, with voltages close to breakdown value, for gap lengths of the order of centimetres - conditions which are of considerable technological interest. There appears to be no reason why these experiments should not be capable of extension to higher gas pressures and longer gap lengths, i.e. to cover breakdown at higher voltages than those used in the present work; an extension of the existing theory of current pulse shape has shown that the effects of inductance, which is likely to be greater in systems using higher voltages, will generally lead to negligible error.

The results of Sections 3 and 4, above, are in accord with the view that each pulse is the result of either an individual electron avalanche or of a "chain" of avalanches generated in rapid succession by a photo-electric secondary

mechanism. In the case of humid air, pulses have been recorded which clearly result from individual electron avalanches, while the results obtained in nitrogen and dry air suggest chains of avalanches. If this interpretation is accepted, then the present results in dry air are not in accord with results obtained by Frommhold[40]; this may be due to the presence of a small quantity of water vapour in the nominally dry air used here.

The values of positive ion drift velocity measured in nitrogen show what might be interpreted as a pressure effect, but it is not clear if this is the correct interpretation. In dry air, any such effect is comparatively slight, and, if anything, in the opposite sense. Measured positive ion drift velocities in humid air (~86% relative humidity) are lower than in dry air, by up to about 20% for the same value of $\frac{E}{p}$.

A photo-electric secondary process has been identified in nitrogen, dry air, and humid air. Secondary avalanches initiated by positive ion bombardment of the cathode did not occur in any of the present experiments.

The effect of a decreased value of secondary ionization coefficient in humid air was evident from the increased amplitude of the pulses.

Measured values of η/α from the pulses observed in dry and humid air are unsatisfactory.

The usefulness of the present results was limited by the presence of noise on the oscillograms, due mainly to pick-up of external interference: it is important to provide more effective screening against such interference in future experiments.

6. RECOMMENDATIONS FOR FURTHER WORK

The need for more effective screening against external interference has already been mentioned on the preceding page.

In order to clarify the discrepancies that exist between the present results and those reported by Vogel[8] and Frommhold[40], with reference to the rise-times of the current pulses, it is important to carry out experiments which will detect individual avalanches with certainty. This will require efficient screening from electrical interference, and probably also the use of a low-noise pre-amplifier. The problem may be simplified somewhat by the choice of a cathode material which will give a lower secondary coefficient, and hence larger individual primary avalanches. It may be necessary to "trigger" large numbers of primary avalanches simultaneously, for example by the radiation from a spark in an auxilliary gap, or by α-particle irradiation (e.g. from polonium).

It would also be useful to carry out measurements of the d.c. gas-amplified current, and obtain values of γ from $\log_e i$, d curves. This would give a useful indication of the average size of avalanche likely to occur in a given condition.

It is important to be sure of the dryness of the gases in future experiments, particularly in the case of dry air, where it appears from the present work that a small proportion of water vapour may have a drastic effect on the rate of avalanche growth. Since outgassing of the Perspex was suspected to take place in the present work, it is suggested that an alternative material should be used. Outgassing of the system by baking would probably be of considerable advantage.

Perhaps the most important feature of experiments of this type is that they appear to be capable of extension to the cases of higher gas pressures and longer gaps.

PART II

MEASUREMENT OF INITIAL IONIZATION CURRENTS WITH RADIUM IRRADIATION

1. INTRODUCTION

The purpose of this part of the work was to obtain information on the factors affecting the intensity of ionization produced in a discharge gap by a capsule of radium bromide enclosed in the anode, approximately 1 mm behind the sparking surface, as in some of the experiments described in Section 3 of Part I, above. To this end, measurements were made of initial ionization current, i.e. the current flowing in the gap with an applied voltage sufficiently high to ensure collection of all the free charge-carriers produced in the gap, but not high enough to allow further ionization by collision of these charge-carriers with neutral molecules.

When a capsule containing radium is enclosed in an electrode as in the present experiments, it is reasonable to assume that the α-radiation from the radium is completely absorbed in the metal surrounding it, and thus has no effect on the gas in the gap. It is therefore necessary to consider the effects of β and γ radiations only. When these pass through solids, they produce considerable secondary radiation; this was discovered fairly early in the study of radioactivity, and some of the results of the early experiments will now be summarised.

1.1 Early Experiments on Secondary Radiation

Experiments were carried out by Eve[50], in which the β and γ radiations from radium were allowed to fall on samples of different materials, and the ionizing power of the secondary radiations from these materials measured in terms of the rate of discharge of a suitably placed electroscope, a thick lead screen shielding the electroscope from the direct radiation from the radium. Using both solid and liquid materials, Eve found that the ionizing power of the secondary radiation from the various materials followed roughly the same order as their densities. Measurements using solid plates of different thicknesses indicated that the secondary radiation came not merely from the surface of the radiating material, but from a total depth ranging from about 1.5 mm for lead to about 3 mm for glass, aluminium, or paper. As would be expected in view of this result, the state of the surface was found to be unimportant.

McClelland[51] carried out measurements somewhat similar to those of Eve, but used an arrangement of lead screens around the radium in an attempt to produce a well-defined pencil of β and γ radiation. Instead of an electroscope, an ionization chamber connected to an electrometer was used to measure the ionizing power of the secondary radiations; the position of the

ionization chamber could be varied in order to measure the secondary radiation emitted at different angles to the radiating surface. The results obtained by McClelland are in general agreement with those of Eve. In addition, it was shown by magnetic deflection of the secondary rays that these consisted of electrons, some having greater energy than the most energetic of the primary β-particles: no γ-rays were detected in the secondary radiation. The measured ionizing power of the secondary radiations depended on the angle at which the primary radiation fell on the test-piece and also on the angle at which the measured secondary radiation came off. Allowing the primary radiation to fall normally on to the material under test, and measuring the secondary radiation coming off at different angles, McClelland was able to compute an integrated ionizing power for the total secondary radiation, and gives values of the ratio p of this integrated ionizing power to the ionizing power of the primary radiation, for a number of chemical elements[52]. When the elements tested were arranged in order according to their p-values, they fell into well-defined groups, these being the groups of the periodic table[52].

This grouping is in accord with the idea that the intensity of the secondary radiation from a particular element depends not only upon the number of electrons in each atom of the element but also upon the energy with which they are bound: such

a dependence would lead to a discontinuous variation in secondary radiation at the boundary of each group of the periodic table.

A similar grouping of the elements was reported by Kleeman[53], with some minor differences in the curves of ionizing power of secondary radiation against atomic weight of the radiating substance. Kleeman's experiments were intended to measure the effect of primary γ radiation only, but Hackett[54] points out that the primary radiation must have contained considerable numbers of β-particles, produced as secondaries when the γ-rays passed through the aluminium side of Kleeman's ionization chamber.

Hackett[54] investigated the effects of γ radiation alone by measuring the ionizing power of the secondary radiation from the upper surface of the material under test when the primary radiations fell on the lower surface - in this way, the primary β radiation was completely absorbed and the radiation measured was produced solely by the more penetrating γ-rays. It was found that the ionizing power of the secondary radiation was practically the same for all elements of atomic weight less than 150, but showed a marked increase for lead and other elements of the same period, and a second marked increase for uranium (the only element of that period investigated).

Crowther[55] carried out experiments to investigate the possible existence of a fatigue effect in a lead plate exposed to radium radiations, as is found with ultra-violet or X-radiation, and now considered to be due to chemical action involving the gases occluded by the metal surface[56]. He found that no diminution occurred in the amount of secondary radiation given out by the metal under the action of the radium radiation itself, although the emission from the plate under the action of ultra-violet or X-radiation was altered by exposure to the radium radiation. Apparently random day-to-day fluctuations of up to 5% in the ionizing power of the secondary radiation with radium were recorded, and Crowther suggests that these may be the result of a humidity effect; humidity was not recorded in his experiments.

1.2 The Mechanism of Discharge Gap Irradiation with Radium

With the radium enclosed in the anode of a discharge gap, β and γ rays will emanate from the anode, most of the β rays being secondaries. Some ionization of the gas will occur as a result of the passage of the β radiation, while direct ionization by the γ rays is likely to be negligible. A fraction of the radiation from the anode will reach the cathode, and there produce further secondary radiation, and hence ionization of the gas, by a similar mechanism[57][58].

Thus, ionization of the gas is brought about by secondary β-radiation, partly from the anode and partly from the cathode. For a fixed radium quantity in a given anode, one would expect the contribution from the anode to be constant, while that from the cathode would be greatest at small gap lengths: with increasing gap length, however, the increased volume of gas available for ionization would tend to make the measured ionization current greater. The effect of changing the cathode material would be most marked in short gaps, and at a fixed gap length would presumably be in accord with McClelland's p-values[52] for the materials used.

Further, from Crowther's work[55], already mentioned, one would expect no fatigue effect, but perhaps a humidity effect or random variations of a few per cent from day to day.

As will be seen, the present results are not entirely in accord with this view, particularly in regard to the effect of different cathode materials.

1.3 Hardy's Initial Ionization Current Measurements with Radium

Initial ionization currents in discharge gaps irradiated with radium have been measured by Hardy[57][58]. The measured current was found to increase with gap length, and no fatigue effect was observed. When different radium quantities were used, the measured current was not proportional to the quantity, but this may be because Hardy used nominal rather than accurate values of radium quantity. (Proportionality between quantity of radioactive material and measured current forms the basis of the use of the ionization chamber for comparative measurements of radioactivity). No dependence of initial ionization current on cathode material was found; the relevant details are given fully in reference (57). The cathode materials used were zinc, magnesium, tin, copper, steel and brass. Only magnesium was different from the others, giving "anomalously low" values of current at small gap lengths (0.1 inch); in some cases the currents measured with a magnesium cathode were apparently negative - a result which Hardy ascribes to zero drift in his measuring apparatus, or to the slight rise in potential of the cathode with respect to the earthed guard-ring closely surrounding it. The present measurements were designed to eliminate both of these possible sources of error.

2. THE PRESENT MEASUREMENTS

In the measurements reported below, initial ionization currents were measured in discharge gaps similar to those used in most of the experiments of Part I, above, i.e. using 100 kV electrodes of the Stephenson profile, between which breakdown takes place in the region of uniform electric field for gap lengths of up to approximately 3.8 cm. Capsules of radium bromide, up to three in number, were situated within the brass anode, in holes drilled to within ~1mm of the sparking surface, and close to the axis of the gap. The guard-ring electrode of Figure 47 was used to measure separately the components of initial ionization current flowing in the uniform-field and non-uniform field regions of the gap. Further measurements employed solid cathodes of carbon, magnesium, aluminium, copper, brass, mild steel and lead.

The measurements were carried out in room air.

2.1 Apparatus

The measurements depended upon passing the current to be measured through a resistor of high value, and measuring the voltage developed across it. A null method of voltage measurement was used, since this made it possible to arrange that the earthy electrode of the discharge gap (or the appropriate part of this electrode, in the guard-ring arrangement) was at earth potential during the measurement.

At first, a Lindemann electrometer was used as the null detector, but greater sensitivity was required than could be achieved conveniently with this instrument. Sensitivity can, of course, be improved by increasing the value of the measuring resistor, but with the high resistance values involved the time-constant of the circuit formed by the measuring resistor and stray capacitance may become troublesome - for example, with a resistor of $10^{11}\Omega$ and a stray capacitance of 10 pF this time-constant is one second, and this is about the maximum that can be used conveniently. If the current is of the order of 10^{-12} amperes, then, in order to measure it to within 1%, the null detector must be capable of detecting a voltage of 1 mV.

For the measurements reported below, the circuit of Figure 48 was used. The gap voltage was provided by a 120V dry

battery; increasing this voltage by a factor of seven was found to produce an increase of less than 1% in the measured initial ionization current at all gap lengths used. R1 served to limit the current in case of an accidental short-circuit. Switch S selected the measuring resistor, which was either (position 2) $10^{11}\Omega$ or (position 3) $10^{10}\Omega$ in parallel with $10^{11}\Omega$. The voltage developed across this measuring resistor was in series opposition with the voltage across the lower arm of a calibrated d.c. potentiometer R4: the double electrometer tetrode BDM10, in conjunction with R5, R6 and galvanometer G, formed a null detector. R7 was a sensitivity control for the galvanometer G.

The apparatus was operated in the following manner. The d.c. potentiometer R4 was first standardized in the usual way against a standard cell (not shown in Figure 48), and R5 was adjusted for zero galvanometer deflection with switch S in position 1. The switch was then turned to position 2 or 3 to select the required measuring resistor, and potentiometer R4 adjusted to return the galvanometer reading to zero, R7 being used to avoid overloading of the galvanometer during this procedure. After the reading on R4 had been noted, the switch S was returned to position 1 to check that the zero of the null detector had not drifted, and the calibration of R4 was checked against the standard cell. If either of these checks was unsatisfactory, the measurement was repeated.

Although the method does not require long-term stability of the null detector, it was found that the drift after several hours of operation could be kept to the equivalent of a few millivolts at the input by observing the precautions usual with such circuits, viz. deriving the power supplies from large accumulators with clean terminals, and turning the apparatus on at least an hour before attempting to take a measurement. The screening indicated in Figure 48 served not only to prevent spurious pick-up on the high-impedance section of the circuit, but also to exclude dust from the discharge gap, switch S, and the measuring resistors. The gap enclosure was of aluminium, fifteen inches square by twenty-four inches high.

2.2 Accuracy of the Measurements

Comparative Accuracy

The comparative accuracy of the present measurements depends primarily on the following factors:

(i) The sensitivity of the null detector.

(ii) Random variations in the value of the measuring resistor.

(iii) Uncertainty in the ratio between the two effective values of measuring resistor (when comparing currents measured on different ranges).

(iv) Variations in the condition of the gas (room air).

The null detector was sufficiently sensitive to introduce negligible error, but accuracy was limited by random variations which were found to occur in the measured current: over a period of the order of a minute, the current varied, apparently randomly, by up to about $\pm$ 0.5% of its mean value. It is considered that the error introduced in this way was always less than 0.5%.

The value of the measuring resistor varies with temperature and applied voltage. The components used here were "Megistors" for which the following data was quoted by the manufacturers:

Temperature coefficient	$<0.3\%$ per °C
Voltage coefficient	$<0.3\%$ per volt

In the course of the measurements, temperatures varied from 18°C to 22°C, and the voltage across the measuring resistor from ~0.1V to ~1.5V. The total error introduced by these effects should therefore be less than $\pm$ 0.8%.

The ratio between the effective values of measuring resistor on the two ranges was estimated by measuring a number of currents of suitable value on both ranges in turn. In fifteen such measurements, with different values of current, the values obtained for this ratio varied from 11.10 to 11.22, with a mean value of 11.14. The uncertainty in this value is not greater than $\pm$ 0.5%.

Variations in the condition of the gas were taken into account by assuming that the measured current is proportional to gas density: on this basis, all results have been reduced to 20°C and 760 mm Hg.

When a high order of accuracy is required in measurements of this kind, it is essential that the position of the radium capsules in the anode be accurately maintained; for this reason the capsules were placed in individual holes in which they were a loose sliding fit, rather than simply being dropped into a single

conveniently oversize hole. It is considered that removal and subsequent replacement of the radium capsules caused negligible difference in the current.

In total, then, the overall comparative accuracy of the present measurements is considered to be better than $\pm$ 2%.

Absolute Accuracy

The absolute accuracy of the results is found by adding the tolerance on the measuring resistors ($\pm$ 10%) to the comparative accuracy given above. Thus, the absolute accuracy is better than $\pm$ 12%.

2.3 Results

A preliminary series of measurements was carried out to determine what degree of repeatability could be expected. Results obtained with an aluminium cathode are shown in Figure 49, and display apparently random day-to-day variations of up to $\pm$ ~8% of the mean value; the other cathode materials gave similar variations. During the period when these measurements were made, the gap enclosure was not opened.

To test for a possible humidity effect, ionization currents were measured with the gap mounted in the large enclosure used for the pulse experiments in room air (Section 3.1.1, Part I). Brass electrodes were used, and the humidity inside the box was raised by the use of a simple humidifier, and measured with a hair hygrometer. In one experiment, the relative humidity was raised from 40% to 70%, and a change of less than 2% in measured current was recorded. A repeat of this experiment, raising relative humidity from 38% to 60%, gave a similar result. It appears, then, that the fluctuations of Figure 49 cannot be the result of a humidity effect.

Figure 50 shows results obtained using the guard-ring electrode as cathode. Two series of measurements were made, one with the radium in the anode, and the other with the radium in the

cathode, at nominally the same depth behind the sparking surface, and at the same (small) distance from the axis in both cases. As Figure 50 shows, the total current was ~2% lower with the radium in the cathode, perhaps due to the radium capsule's not being at precisely the same depth behind the sparking surface in the two different electrodes: in spite of this, the currentto the inner portion of the guard-ring electrode was greater in this case, by ~3% in the shortest gaps and ~10% in the longest. (Note that these electrodes are most likely to be used at spacings of less than 3.8 cm, where breakdown occurs in the uniform-field region of the gap). Figure 51 shows the fraction of total initial ionization current that flows to the inner portion of the guard-ring electrode, and therefore in the substantially uniform-field region of the gap. The surface area of this inner portion is 12% of the projected area of the whole electrode. In the experiments with the guard-ring electrode, it was found that day-to-day variations in the current to the inner portion were considerably less than those in the total current: thus, in a series of measurements with a 2 cm gap, a variation of 9% in the total current was accompanied by a variation of less than 1% in the current to the inner portion - this latter variation may be entirely due to experimental inaccuracy.

Results obtained with different quantities of radium in the anode indicate that the initial ionization current is

proportional to this quantity. Figure 52 shows the values of current measured on the inner portion of the guard-ring electrode; similar results were obtained by measuring the current to the outer part of this electrode, and also in the case of a solid brass cathode.

Measured values of initial ionization current with different cathode materials are compared in Figures 53 and 54. Each point represents the mean of 3 to 12 measurements, made on different days so that the effects of random day-to-day variations have been averaged out. As a check, some of the measurements were repeated with a larger quantity of radium, giving the results shown in Figures 55 and 56. Values of i_o obtained with a brass cathode were virtually identical with those for the copper cathode. In the present case, no anomalous effect was found with the magnesium cathode, as in Hardy's work[57].

3. CONCLUSIONS

Considerable day-to-day variations occur in the initial ionization currents measured using solid electrodes: when, however, the cathode is divided into two separate parts, the component of current measured in the uniform-field region of the gap displays variations no larger than those attributable to experimental error. It follows from this latter result that these variations are likely to be of no consequence in experiments where the radium is required to irradiate only the uniform-field region of the gap. The variations occurring with solid electrodes are perhaps to be identified with the day-to-day variations reported in Crowther's work[55]. In the present case at least, they do not result from a humidity effect.

Results obtained with the guard-ring cathode indicate the error that would be introduced if the component of initial ionization current flowing in the uniform-field region of the gap were estimated from the total simply by multiplying by the ratio (surface area of flat inner portion of cathode)/(total projected area). In the present case, the estimated current would be too low by a factor of ~ 1.6, the exact value depending on gap length: the error is greatest for small gaps. (These electrodes are most likely to be used with gap lengths of $\lesssim 3.8$ cm, where breakdown is confined to the uniform-field region).

The variation of initial ionization current resulting from the use of different cathode materials is only a few per cent, except for lead, and this factor is not likely to influence the choice of cathode material in any practical application, the advantage of increased ionization with lead being offset by the difficulty of working this material satisfactorily. The variation of initial ionization current with cathode material is not the same at all gap lengths. The mechanism is probably more complicated than indicated in Section 1.2, above; and the following, purely tentative, explanation may be put forward. For gaps longer than 2 cm, all materials gave very similar results, with the exception of lead, for which the ionization was considerably greater. On the basis of Hackett's results[54], this would be expected if the radiation on the cathode were wholly γ radiation: thus it may be supposed that the secondary β radiation from the anode is severely attenuated in traversing 2 cm in air. In gaps considerably shorter than 2 cm, this β radiation is presumably the major factor in determining the amount of secondary radiation produced at the cathode, leading to an entirely different kind of behaviour.

4. RECOMMENDATIONS FOR FURTHER WORK

It would be of interest to investigate the cause of the random day-to-day variations that have been found in the initial ionization currents measured with solid electrodes.

One approach to this problem would be to find if such variations occur in the initial ionization currents measured using thoroughly outgassed electrodes in an inert gas atmosphere: if, as seems likely, they do not, it would remain to be determined whether the variations in the present measurements result from changes in the content of the atmospheric air, or from chemical changes at the electrode surfaces - it may be difficult to separate these effects experimentally. The results above have shown that the random variations in the current to the inner part of the electrodes are significantly less than for the outer part, and it is difficult to see how variations in the gas content could lead to this kind of behaviour. If it is assumed that the state of the anode surface influences the angular distribution of the emergent radiation, it is conceivable that such a behaviour could result. This angular distribution could be measured by means of a counter. It would be useful to be able to distinguish between β and γ radiation, as a similar experiment would then throw light on the feasibility of the tentative explanation proposed above for the variation of initial ionization current with cathode material.

ACKNOWLEDGEMENTS

The author wishes to express his gratitude to Professor F. M. Bruce for his encouragement and guidance throughout this work.

Thanks are due also to other members of the Electrical Engineering Department of the Royal College of Science and Technology, especially to Dr. J. E. Matthews for much valuable guidance, and to Dr. D. J. Tedford for many hours of useful discussion and practical assistance, as well as to the members of the departmental workshop, and library, for their co-operation.

Invaluable assistance in the construction of the glassware was generously given by members of the Chemistry Department.

Receipt of a Scholarship from the Sir James Caird's Travelling Scholarships Trust is gratefully acknowledged.

REFERENCES

(1) D.J. Tedford, Thesis for Ph.D., Glasgow, 1957.

(2) S.C. Kapoor, Thesis for Post-graduate Diploma, Royal College of Science and Technology, Glasgow, 1956.

(3) D.T.A. Blair, Thesis for Associateship, Royal College of Science and Technology, Glasgow, 1957.

(4) D.T.A. Blair, F.M.Bruce, J.E. Matthews, and D.J. Tedford, Proc. Phys. Soc. 75 (1960) 729.

(5) H..Raether, App. Sci. Res. B5 (1956) 23.

(6) K.J. Schmidt, Z. Phys. 139 (1954) 251.

(7) J.K. Vogel and H. Raether, Z. Phys. 147 (1957) 141.

(8) J.K. Vogel, Z. Phys. 148 (1957) 355.

(9) F. Llewellyn-Jones, Ionization and Breakdown in Gases (Methuen, 1957) p.47.

(10) L.B. Loeb, Basic Processes of Gaseous Electronics (University of California Press, 1955) p.711.

(11) H. Schlumbohm, Z. Naturforshg. 16a (1961) 510.

(12) J. Dutton, S.C. Haydon, and F. Llewellyn Jones, Proc. Roy. Soc. A 213 (1952) 203.

(13) A.N. Prasad and J.D. Craggs, E.R.A. Report L/T 378 (1958).
A.N. Prasad, Proc. Phys. Soc. 74 (1959) 33.

(14) J. Dutton, F. Llewellyn Jones and R.W. Palmer, Proc. 4th. Int. Conf. on Ionization Phenomena in Gases (Uppsala, 1959)1137.

(15) A.N. Prasad and J.D. Craggs, E.R.A. Report L/T 390 (1959). Proc. Phys. Soc. 76 (1960) 223.

(16) J.M. Meek, Proc.4th Int. Conf. on Ionization Phenomena in Gases (Uppsala, 1959)1146.

(17) G.A. Schröder, Z. angew. Phys. 13 (1961) 367.

(18) H. Schlumbohm, Z. Phys. 166 (1962) 93.

(19) L.B. Loeb, Basic Processes of Gaseous Electronics (University of California Press, 1955) p.251.

(20) K.R. Allen and K. Philips, J. Electronics and Control 8 (1960) 273.

(21) S.A. Korff, Electron and Nuclear Counters (van Nostrand, 1947) 36 (or other standard texts on counters).

(22) R.W. Pidd and L. Madansky, Phys. Rev. 75 (1949) 1175.

(23) K.J. Schmidt, Z. Phys. 139 (1954) 266.

(24) S.A. Korff and R.D. Present, Phys. Rev. 65 (1944) 274.

(25) W. Legler, Z. Phys. 143 (1955) 173.

(26) U. Dibbern, Z. Phys. 163 (1961) 582
Proc. 5th Int. Conf. on Ionization Phenomena in Gases (Munich, 1961).

(27) R.A. Wijsman, Phys. Rev. 75 (1949) 833.

(28) S.C. Curran, A.L. Cockroft and J. Angus, Phil. Mag. 40 (1949) 929.

(29) W. Legler, Z. Phys. 140 (1955) 221.

(30) L. Frommhold, Z. Phys. 144 (1956) 396.
see also:
H. Schlumbohm Z. angew. Phys. 11 (1959) 156.
Proc. 4th Int. Conf. on Ionization Phenomena in Gases (Uppsala, 1959) 1 127.

(31) L. Frommhold, Z. Phys. 150 (1958) 172.
see also:
H. Schlumbohm, as in (30), above.

(32) W. Legler, Z. Naturforsg. 16a (1961) 253.

(33) H. Schlumbohm, Z. Phys. 151 (1958) 563.

(34) L. Frommhold, Z. Phys. 156 (1959) 144.
Proc. 4th Int. Conf. on Ionization Phenomena in Gases (Uppsala, 1959) 1 115.

(35) K. Richter, Z. Phys. 157 (1959) 130.

(36) H. Raether, Naturw. 33 (1961) 175.

(37) J.M. Meek and J.D. Craggs,
Electrical Breakdown of Gases (Oxford, 1953) p.252.

(38) J. Pfaue and H. Raether,
Z. Phys. 153 (1959) 523.
H. Raether, Proc. 4th Int. Conf. on Ionization Phenomena in Gases (Uppsala, 1959) 1 124.

(39) K. Richter, Z. Phys. 158 (1960) 312.

(40) L. Frommhold, Z. Phys. 160 (1960) 554.

(41) J.A. Hornbeck, Phys. Rev. 83 (1951) 374.

(42) C.D. Thomas, Rev. Sci. Inst. 20 (1949) 147.

(43) J.D. Cobine, Gaseous Conductors (Dover, 1958) p.56.

(44) N.F. Astbury, Introduction to Electrical Applied Physics (Chapman and Hall, 1956) p.61.

(45) F.M. Bruce, J.I.E.E. 94 Part II (1947) 140.

(46) D.T.A. Blair, J. McNaull, D.J. Tedford, and F.M. Bruce,
Proc. 5th Int. Conf. on Ionization Phenomena in Gases (Munich, 1961) 1 162.

(47) D.J. Tedford and D.T.A. Blair,
Proc. Phys. Soc. 79 (1962) 310.

(48) M.A. Harrison and R. Geballe,
Phys. Rev. 91 (1953) 1.

(49) R.A. Nielsen and N.E. Bradbury,
Phys. Rev. 51 (1937) 69.

(50) A.S. Eve, Phil. Mag. 8 (1904) 669.

(51) J.A. McClelland, Phil. Mag. 9 (1905) 230
Sci. Trans. Roy. Dublin Soc. 8 (1905) 169.

(52) J.A. McClelland, Sci. Trans. Roy. Dublin Soc. 9 (1905) 1.

(53) R.D. Kleeman, Phil. Mag. 14 (1907) 618.

(54) F.E. Hackett, Sci. Trans. Roy. Dublin Soc., 9
(1909) 201.

(55) J.A. Crowther, Proc. Camb. Phil. Soc. 14 (1907) 340.

(56) A.L. Hughes and L.A. Du Bridge,
Photoelectric Phenomena (McGraw-Hill,
1932) 49.

(57) D.R. Hardy, Thesis for M.Sc., London, 1948.

(58) D.R. Hardy and J.D. Craggs,
Trans. A.I.E.E. 69 (1950) 584.

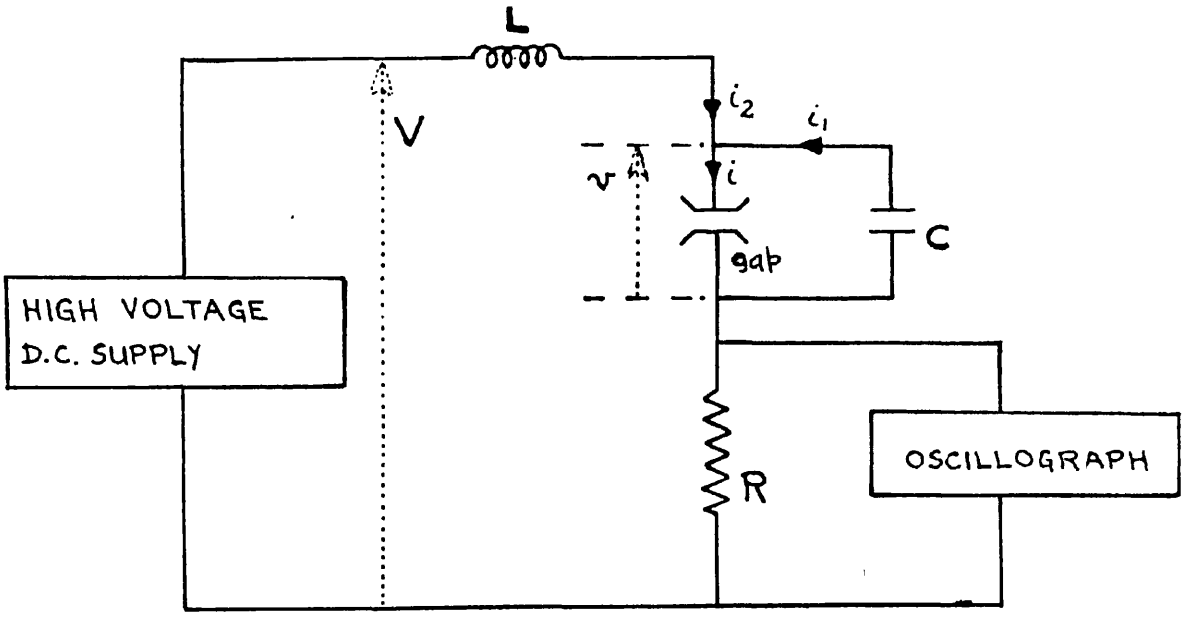

FIG. 1. EQUIVALENT CIRCUIT OF THE EXPERIMENTAL APPARATUS. The symbols are defined on p.33.

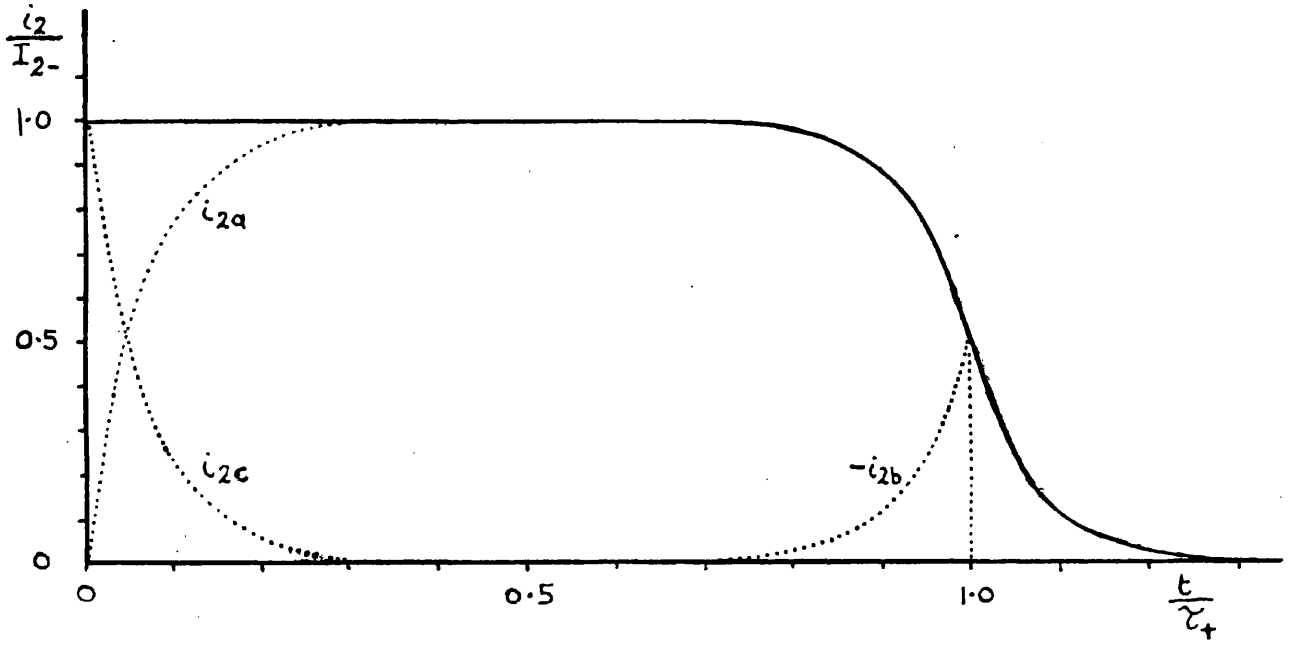

FIG. 2. CALCULATED CURRENT PULSE SHAPE FOR $\alpha d = 15, \psi = 1$.

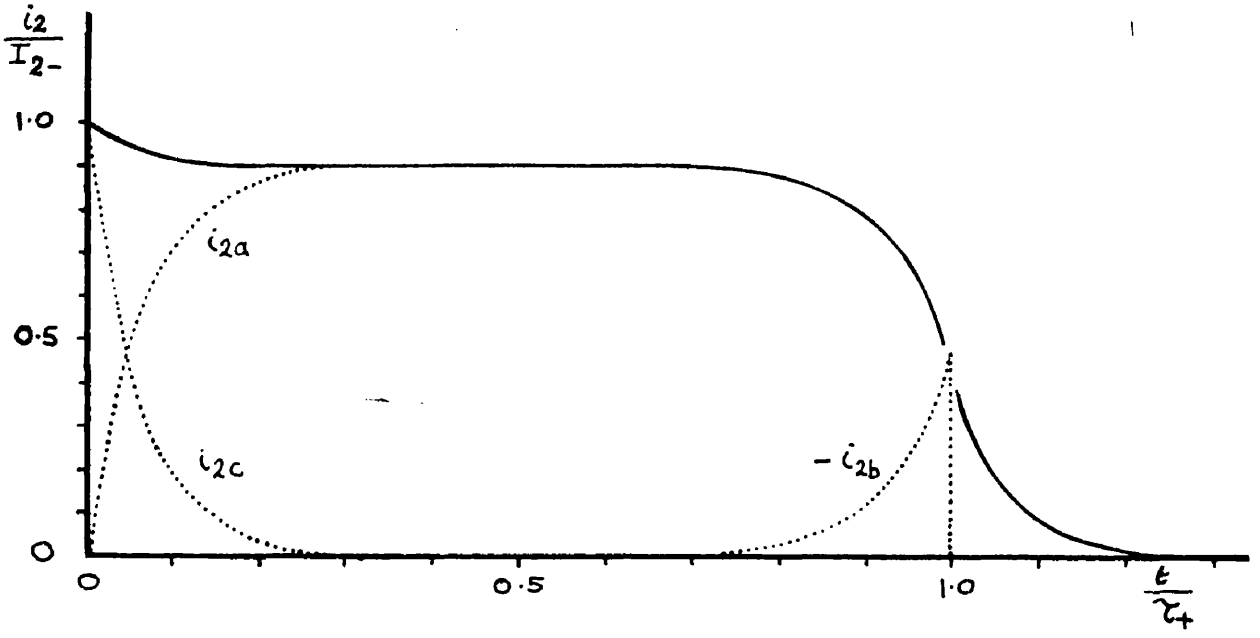

FIG. 3. CALCULATED CURRENT PULSE SHAPE FOR $\alpha d = 15$, $\gamma = 0.9$.

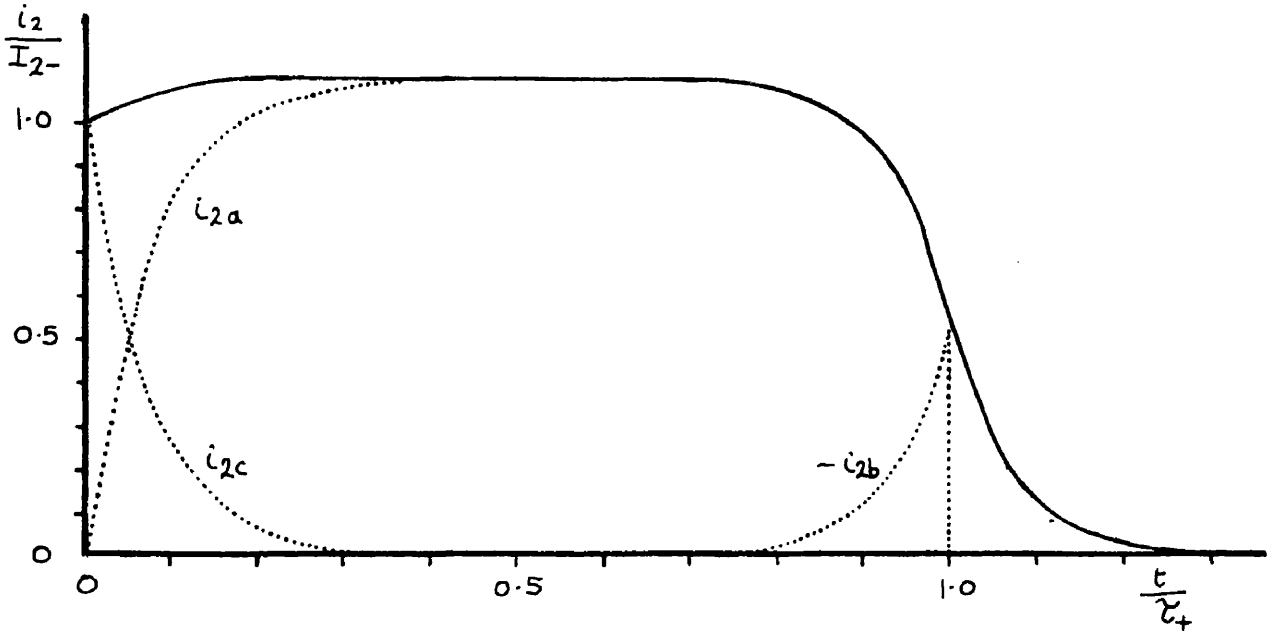

FIG. 4. CALCULATED CURRENT PULSE SHAPE FOR $\alpha d = 15$, $\gamma = 1.1$.

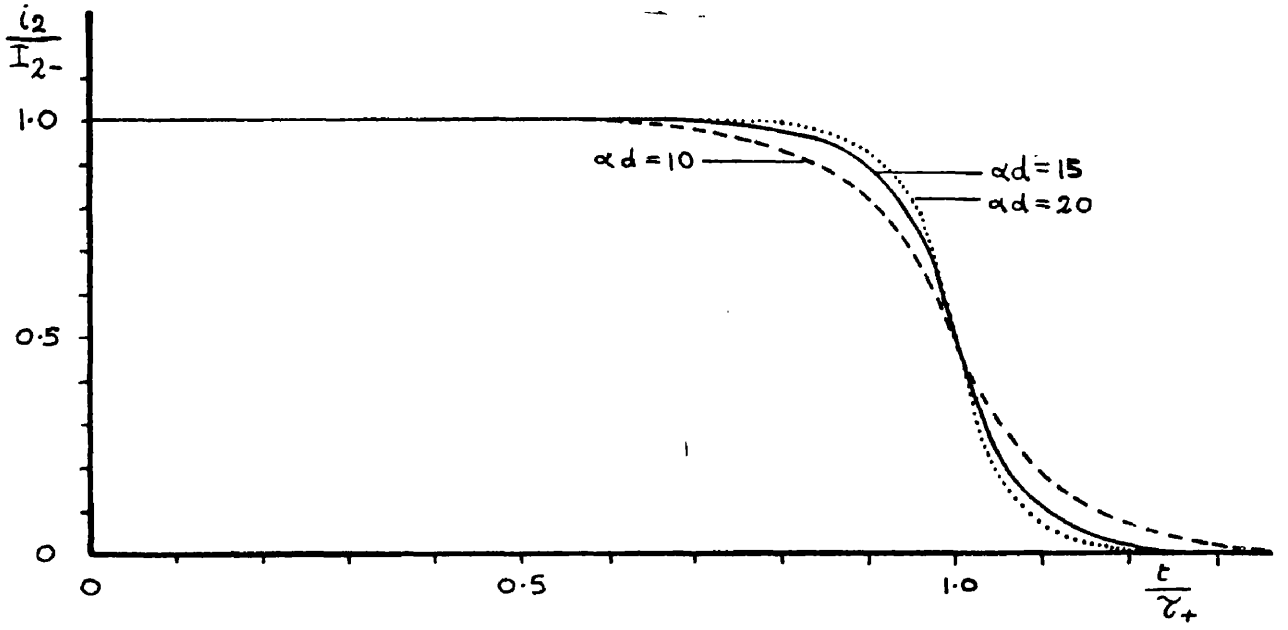

FIG. 5. CALCULATED CURRENT PULSE SHAPES FOR $\Psi = 1$, $\alpha d = 10, 15$ and 20.

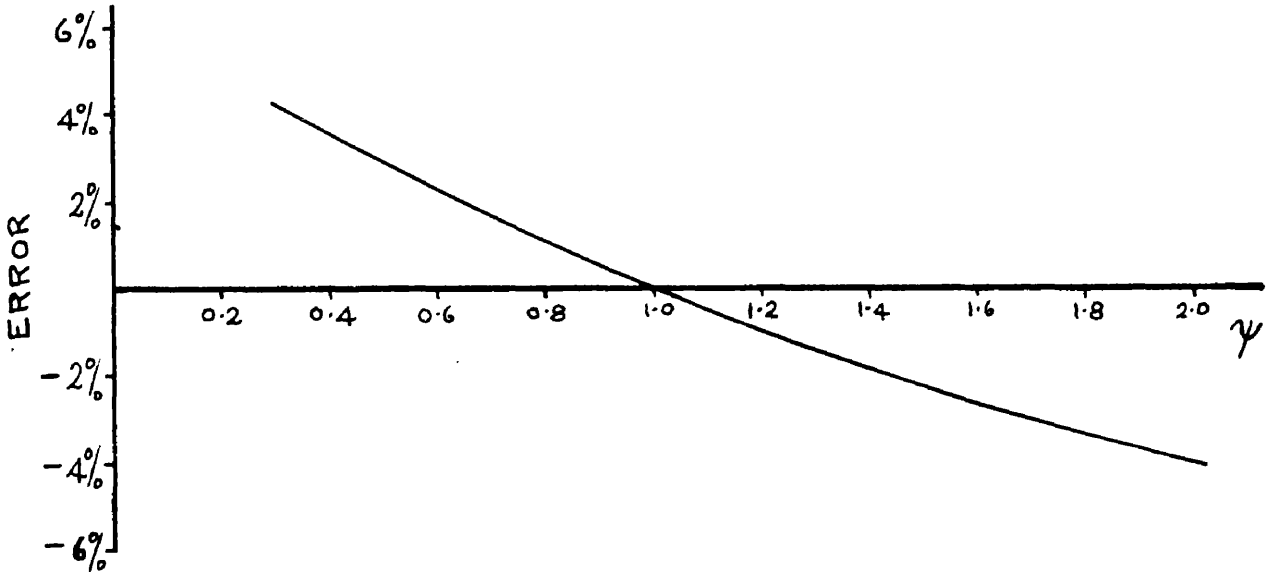

FIG. 6. THE ERROR IN MEASURED τ_+ FOR $\Psi \neq 1$.

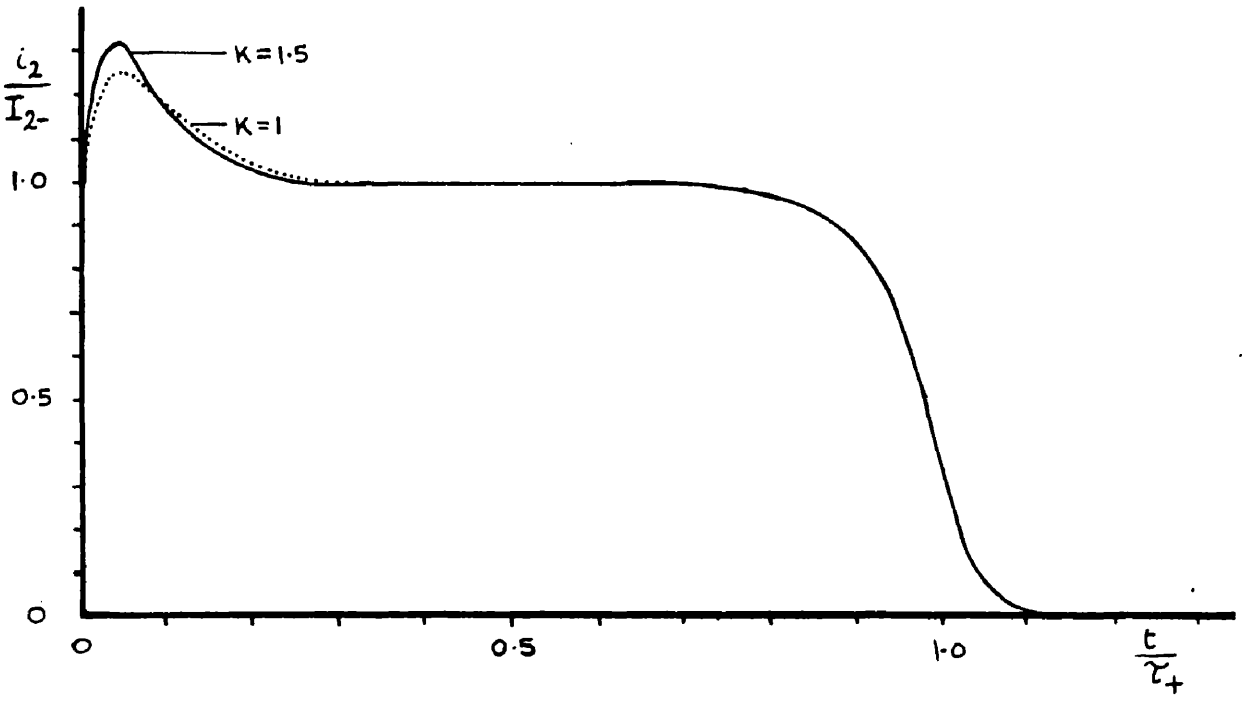

FIG.7. CALCULATED CURRENT PULSE SHAPE FOR $\alpha d=30$, $\psi=1$, $f=0.5$, $K=1$ and 1.5.

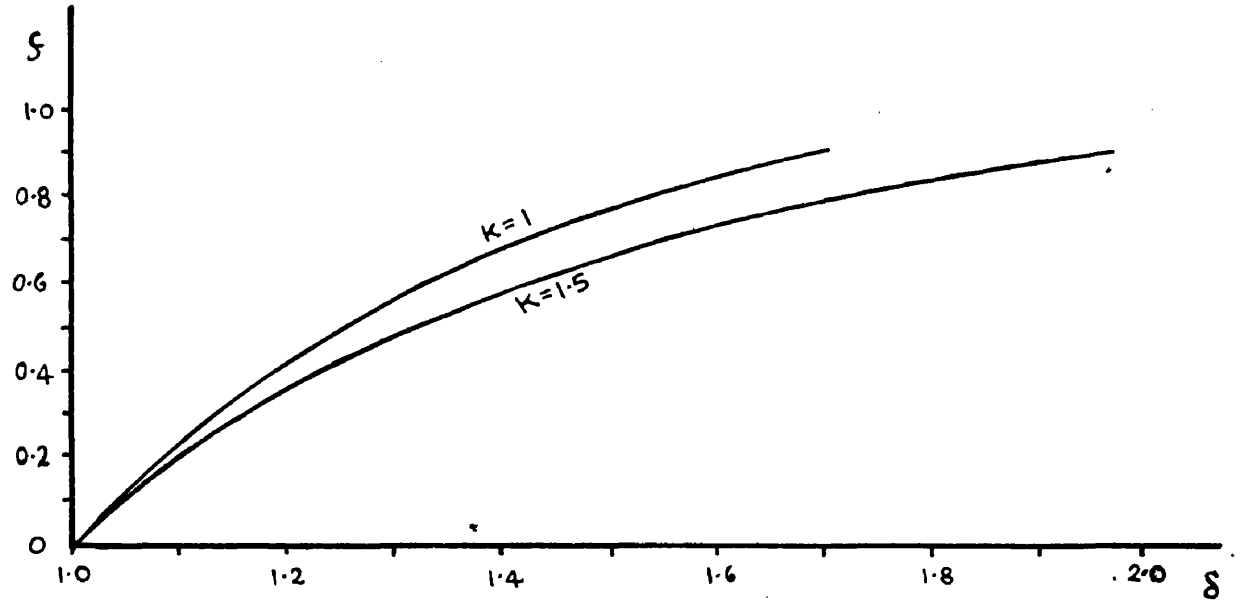

FIG.8. THE RELATION BETWEEN f AND δ.

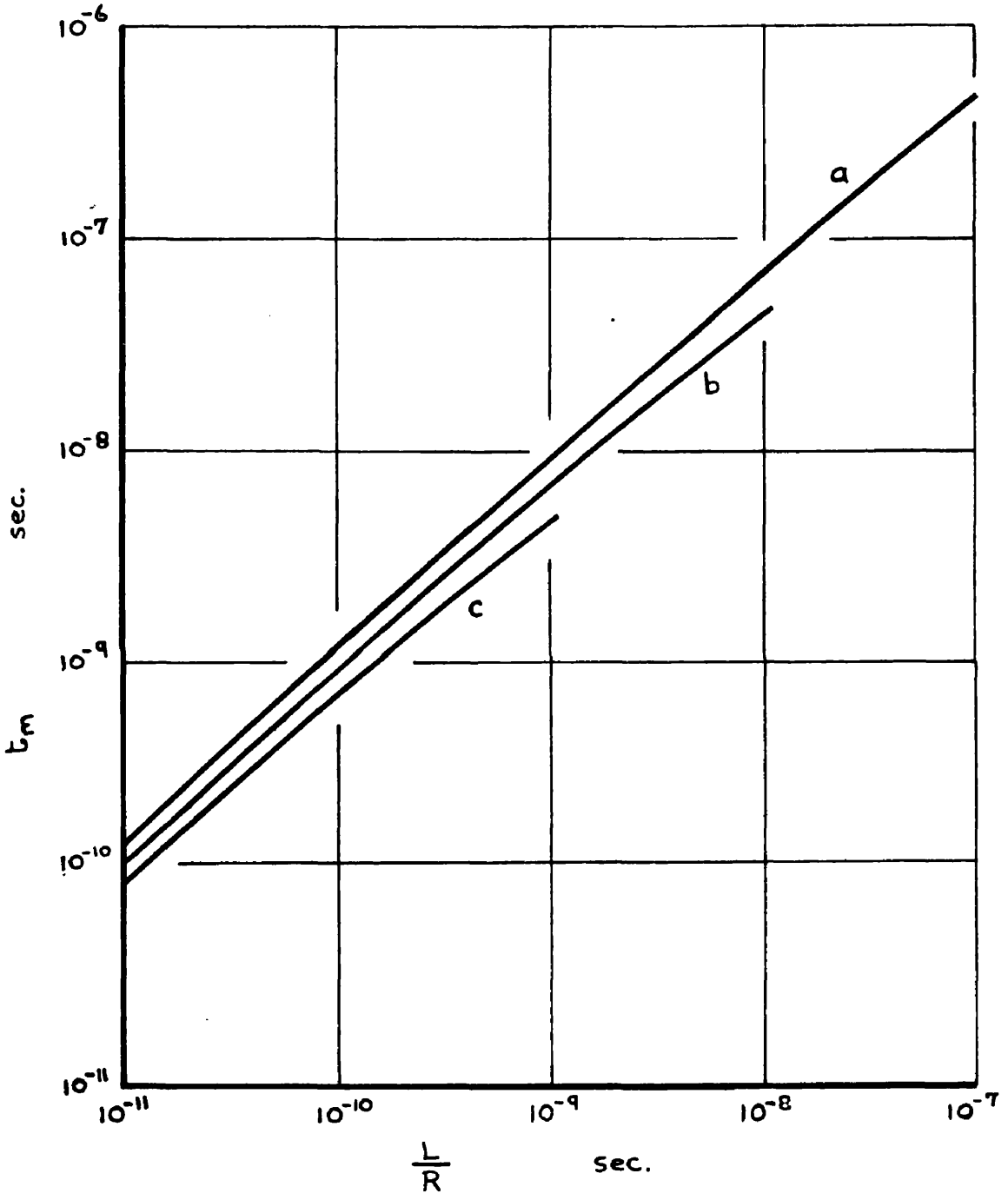

FIG. 9. t_m AS A FUNCTION OF $\frac{L}{R}$ FOR DIFFERENT VALUES OF CR.

a - $CR = 10^{-5}$ sec.
b - $CR = 10^{-6}$ sec.
c - $CR = 10^{-7}$ sec.

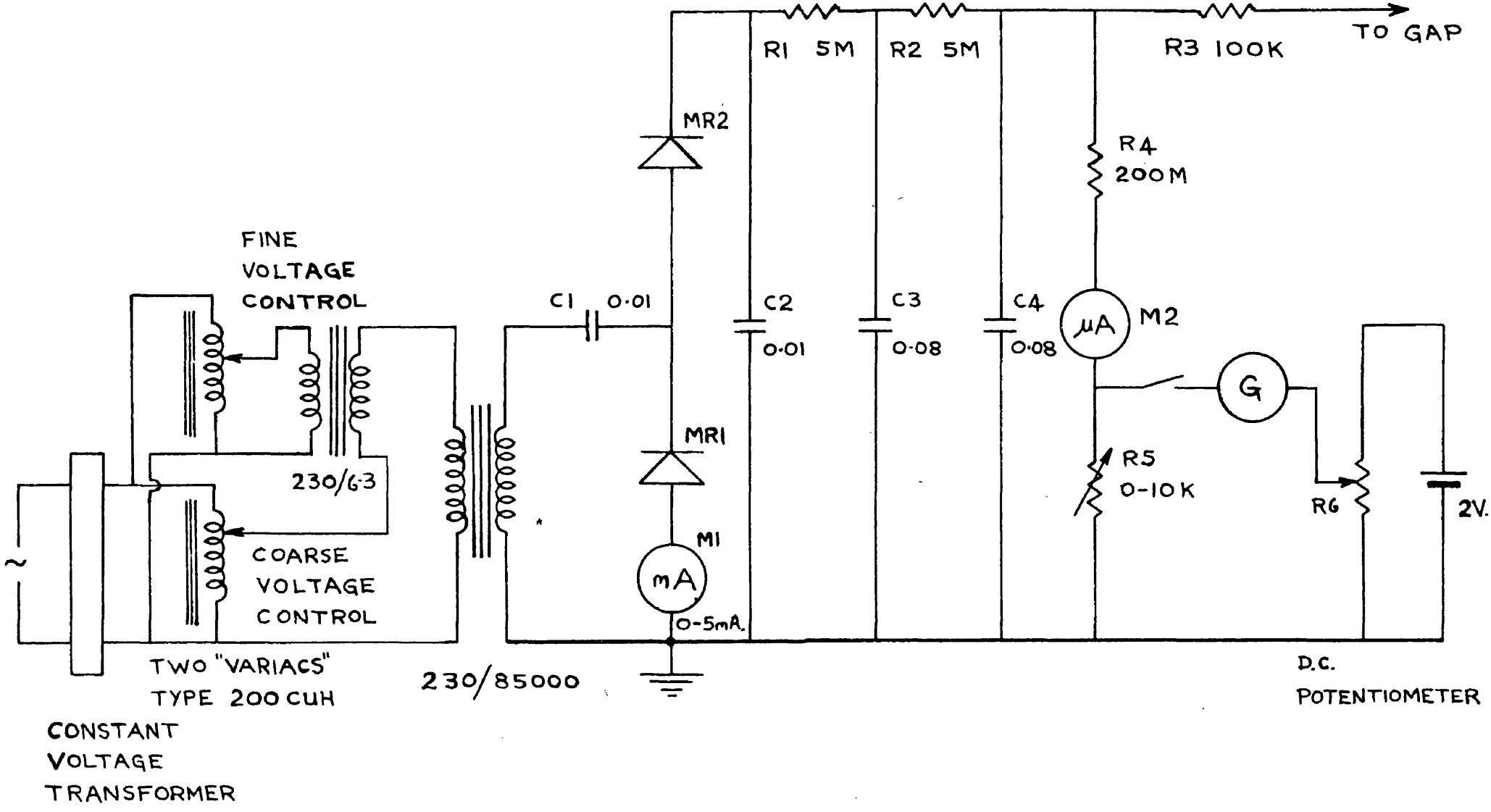

FIG. 10. THE HIGH VOLTAGE D.C. SUPPLY.

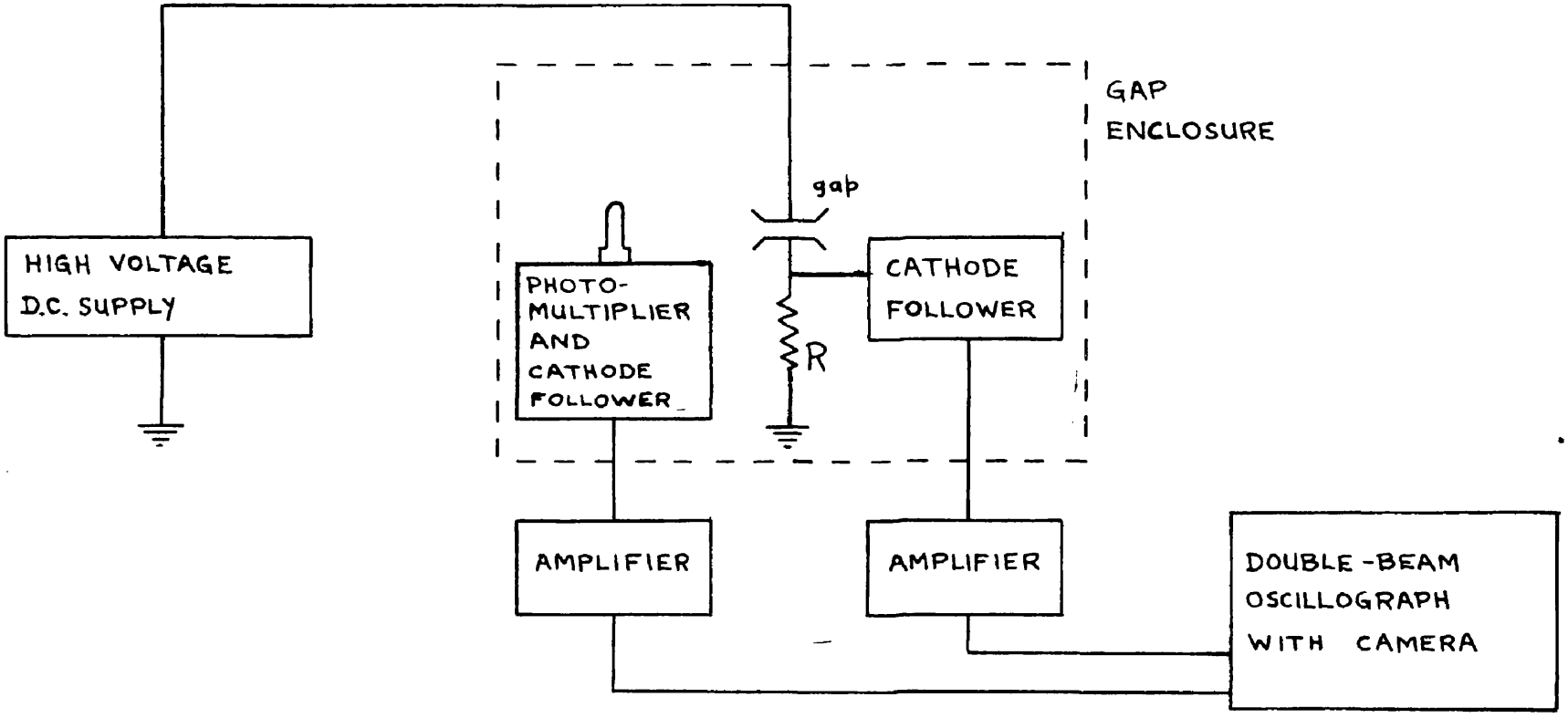

FIG. II. BLOCK DIAGRAM OF THE APPARATUS USED TO RECORD CURRENT AND LIGHT PULSES SIMULTANEOUSLY.

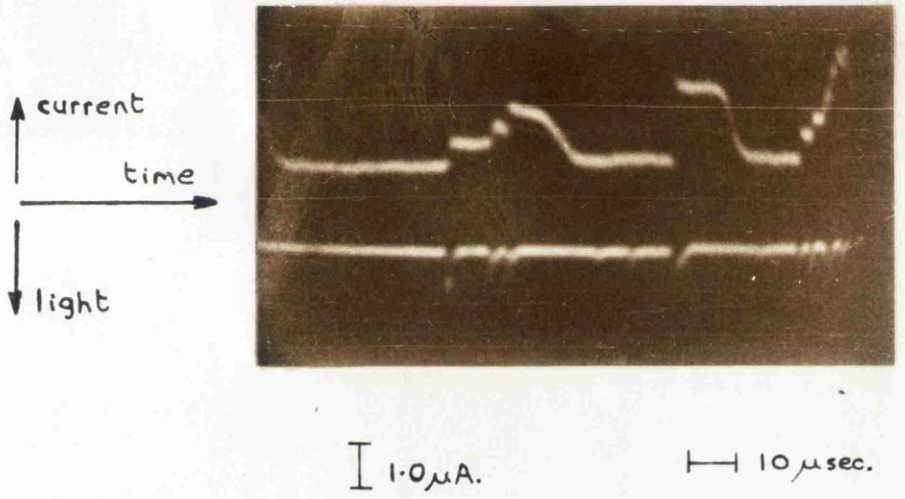

FIG.12. A TYPICAL OSCILLOGRAM OF CURRENT AND LIGHT PULSES IN ROOM AIR : 1 cm. GAP. (avalanches in uniform-field region).

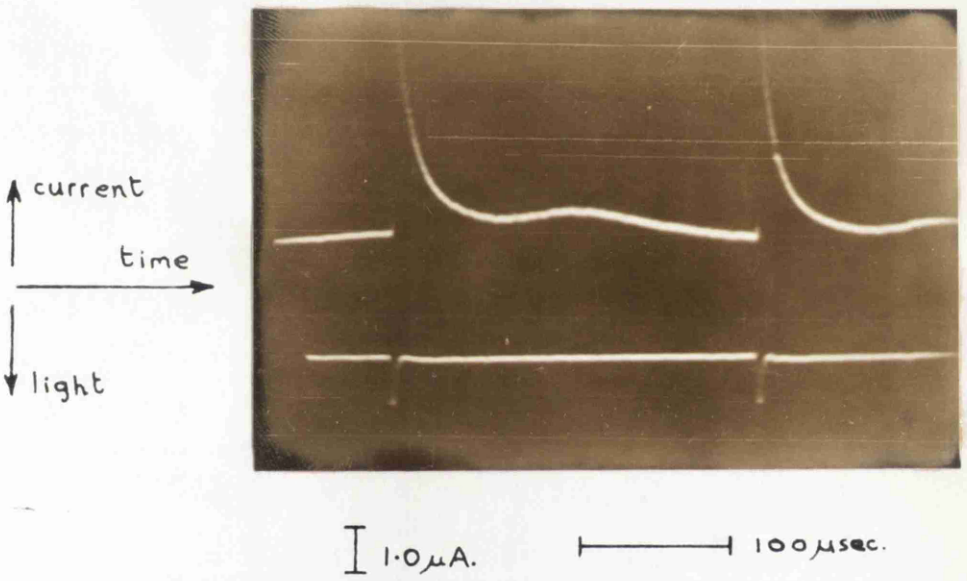

FIG.13. A TYPICAL OSCILLOGRAM OF CURRENT AND LIGHT PULSES IN ROOM AIR : 5 cm. GAP (avalanches in non-uniform field region).

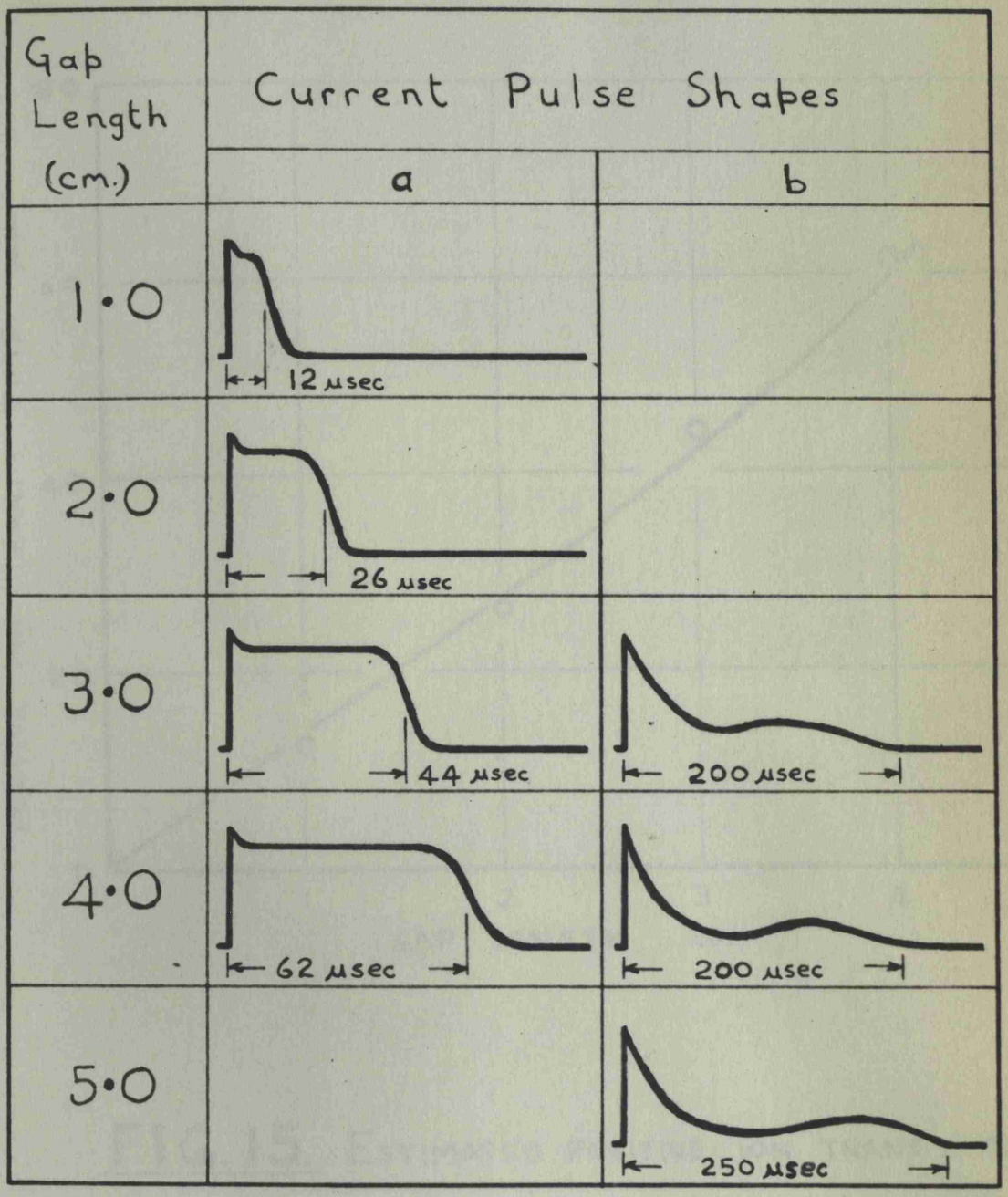

FIG. 14. CURRENT PULSE SHAPES OBSERVED AT DIFFERENT GAP LENGTHS IN ROOM AIR.

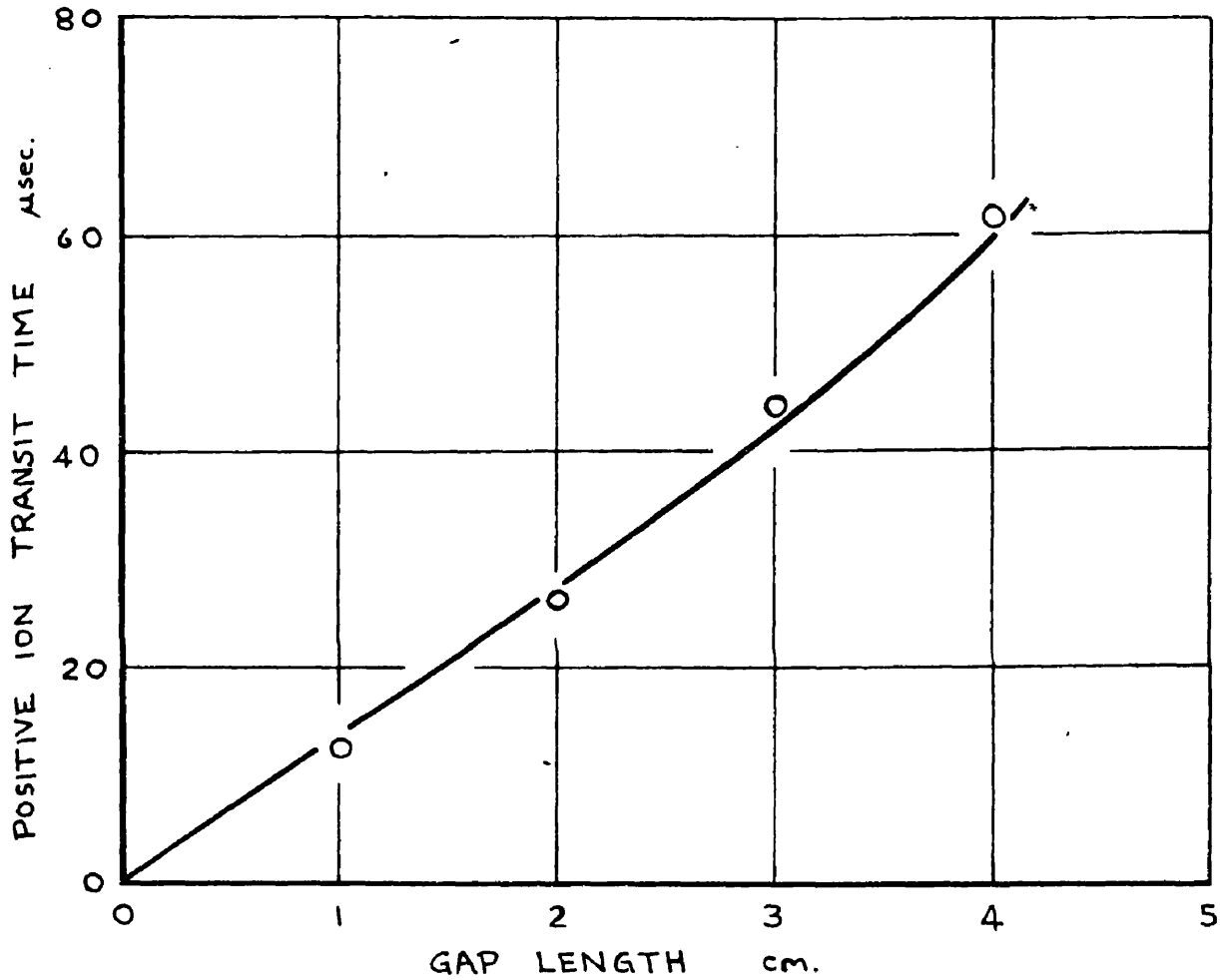

FIG. 15. ESTIMATED POSITIVE ION TRANSIT TIMES IN ROOM AIR, COMPARED WITH VALUES CALCULATED FROM A MOBILITY OF 2·6 $cm.^2 sec.^{-1} V.^{-1}$

o MEASURED

— CALCULATED

Relative humidity 35–40%

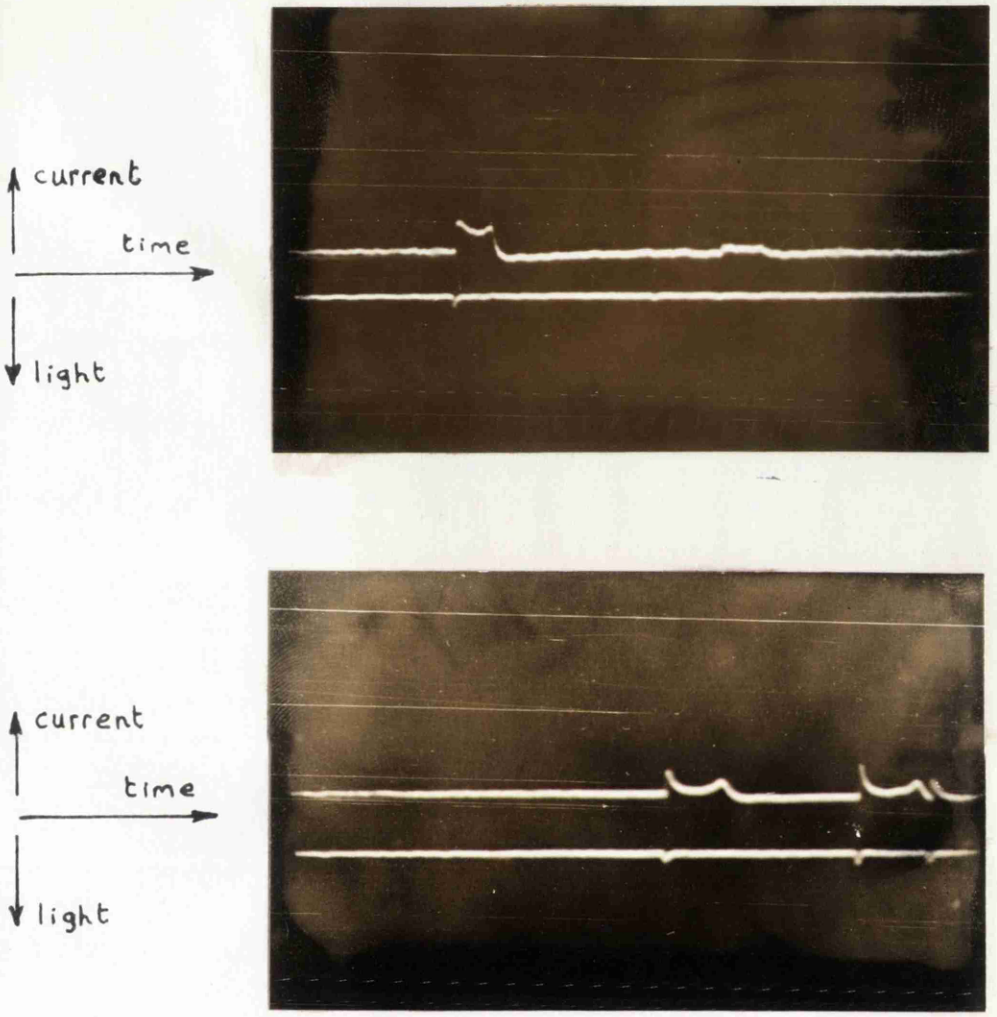

FIG. 16. OSCILLOGRAMS OF CURRENT AND LIGHT PULSES IN ROOM AIR : SPHERE GAPS.

(a) 2 cm. gap : 6·25 cm. spheres.
(b) 2 cm. gap : 2 cm. spheres.

Irradiation was provided by 2mg radium in the anode in each case.

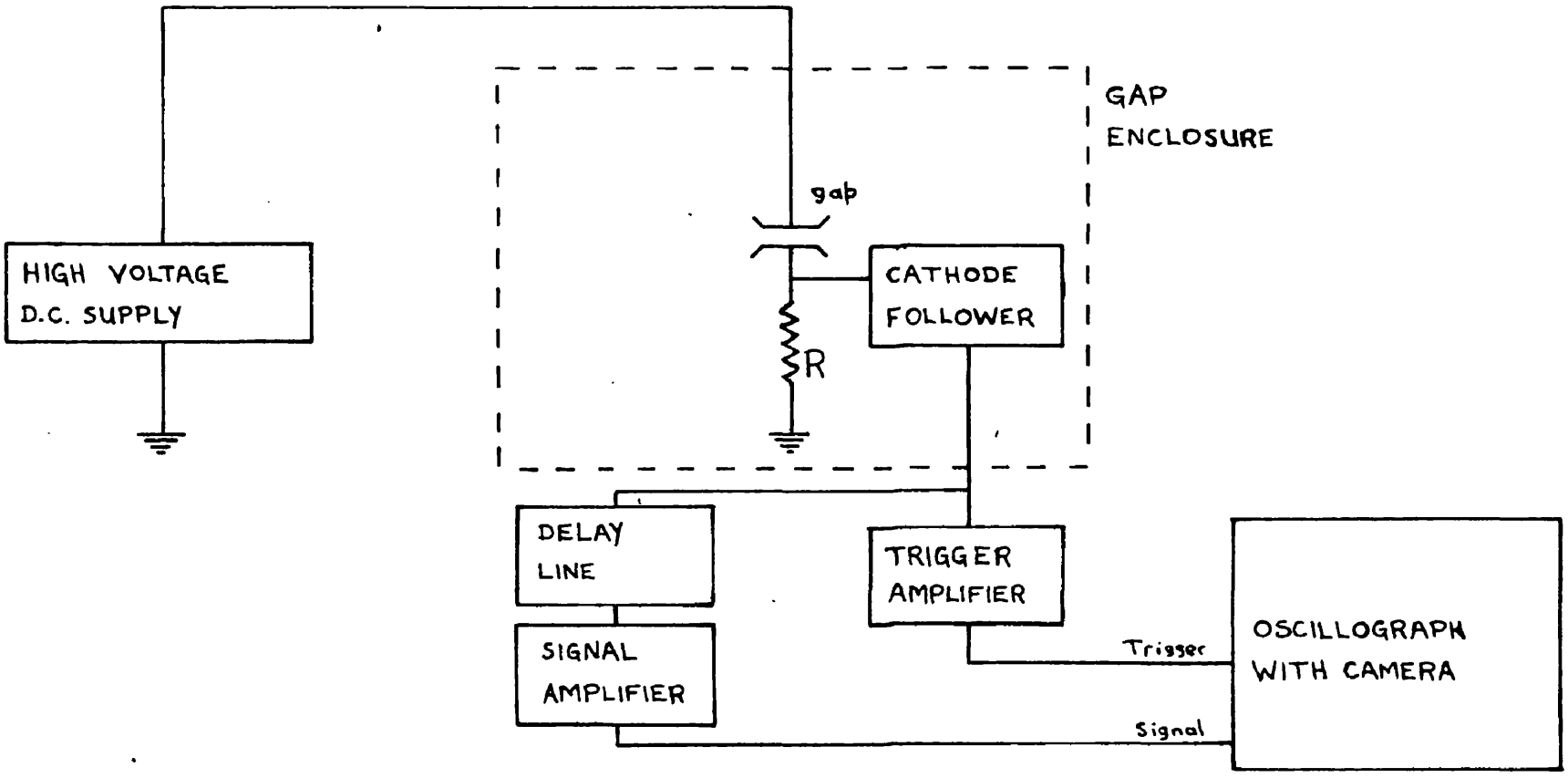

FIG. 17. BLOCK DIAGRAM OF THE APPARATUS USED TO RECORD INDIVIDUAL CURRENT PULSES.

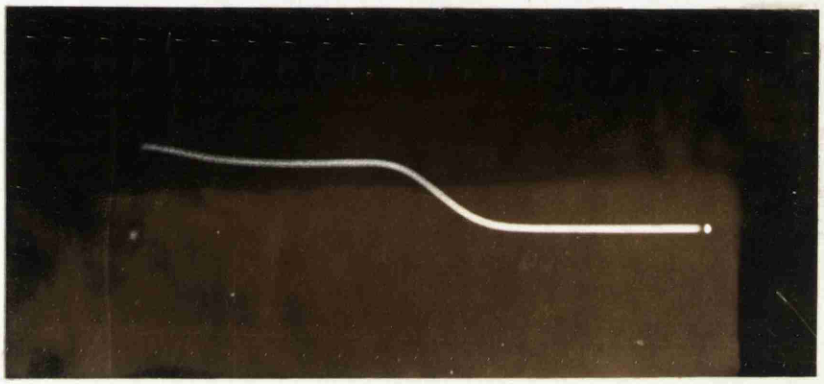

10 μsec.

FIG. 18. OSCILLOGRAM OF AN INDIVIDUAL CURRENT PULSE IN ROOM AIR: 3cm. GAP. (uniform field).

(a)

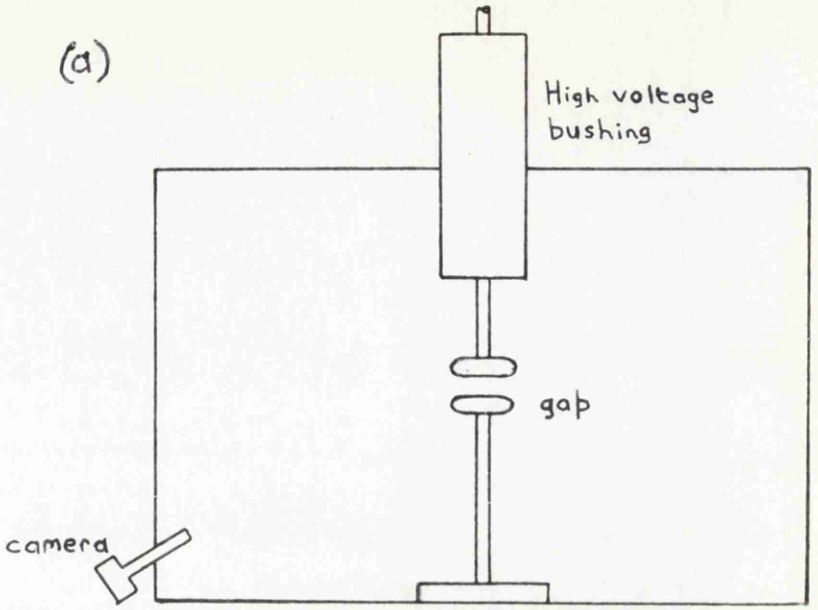

(b)

FIG. 19. (a) APPARATUS USED TO OBTAIN ANODE GLOW PHOTOGRAPHS. (Diagrammatic only ; not to scale).

(b) A PHOTOGRAPH OF THE ELECTRODES TAKEN WITH THIS APPARATUS. (To the same scale as the photographs of FIG. 20).

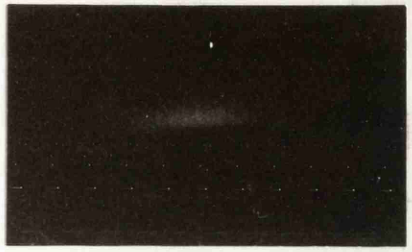

1cm

2cm

3cm

4cm

5cm

FIG. 20. THE ANODE GLOW IN ROOM AIR, AT DIFFERENT GAP LENGTHS.

Irradiation was provided by 2mg. of radium.

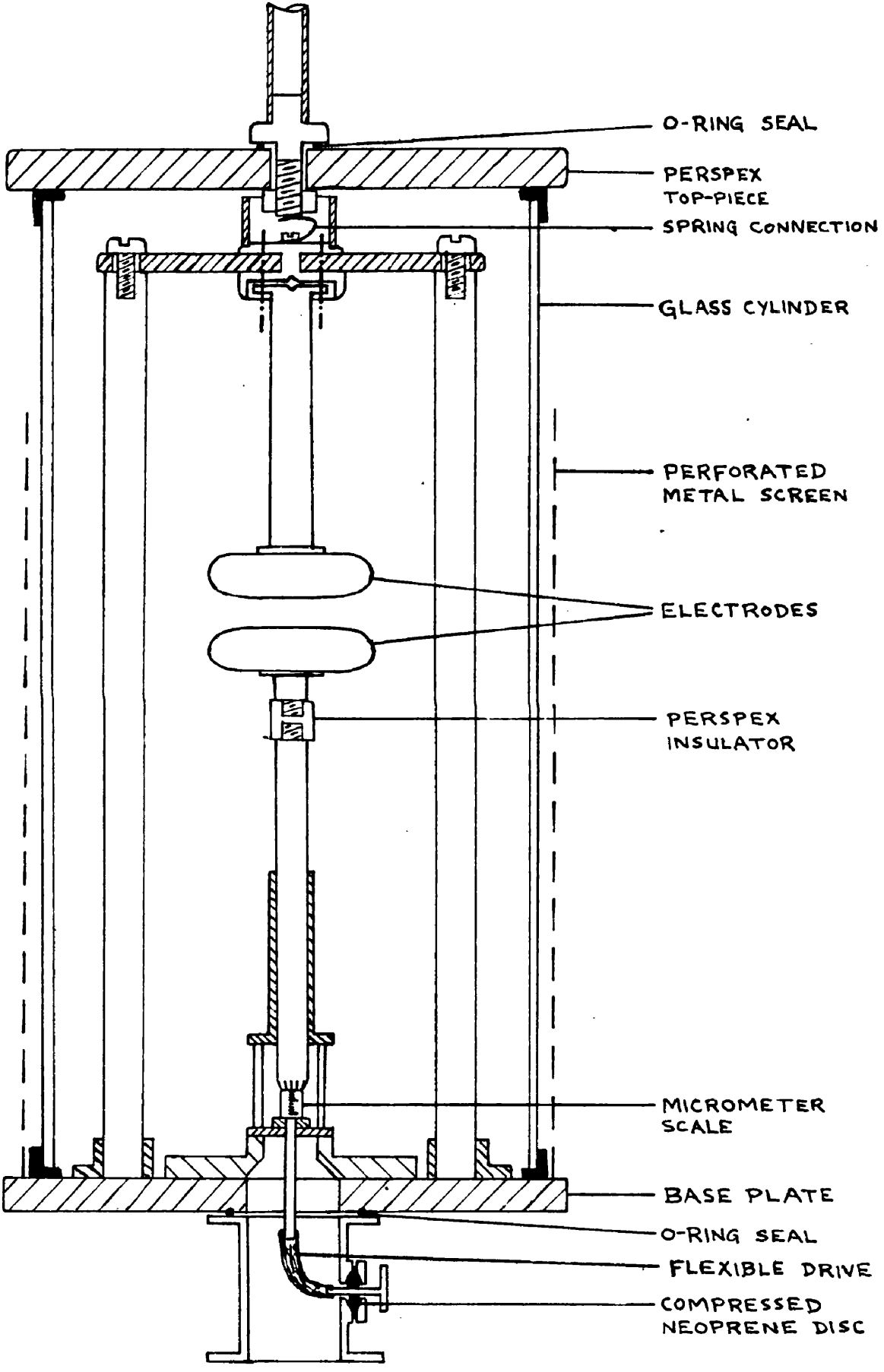

FIG. 21. THE EXPERIMENTAL VESSEL.

(Abbrox. one quarter full size).

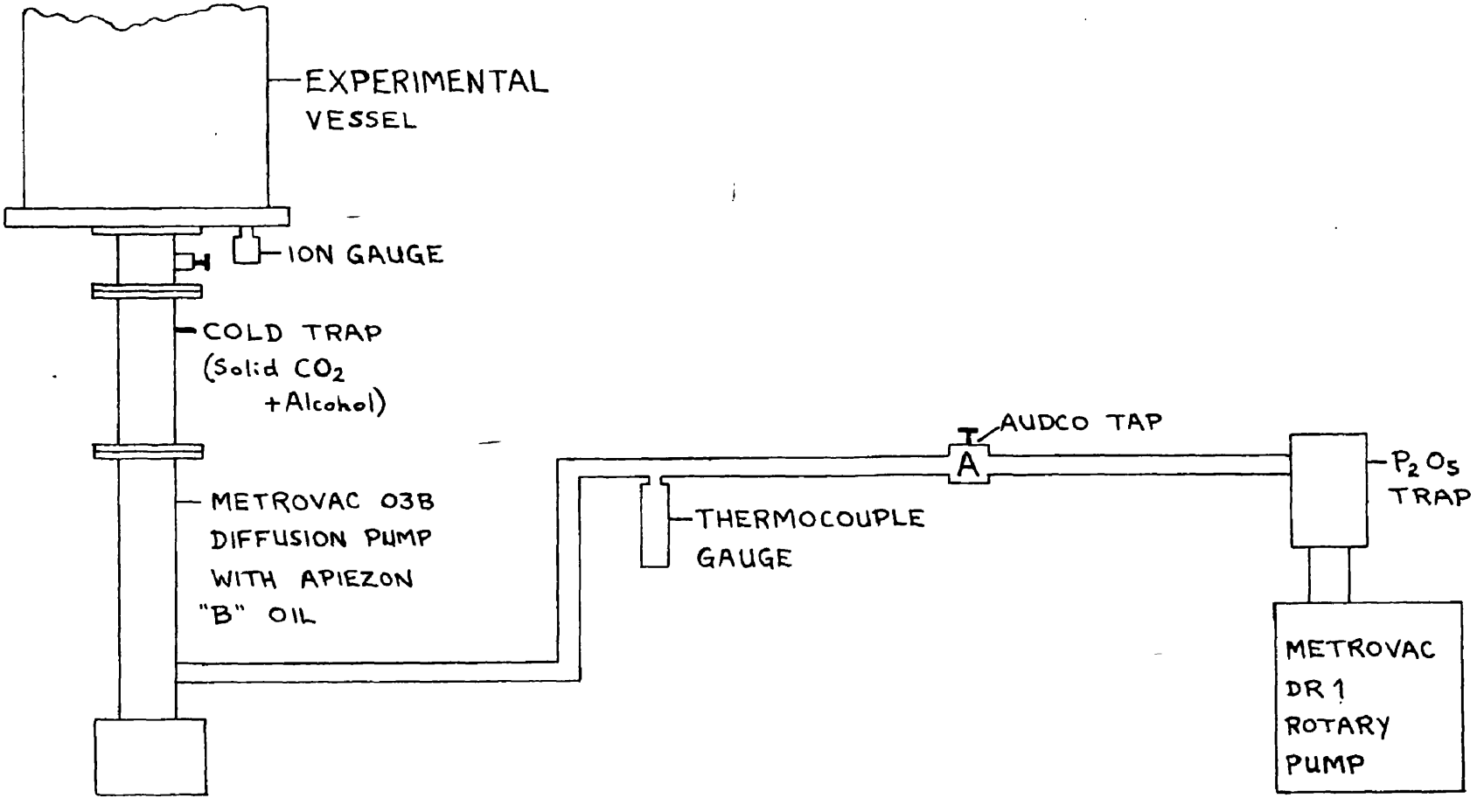

FIG. 22. THE VACUUM SYSTEM. (Diagrammatic only : not to scale).

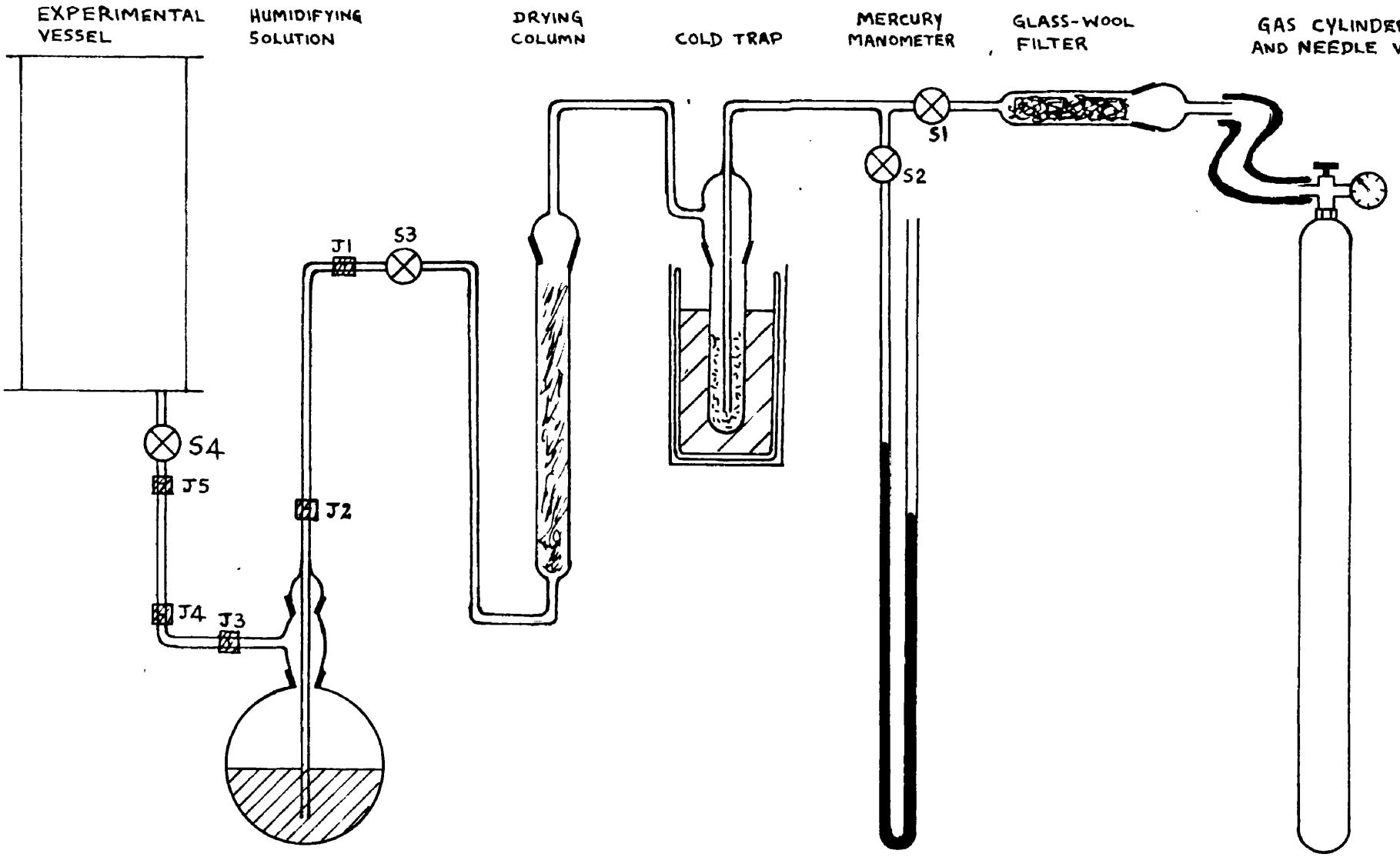

FIG. 23. THE GAS SYSTEM. (Diagrammatic only : not to scale).

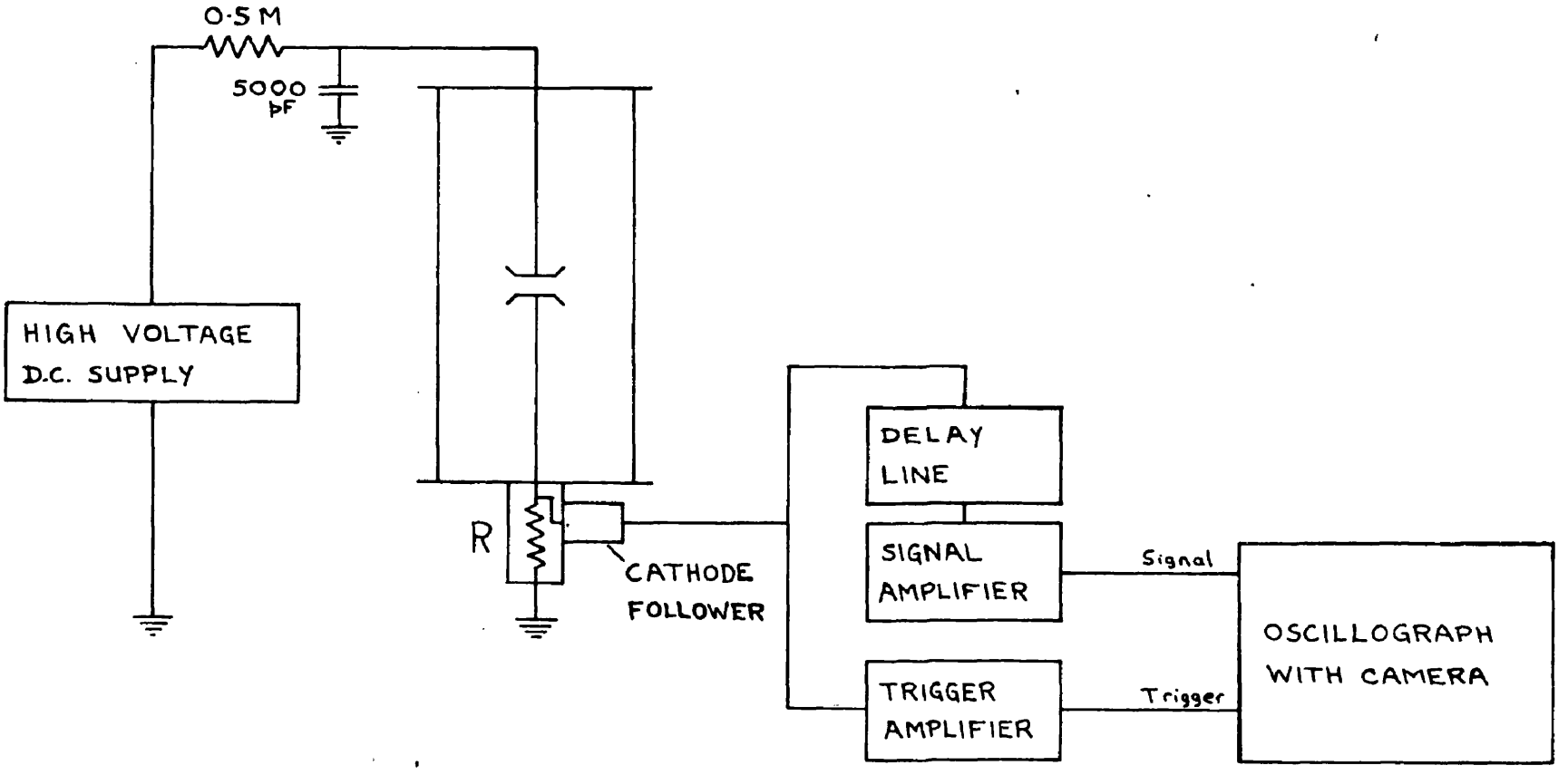

FIG. 24. BLOCK DIAGRAM OF THE PULSE RECORDING APPARATUS.

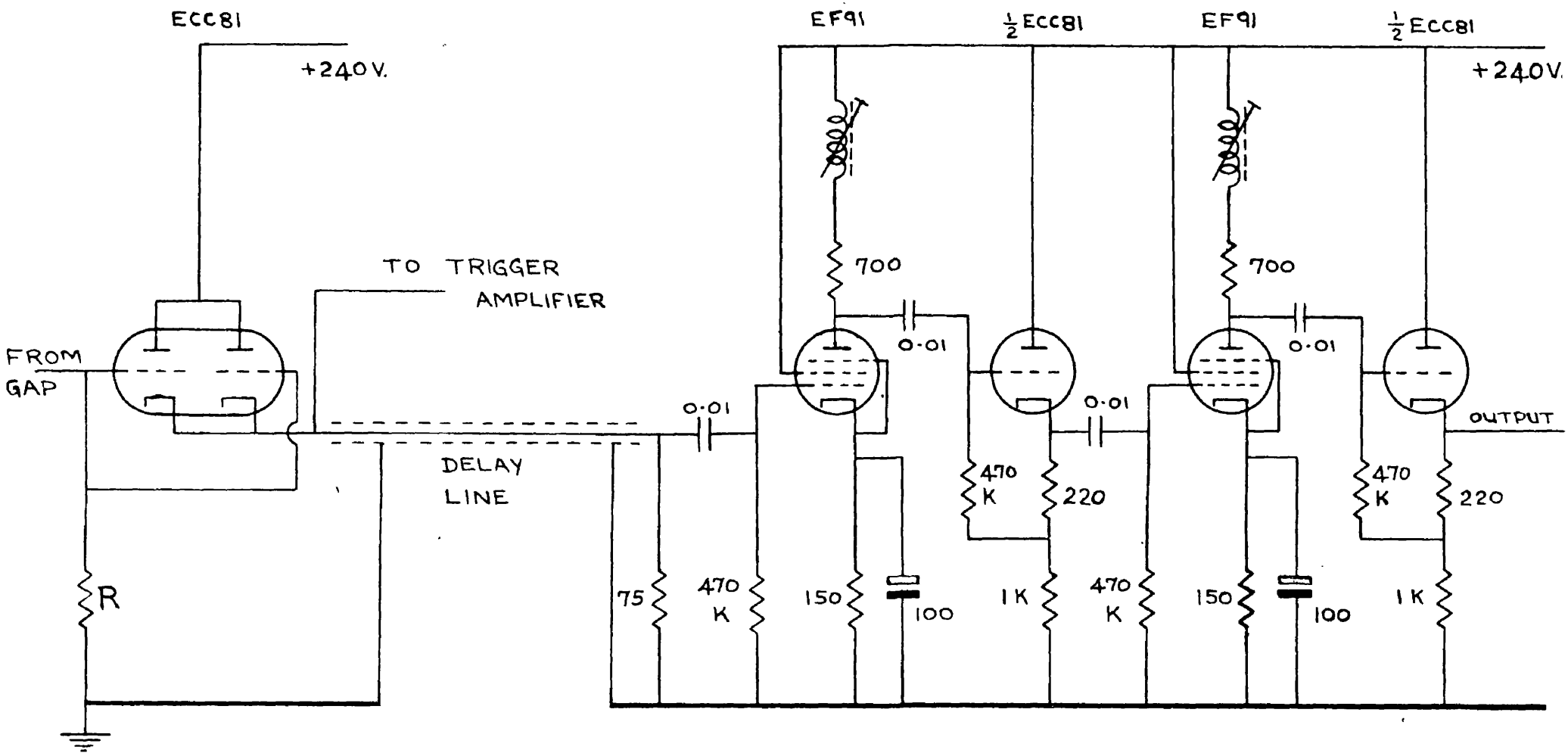

FIG. 25. THE CATHODE FOLLOWER AND SIGNAL AMPLIFIER OF FIG. 24.

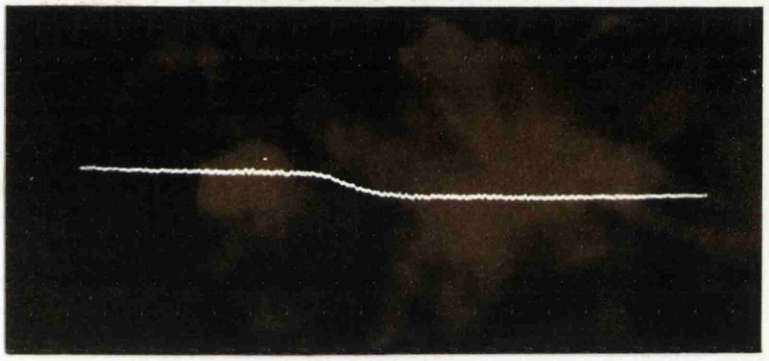

⟷ 10 μsec.

FIG. 26. OSCILLOGRAM OF A CURRENT PULSE OF BALANCED FORM, IN NITROGEN.

$\frac{E}{p} = 36{\cdot}6 \text{ V.cm}^{-1}\text{(mm. Hg)}^{-1}$

$p = 700$ mm. Hg.

$d = 3$ cm.

$n \approx 10^6$ electrons.

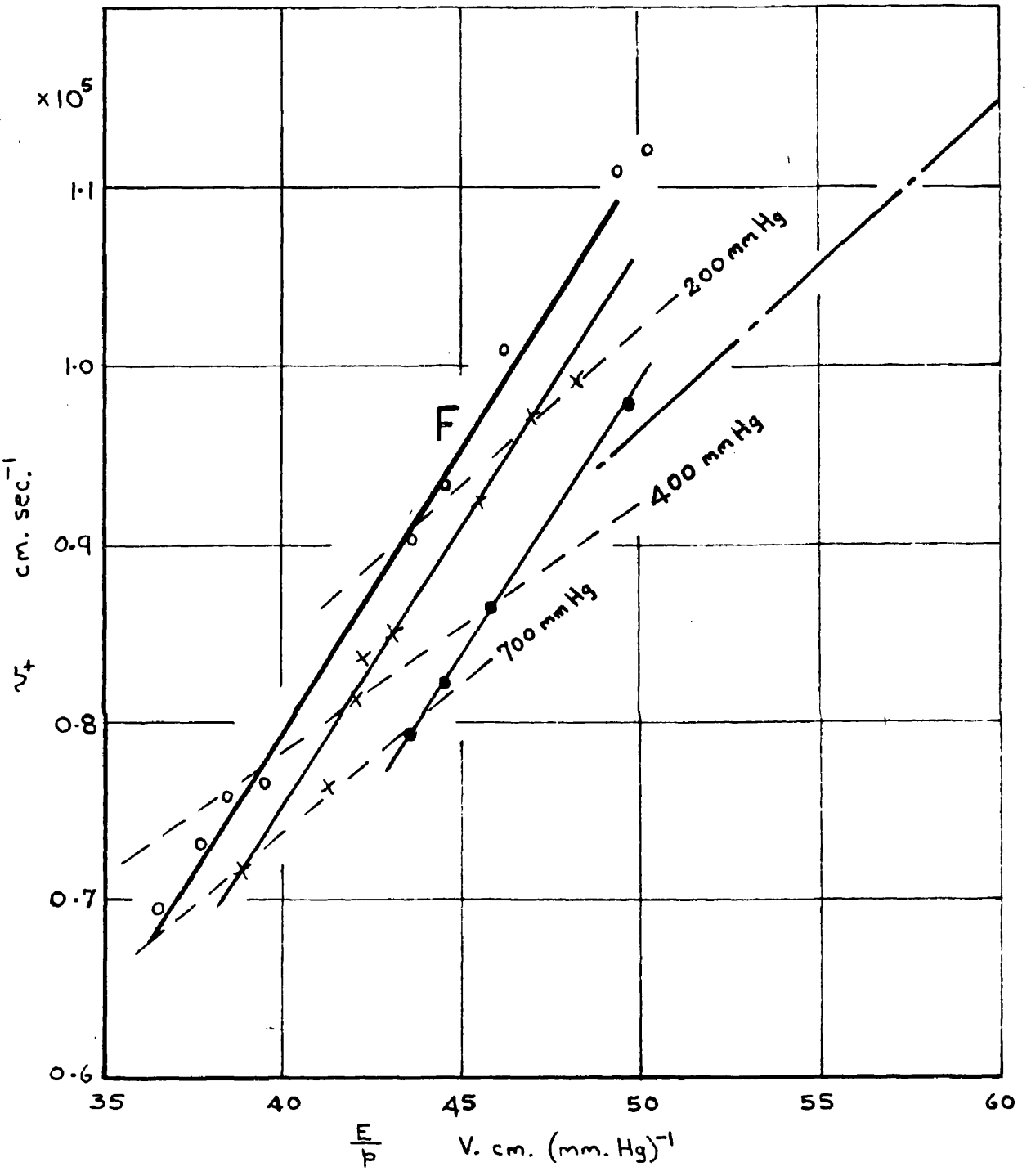

FIG. 27. MEASURED POSITIVE ION DRIFT VELOCITIES v_+ IN NITROGEN.

• 1cm. gap
× 2cm. gap
o 3cm. gap

F Frommhold[40]: 3cm. gap.

Vogel[8]: 2cm. gap.

constant pressure lines.

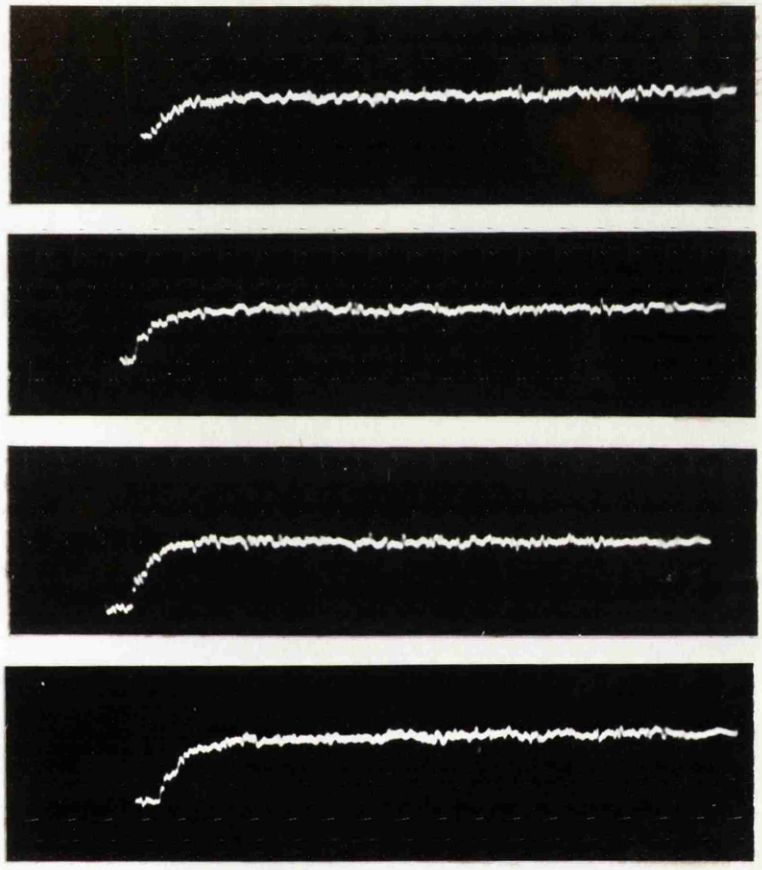

1·0 μsec.

FIG. 28. ELECTRON COMPONENTS OF CURRENT PULSES IN NITROGEN.

$\frac{E}{p} = 37{\cdot}8$ V. cm^{-1} (mm. Hg)$^{-1}$

$p = 491$ mm. Hg.

$d = 3$ cm.

$n \approx 10^6$ electrons.

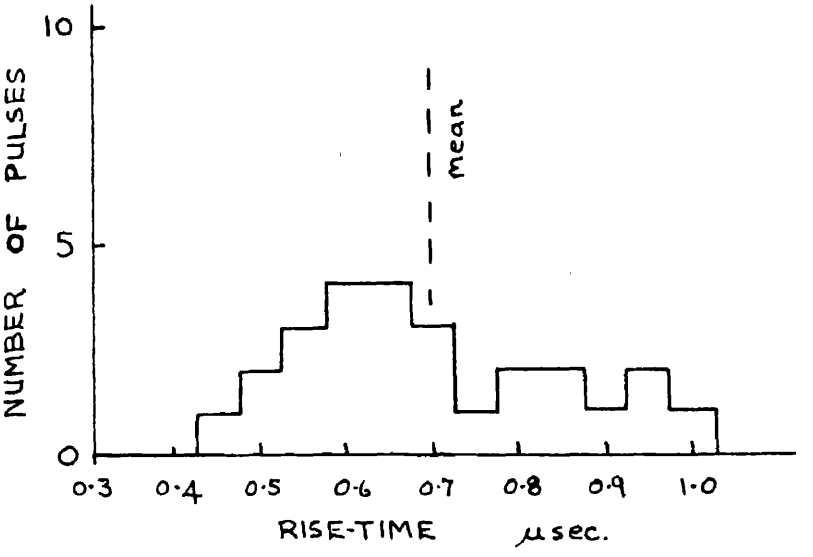

FIG. 29. TYPICAL DISTRIBUTION OF MEASURED CURRENT PULSE RISE-TIMES IN NITROGEN.

$\frac{E}{p} = 37{\cdot}8$ V. cm.$^{-1}$(mm. Hg).$^{-1}$

$p = 491$ mm. Hg.

$d = 3$ cm.

n of the order of 10^6 electrons per pulse.

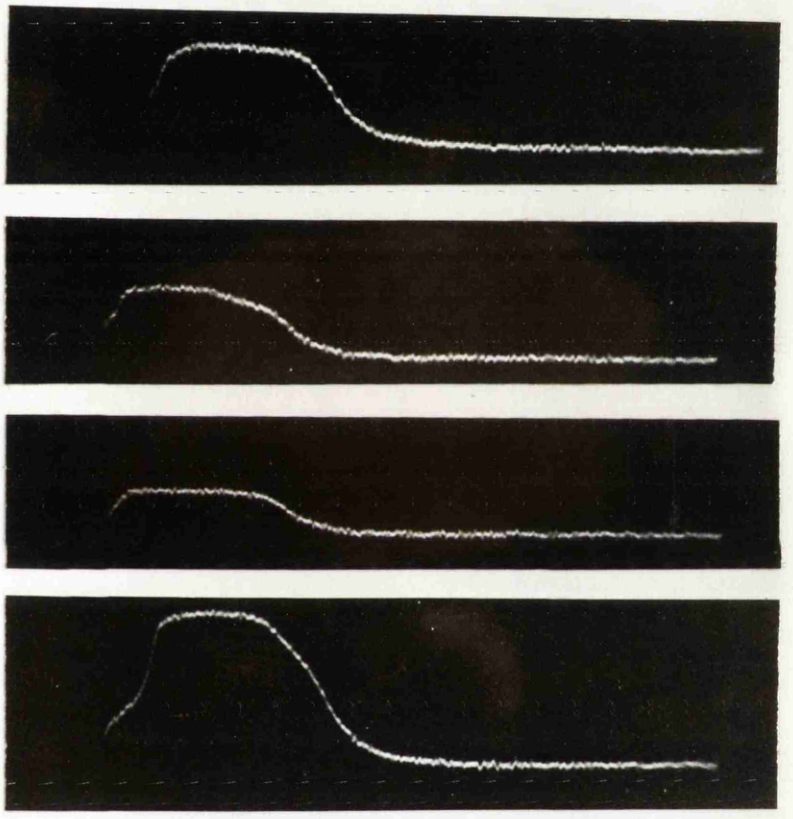

10 μsec.

FIG. 30. CURRENT PULSES IN NITROGEN, SHOWING THE EFFECT OF A PHOTO-ELECTRIC SECONDARY PROCESS.

$\frac{E}{p} = 50{\cdot}3 \text{ V.cm}^{-1}\text{(mm.Hg)}^{-1}$.

$p = 92{\cdot}2$ mm. Hg.

$d = 3$ cm.

$n \approx 2$ to 5×10^6 electrons per pulse.

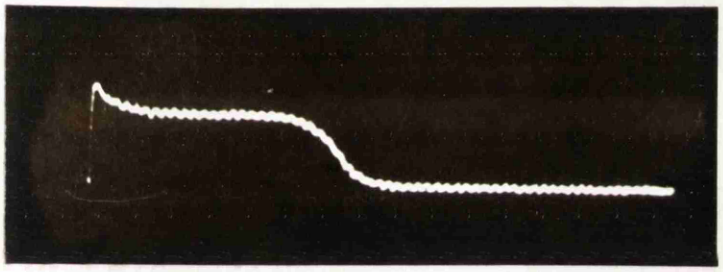

10 μsec.

FIG. 31. OSCILLOGRAM OF A CURRENT PULSE OF BALANCED FORM, IN DRY AIR.

$\frac{E}{p} = 39{\cdot}8$ V. cm.$^{-1}$ (mm.Hg)$^{-1}$

$p = 700$ mm. Hg.

$d = 3$ cm.

$n \approx 10^7$ electrons.

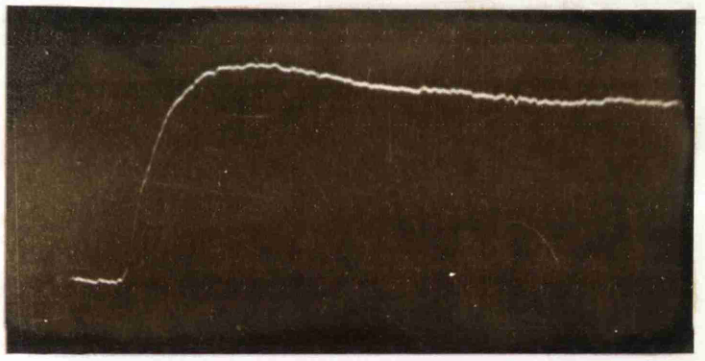

⊢⊣ 0·5 μsec.

FIG. 32. As FIG. 31, BUT SHOWING ELECTRON AND NEGATIVE ION COMPONENTS IN GREATER DETAIL.

$\frac{E}{p} = 40{\cdot}4$ V.cm^{-1} (mm. Hg)$^{-1}$

$p = 508$ mm. Hg.

$d = 2$ cm.

$n \approx 3 \times 10^7$ electrons.

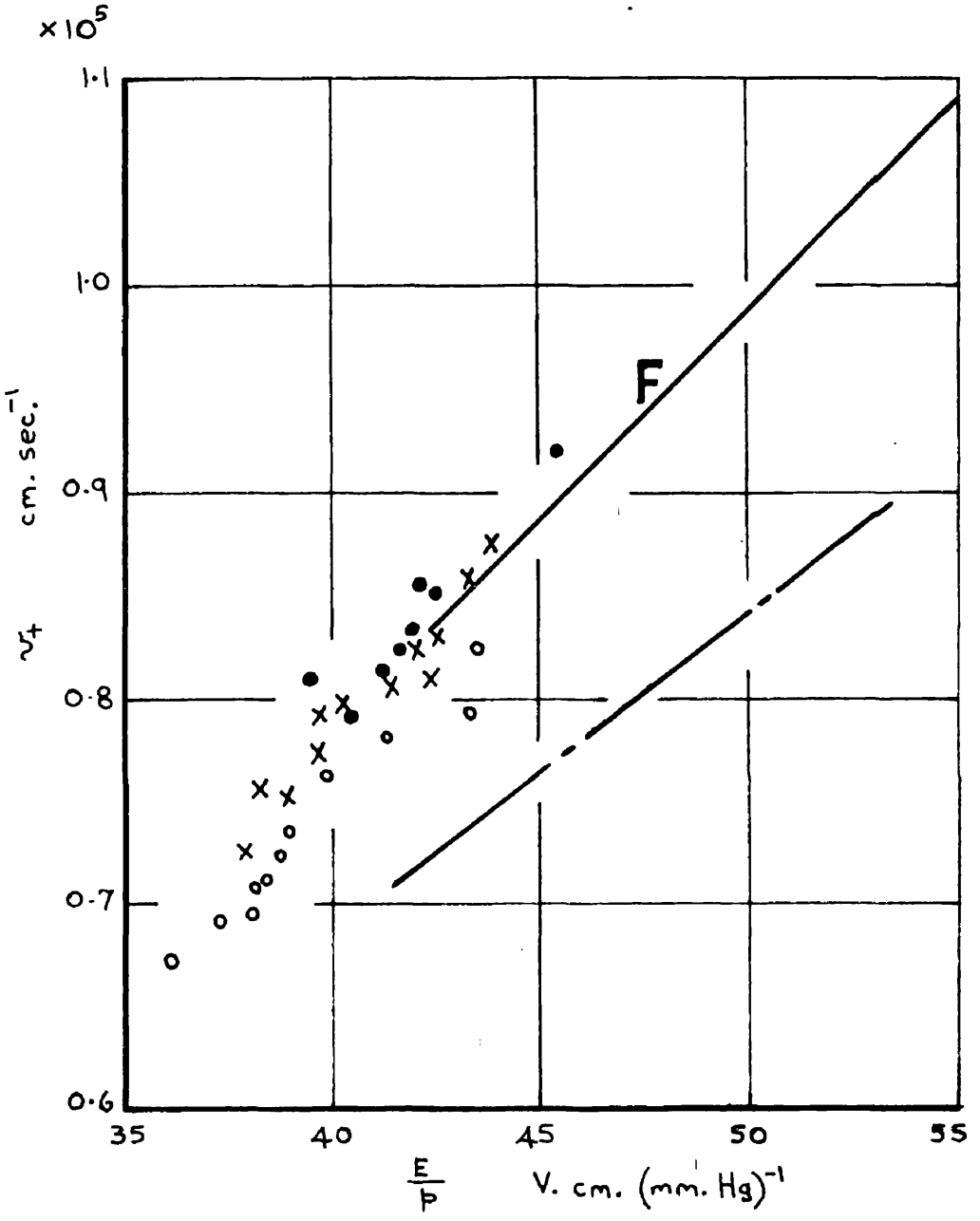

FIG. 33. MEASURED POSITIVE ION DRIFT VELOCITIES v_+ IN DRY AIR.

• 1cm. gap
× 2cm. gap
o 3cm. gap

F Frommhold[40] : 3cm. gap.

Vogel[8] : 2cm. gap.

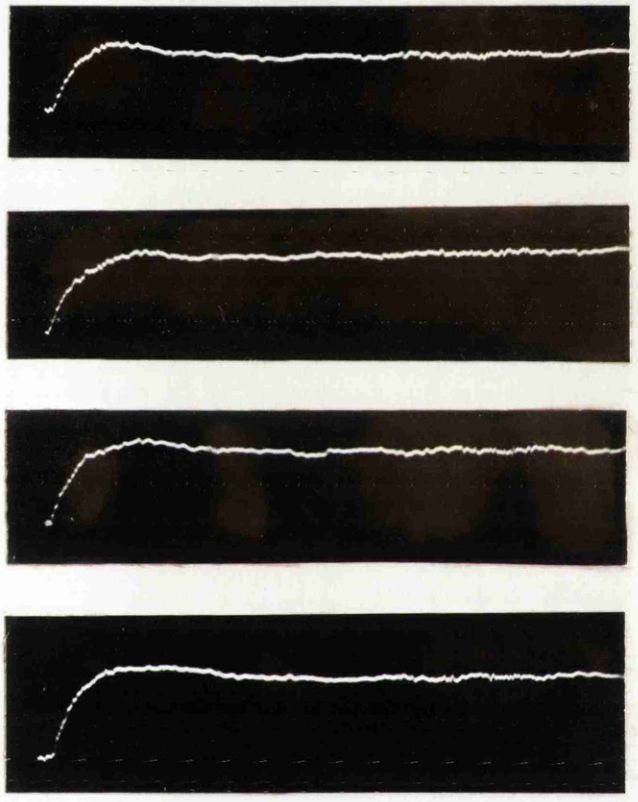

1·0 μsec.

FIG. 34. ELECTRON COMPONENTS OF CURRENT PULSES IN DRY AIR.

$\frac{E}{p} = 43{\cdot}6$ V. cm^{-1} (mm. Hg)$^{-1}$.

$p = 205$ mm. Hg.

$d = 3$ cm.

$n \approx 2 \times 10^{7}$ electrons.

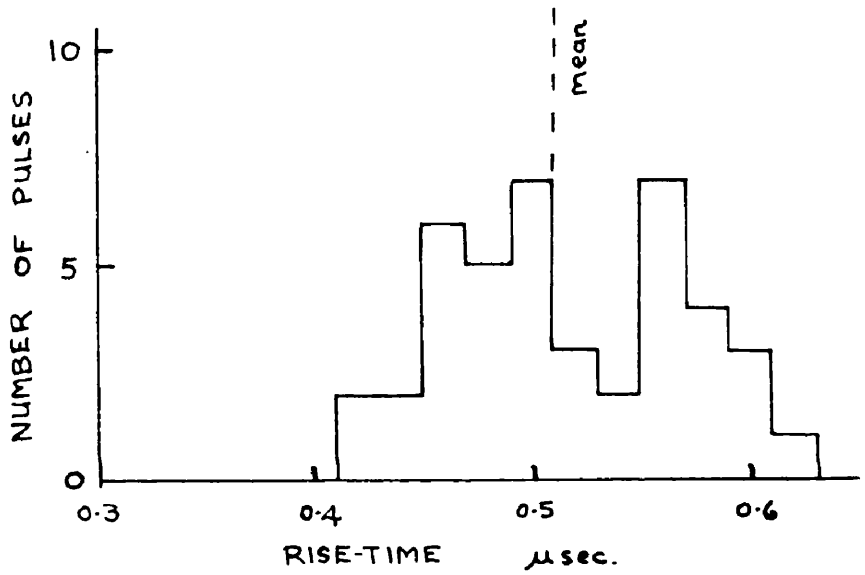

FIG. 35. TYPICAL DISTRIBUTION OF MEASURED CURRENT PULSE RISE-TIMES IN DRY AIR.

$\frac{E}{p} = 43{\cdot}6$ V. cm.$^{-1}$ (mm. Hg)$^{-1}$.

$p = 205$ mm. Hg.

$d = 3$ cm.

n of the order of 10^7 electrons per pulse.

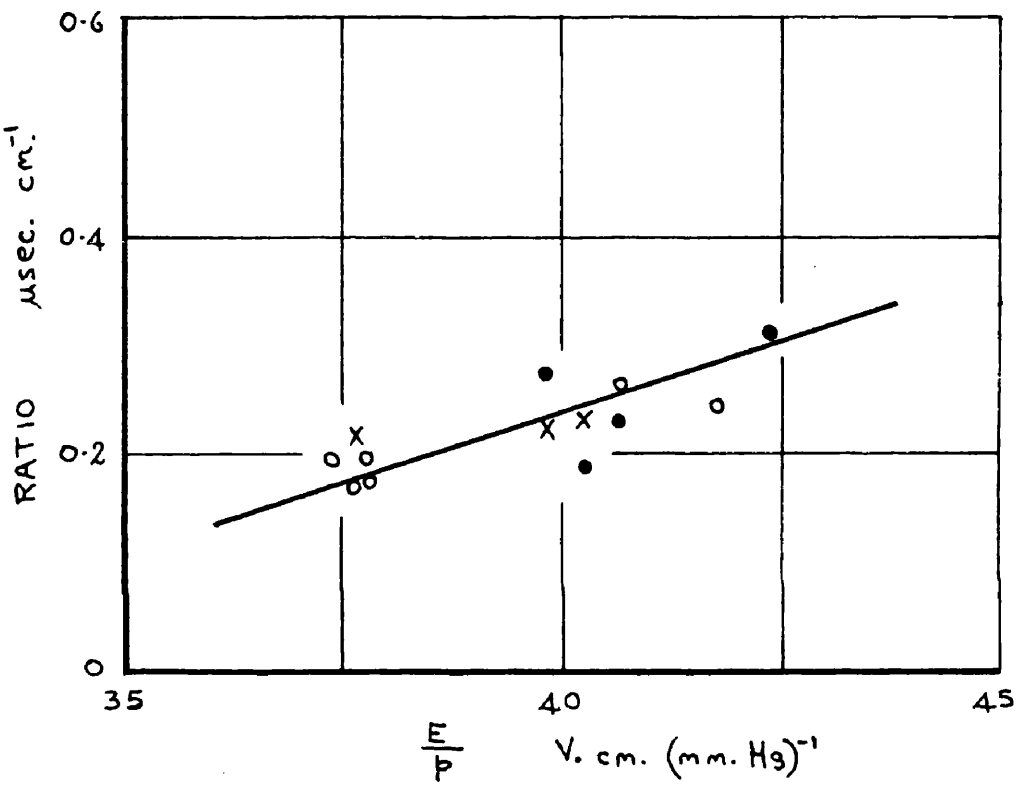

FIG.36. MEASURED VALUES OF THE RATIO $\frac{\text{MEAN RISE-TIME } (\mu\text{sec.})}{\text{GAP LENGTH (cm.)}}$ IN DRY AIR.

• 1cm. gap
× 2cm. gap
o 3cm. gap

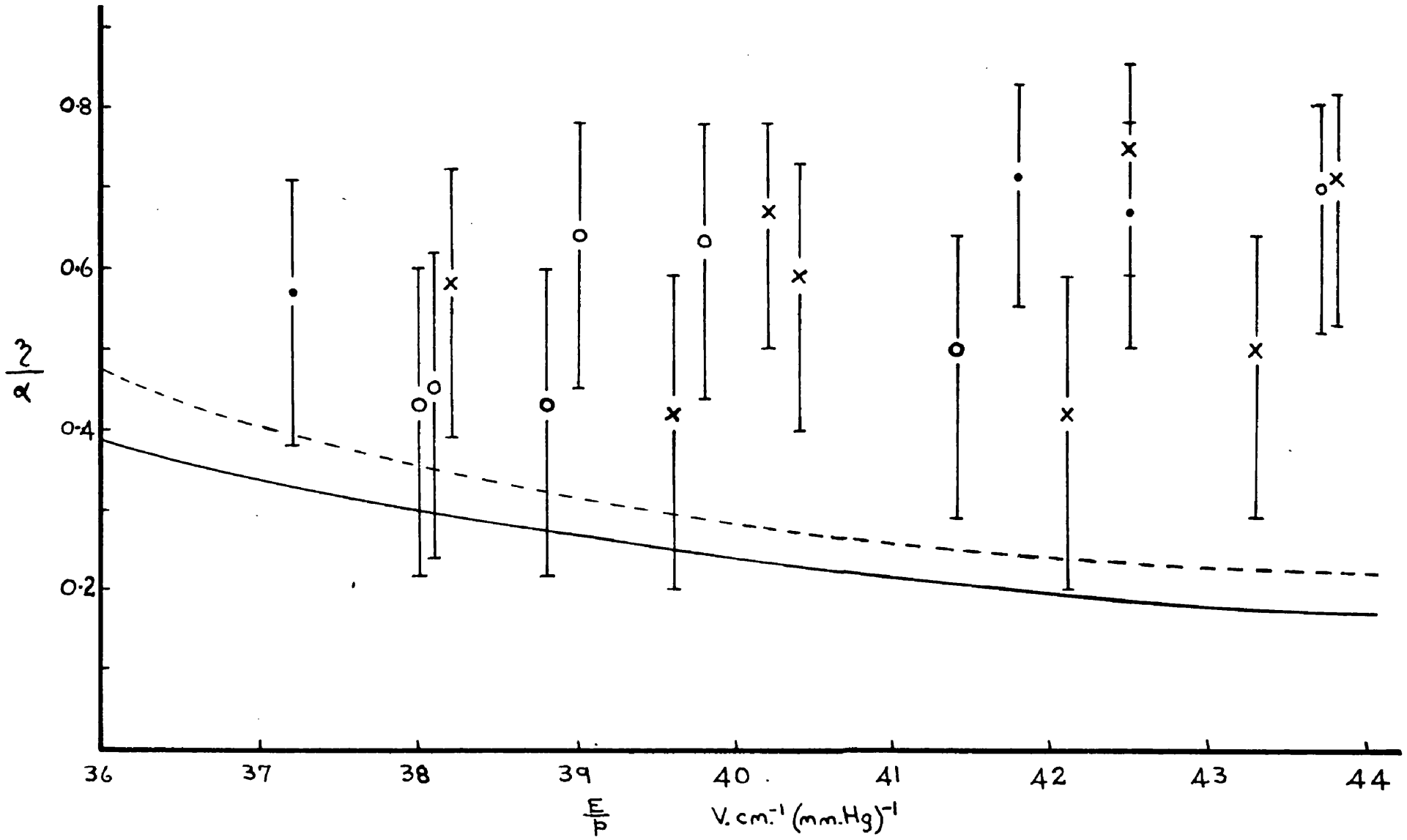

FIG. 37. MEASURED VALUES OF η/α IN DRY AIR.

• 1cm. gap. x 2cm. gap.. o 3cm. gap. ---- Harrison and Geballe[48] —— Prasad[13]

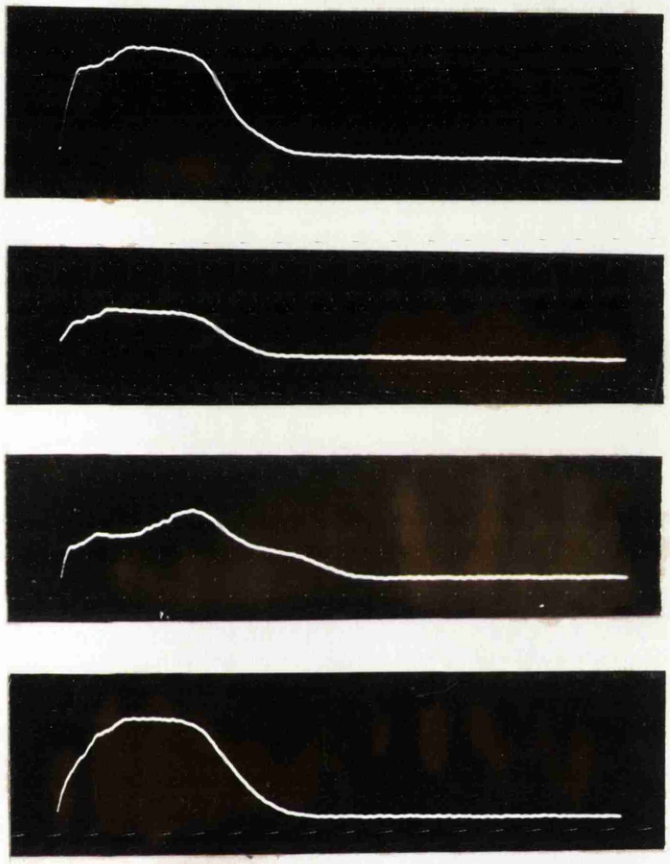

⟝ 10 μsec.

FIG. 38. CURRENT PULSES IN DRY AIR, SHOWING THE EFFECT OF A PHOTO-ELECTRIC SECONDARY PROCESS.

$\frac{E}{p} = 43{\cdot}1 \text{ V.cm}^{-1}\text{(mm.Hg)}^{-1}$.

$p = 302$ mm. Hg.

$d = 2$ cm.

$n \approx 10^8$ electrons per pulse.

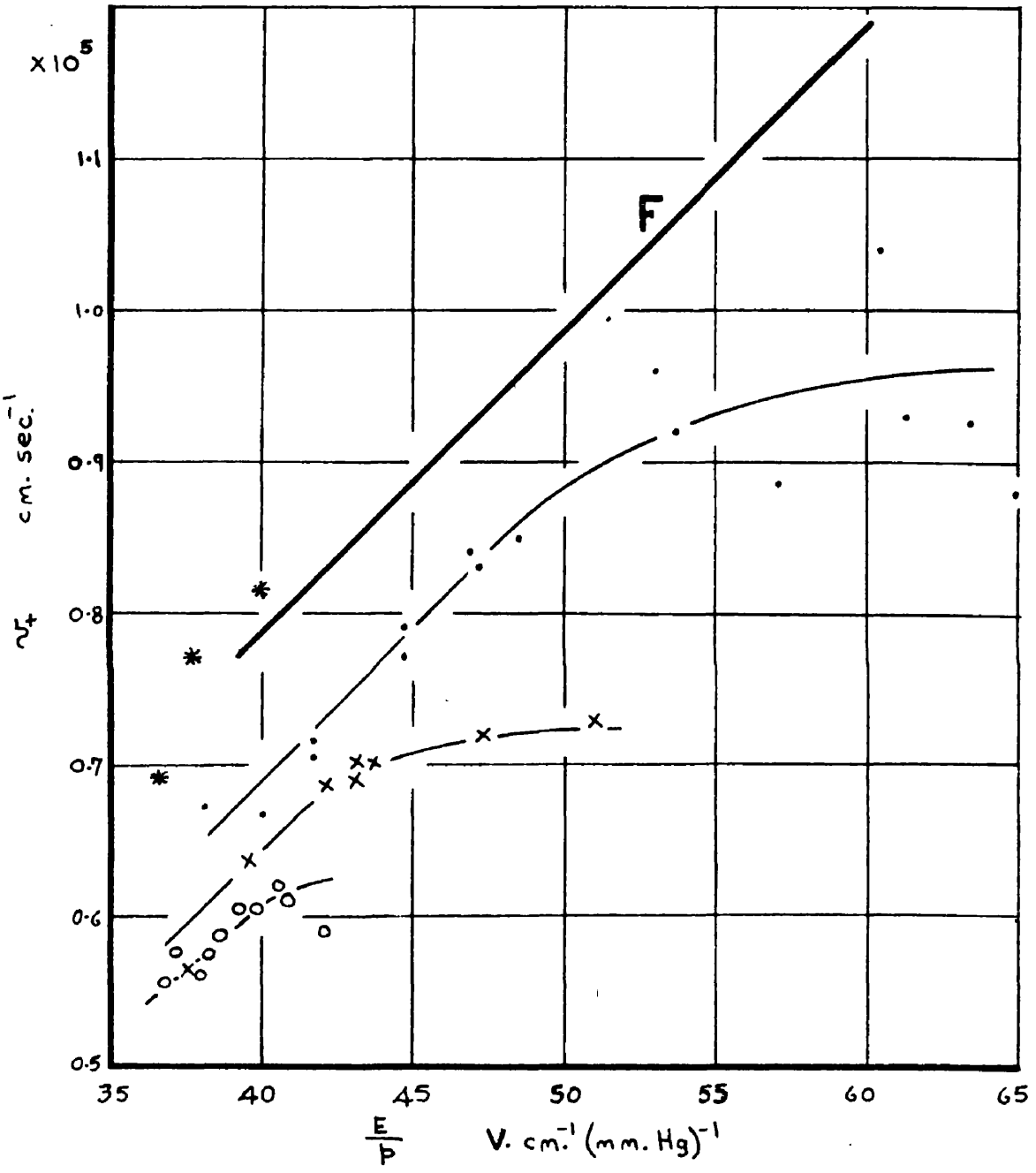

FIG. 39. MEASURED POSITIVE ION DRIFT VELOCITIES v_+ IN HUMID AIR.

• 1cm. gap
× 2cm. gap
o 3cm. gap

F Frommhold[40]
3cm. gap in dry air:
compare FIG. 33.

* Results in room air (Section 3)

⊢ 0·1 μsec.

FIG. 40. THE ELECTRON COMPONENT OF A CURRENT PULSE IN HUMID AIR.

$\frac{E}{p} = 42{\cdot}2$ V.cm^{-1} (mm.Hg)$^{-1}$.

$p = 114$ mm. Hg.

$d = 3$ cm.

$n \approx 1{\cdot}5 \times 10^{7}$ electrons.

water vapour partial pressure 16·2 mm. Hg.

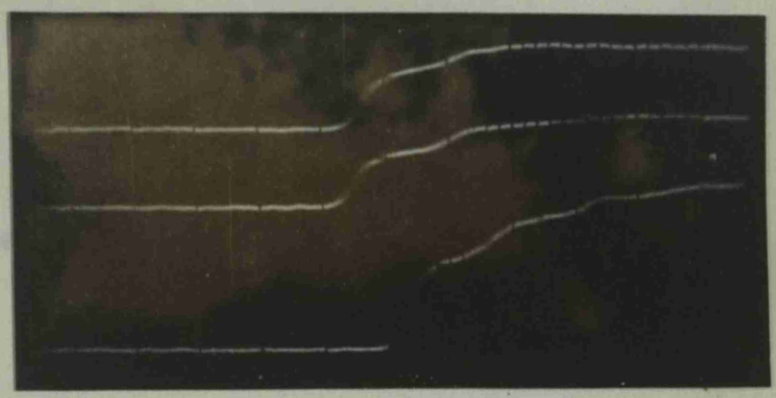

0·1 μsec.

FIG. 41. ELECTRON COMPONENTS OF CURRENT PULSES IN HUMID AIR, SHOWING INDIVIDUAL SECONDARY AVALANCHES PRODUCED BY A PHOTO-ELECTRIC MECHANISM.

$\frac{E}{p} = 44{\cdot}2$ V. cm^{-1} (mm. Hg)$^{-1}$.

$p = 114$ mm. Hg.

$d = 3$ cm.

$n \approx 10^8$ electrons per avalanche.

water vapour partial pressure 16·2 mm. Hg.

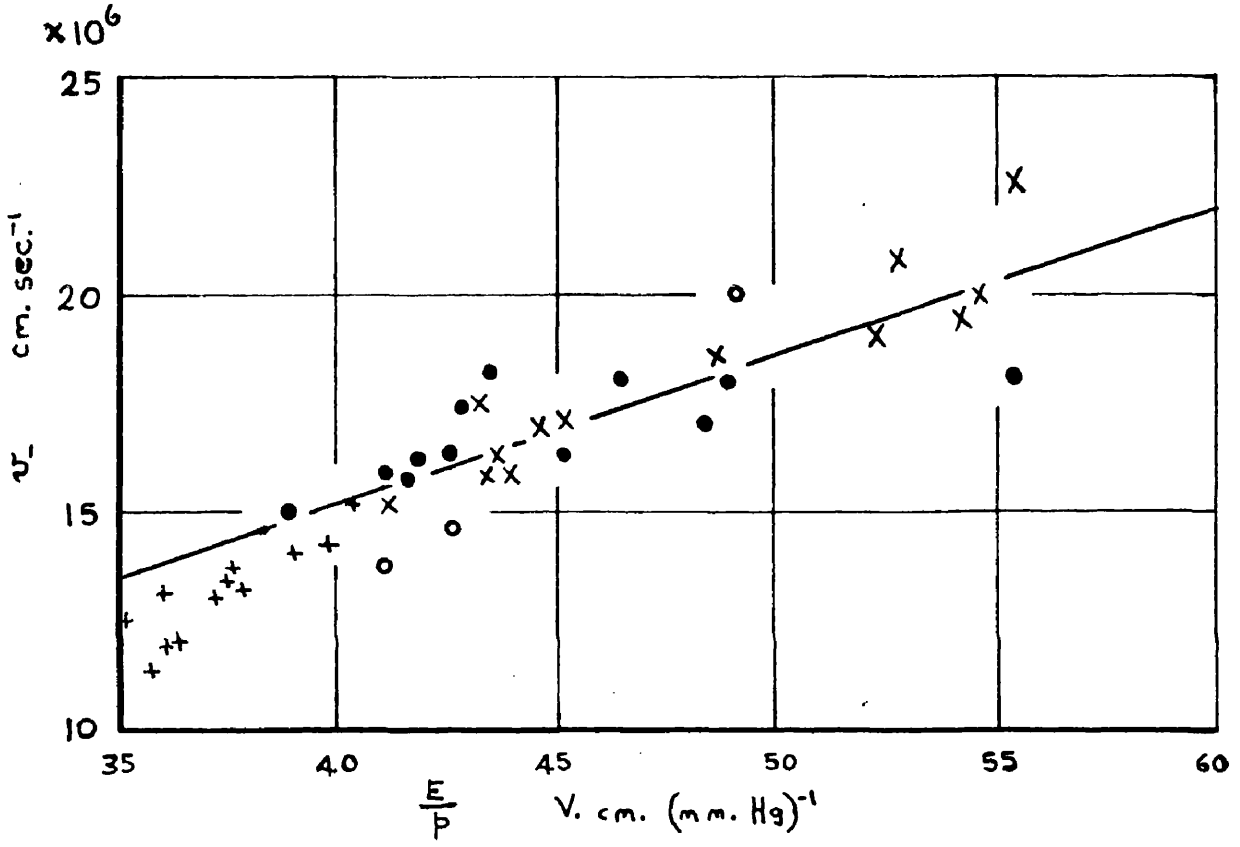

FIG. 42. MEASURED ELECTRON DRIFT VELOCITIES v_- IN HUMID AIR.

• 1cm. gap
× 2cm. gap
o 3cm. gap

——— Nielsen and Bradbury[49] for dry air (extrapolated).

\+ Schröder[17]

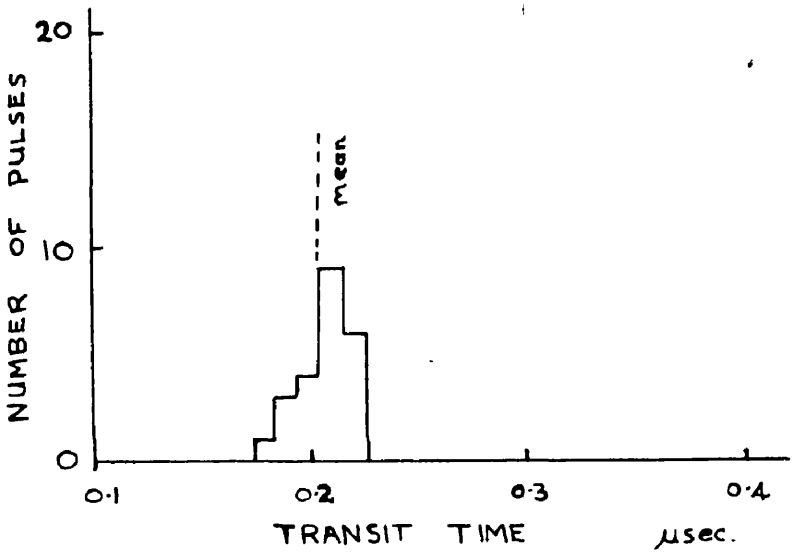

FIG. 43. TYPICAL DISTRIBUTION OF MEASURED ELECTRON TRANSIT TIMES IN HUMID AIR.

$\frac{E}{p} = 42{\cdot}9$ V.cm.$^{-1}$(mm.Hg)$^{-1}$.

$p = 248$ mm. Hg.

$d = 3$ cm.

n of the order of 10^8 electrons per avalanche.

water vapour partial pressure 16·5 mm Hg.

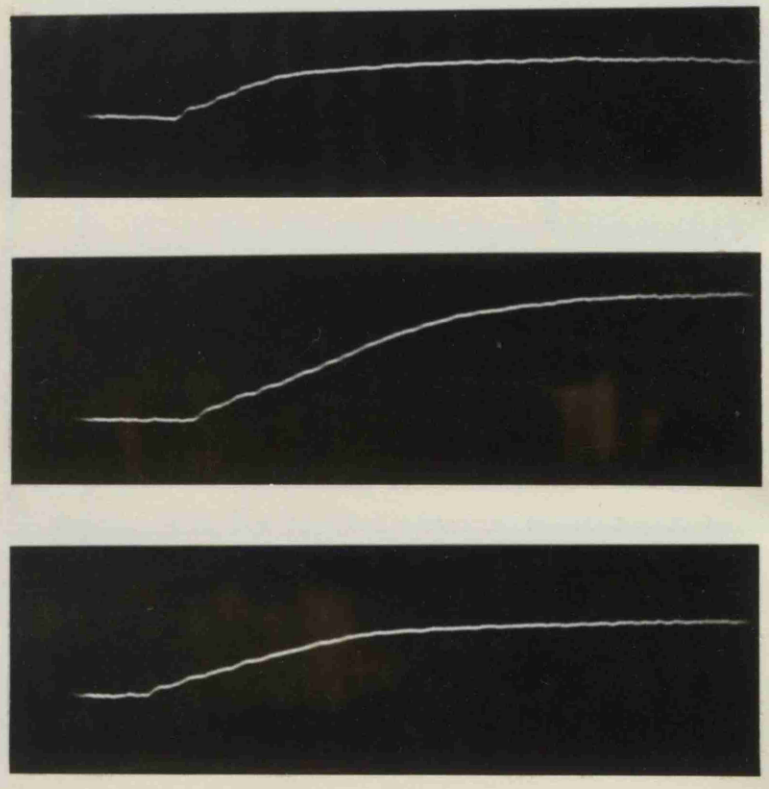

0·2 μsec.

FIG. 44. ELECTRON COMPONENTS OF CURRENT PULSES IN HUMID AIR, WITH MANY PHOTO-ELECTRIC SECONDARY AVALANCHES.

$\frac{E}{p} = 56{\cdot}6$ V. cm.$^{-1}$ (mm. Hg)$^{-1}$.

$p = 72$ mm. Hg.

$d = 2$ cm.

$n \approx 10^9$ electrons per pulse.

water vapour partial pressure 18·7 mm. Hg.

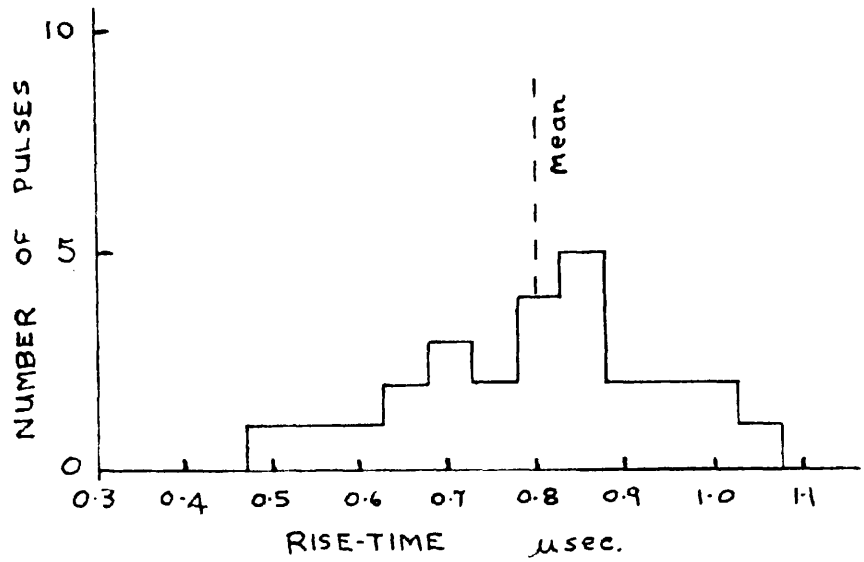

FIG. 45. TYPICAL DISTRIBUTION OF MEASURED CURRENT PULSE RISE-TIMES IN HUMID AIR, FOR PULSES OF THE TYPE SHOWN IN FIG. 44.

$\frac{E}{p} = 56{\cdot}6$ V.cm.$^{-1}$(mm.Hg)$^{-1}$.

$p = 72$ mm. Hg.

$d = 2$ cm.

n of the order of 5×10^8 electrons per pulse

water vapour partial pressure 18·7 mm.Hg.

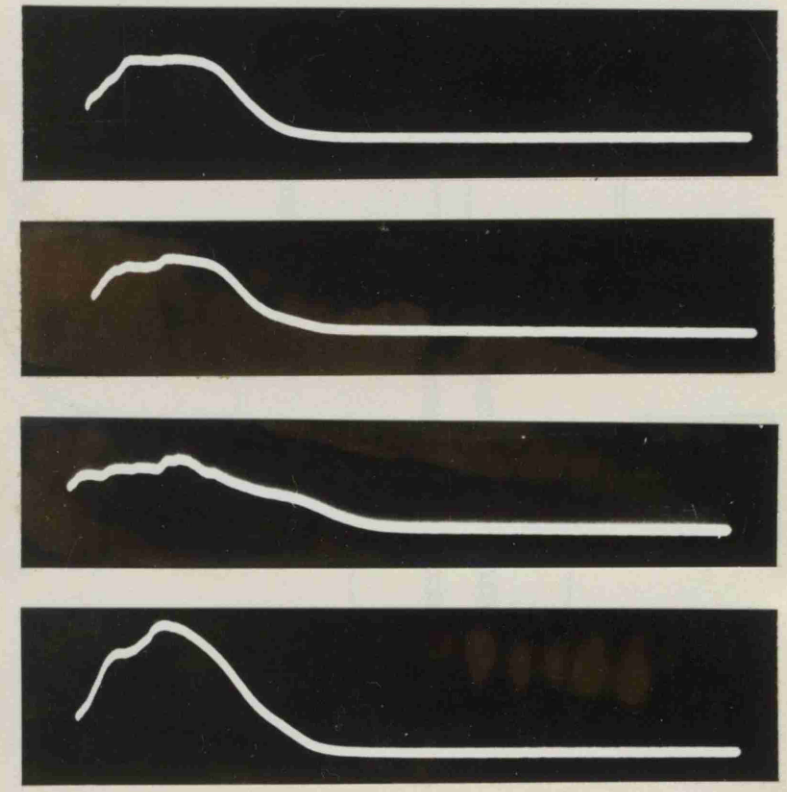

5·0 μsec.

FIG. 46. CURRENT PULSES IN HUMID AIR, AT A VOLTAGE CLOSE TO BREAKDOWN VALUE.

$\frac{E}{p} = 47{\cdot}2$ V. cm.$^{-1}$ (mm. Hg)$^{-1}$.

$p = 278$ mm. Hg.

$d = 1$ cm.

$n \approx 10^9$ electrons per pulse.

water vapour partial pressure 18·7 mm. Hg.

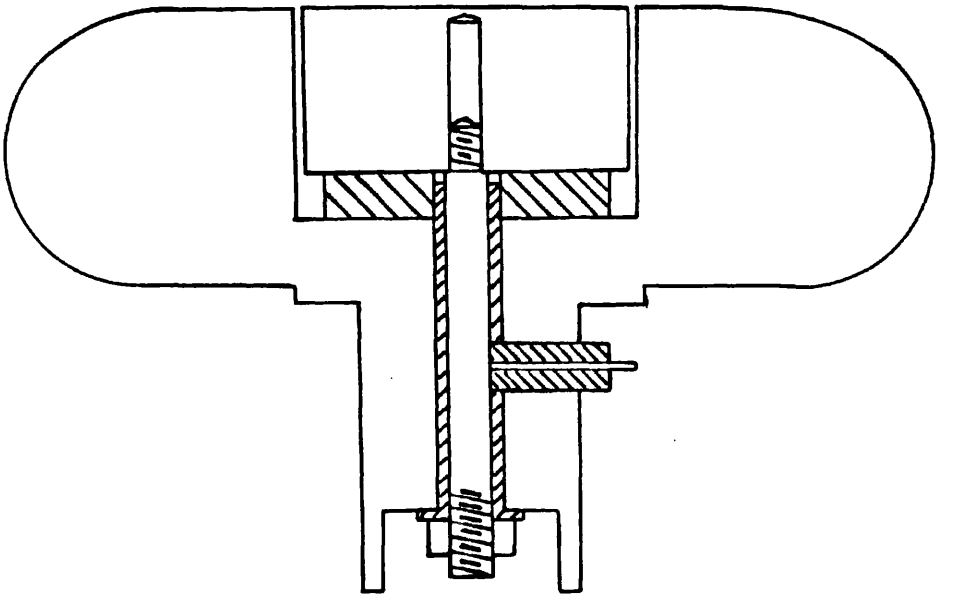

FIG. 47. THE GUARD-RING ELECTRODE.

(Approx. full size).

The insulating parts – shown hatched – are of polystyrene: the remainder brass.

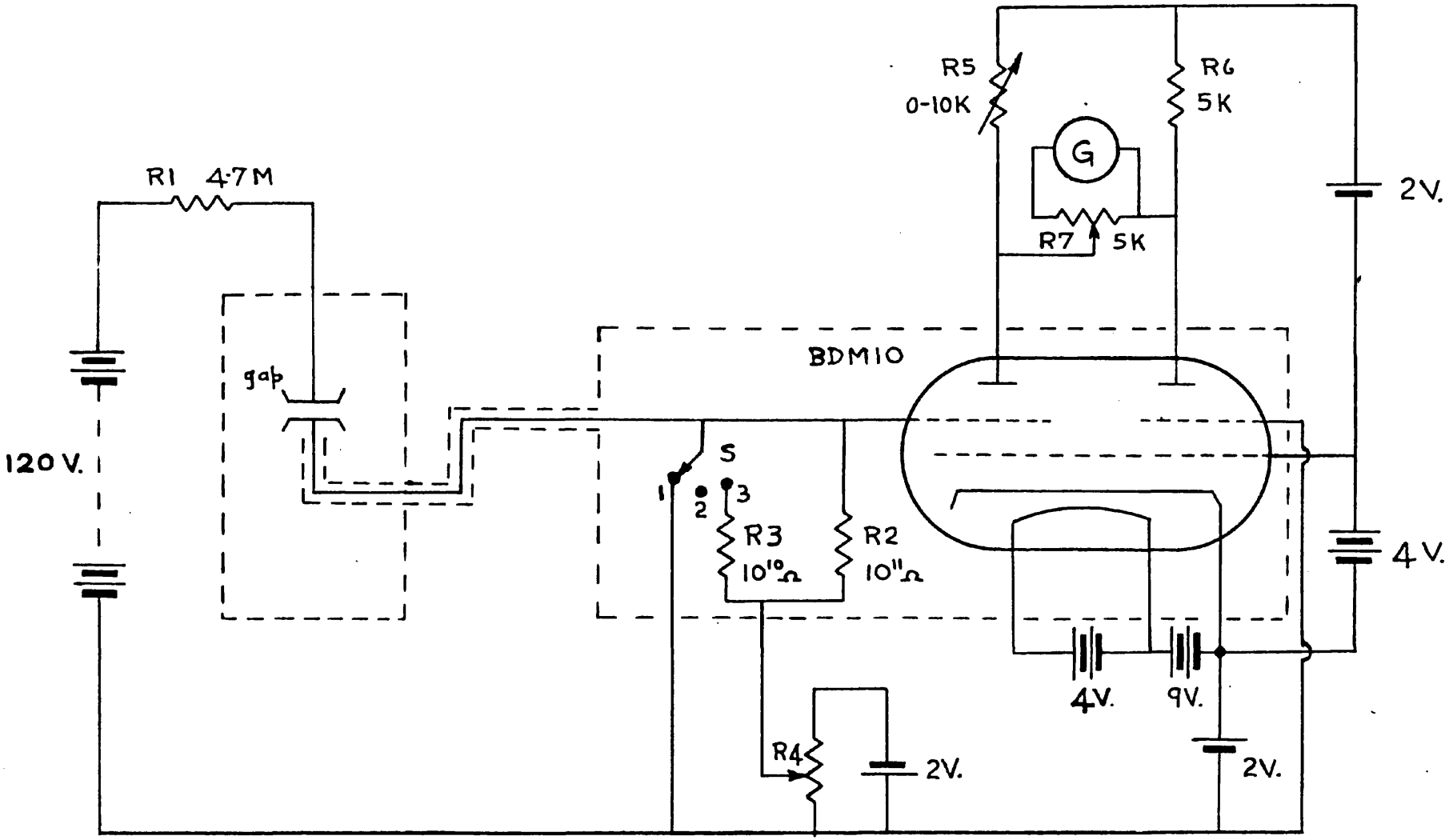

FIG. 48. APPARATUS FOR INITIAL IONIZATION CURRENT MEASUREMENTS.

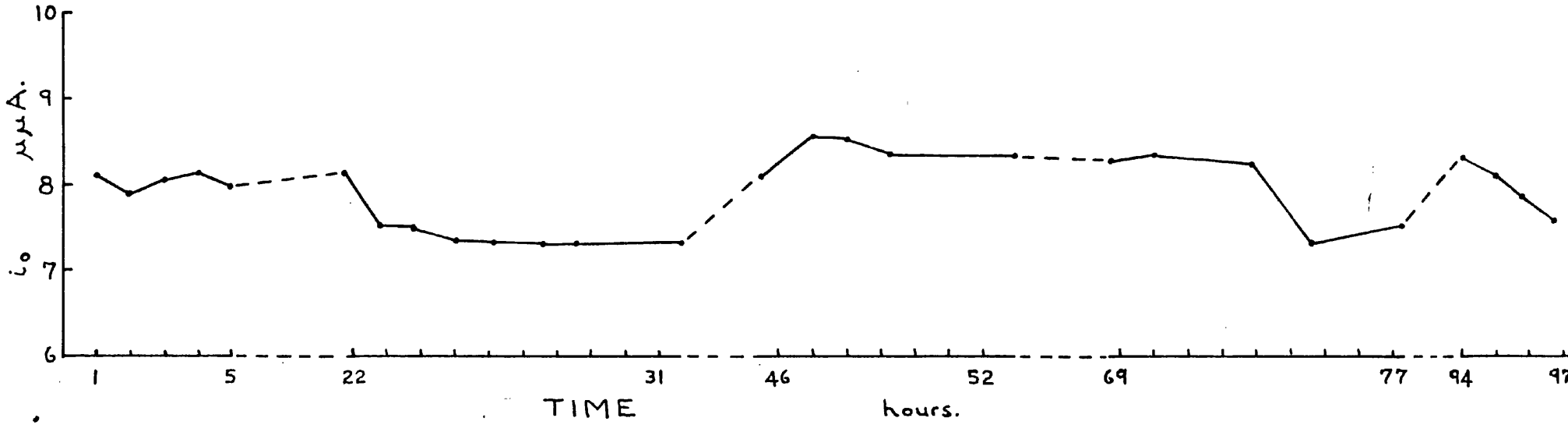

FIG. 49. DAY-TO-DAY VARIATIONS IN MEASURED INITIAL IONIZATION CURRENT i_o

Aluminium cathode : brass anode. 0·46 mg. radium in anode.

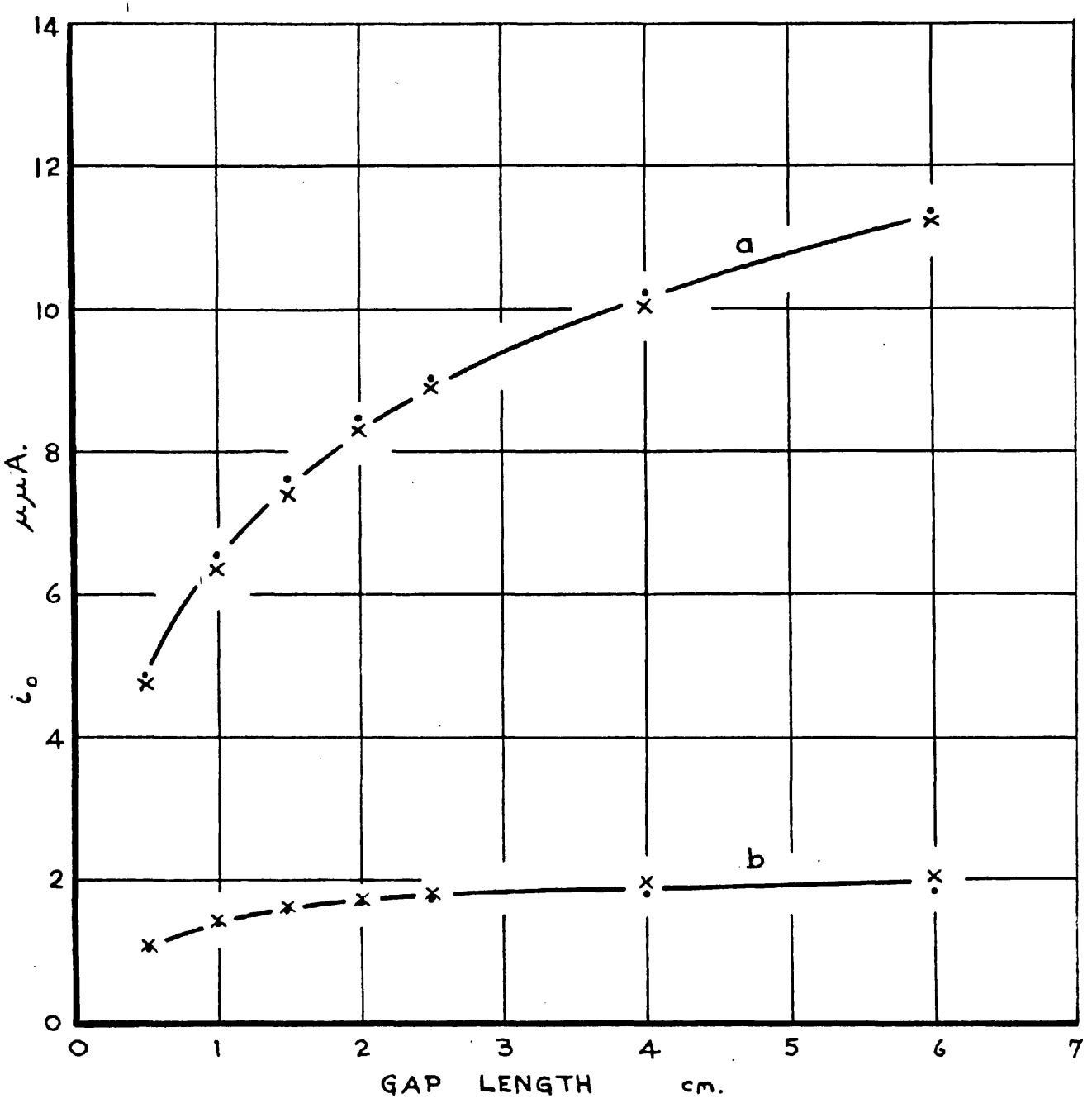

FIG. 50. MEASURED INITIAL IONIZATION CURRENTS i_o WITH THE GUARD-RING ELECTRODE AS CATHODE.

a total current

b current to inner portion

• 0·46 mg. radium in cathode

x " " " in anode.

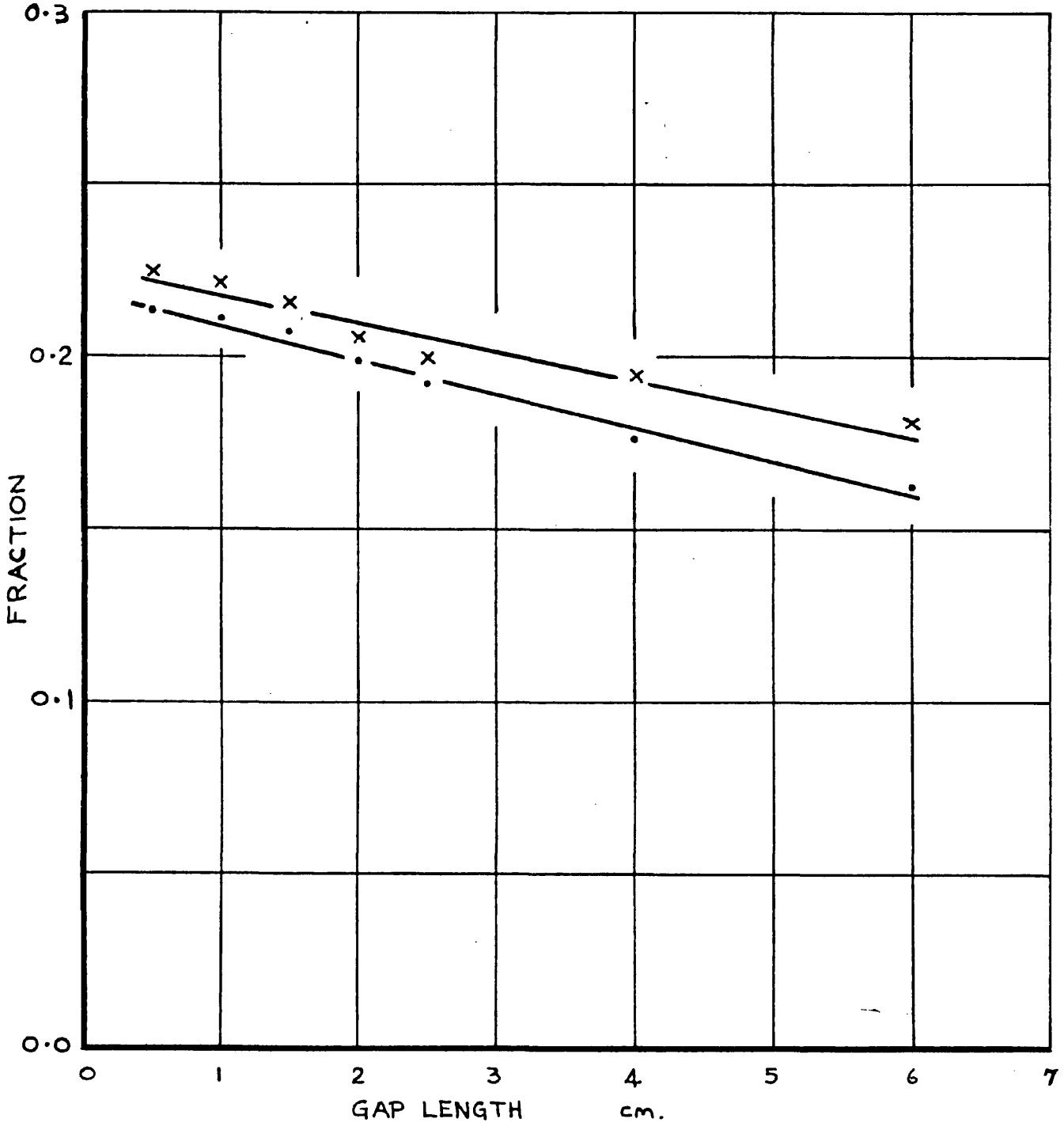

FIG.51. THE FRACTION OF THE TOTAL INITIAL IONIZATION CURRENT COLLECTED BY THE INNER PORTION OF THE GUARD-RING ELECTRODE.

• 0·46 mg. radium in cathode
× " " " in anode.

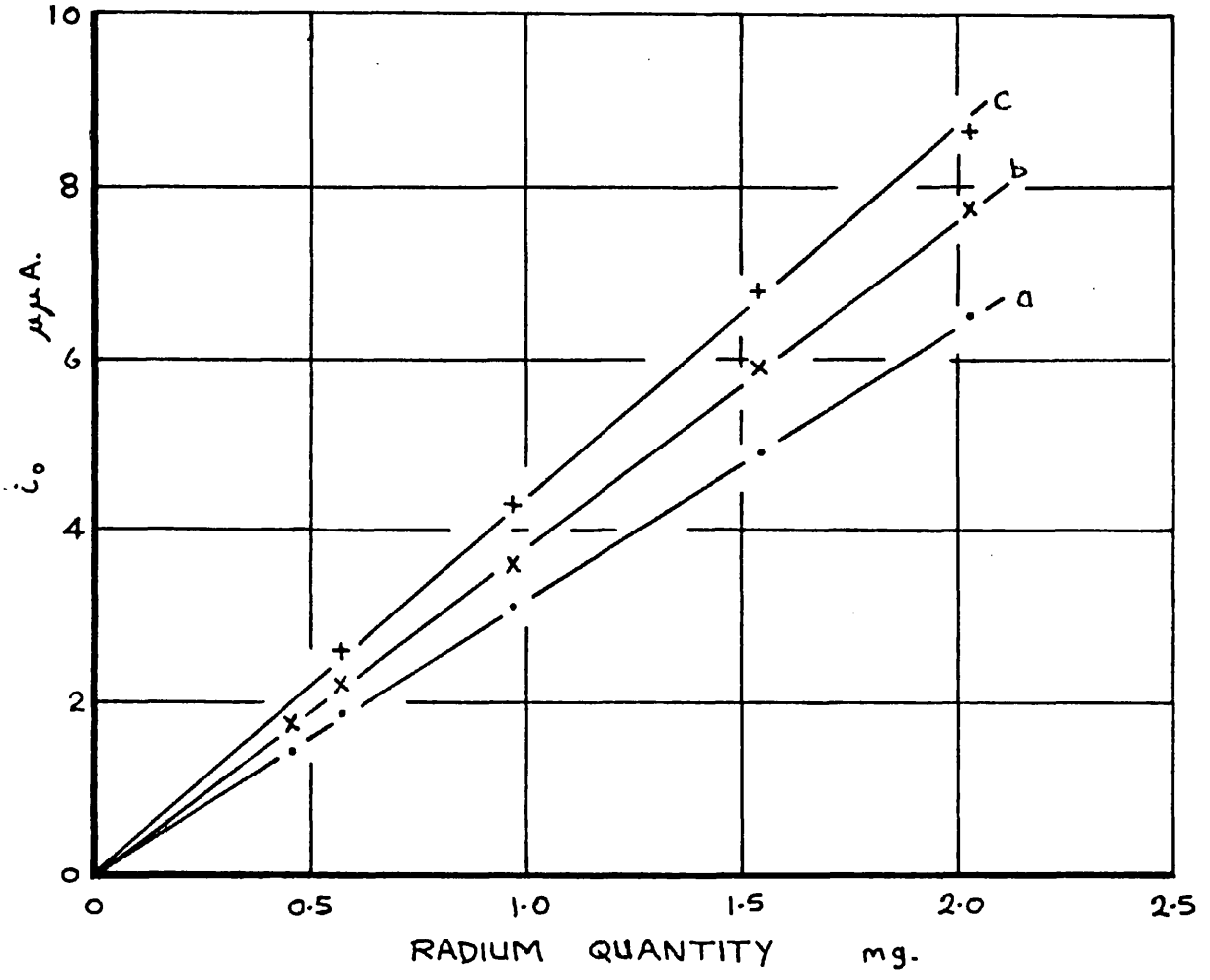

FIG. 52. VARIATION WITH RADIUM QUANTITY OF MEASURED INITIAL IONIZATION CURRENT i_o TO THE INNER PORTION OF THE GUARD-RING ELECTRODE.

The radium was placed in the (solid) brass anode.

a - 1cm. gap
b - 2cm. gap
c - 7cm. gap

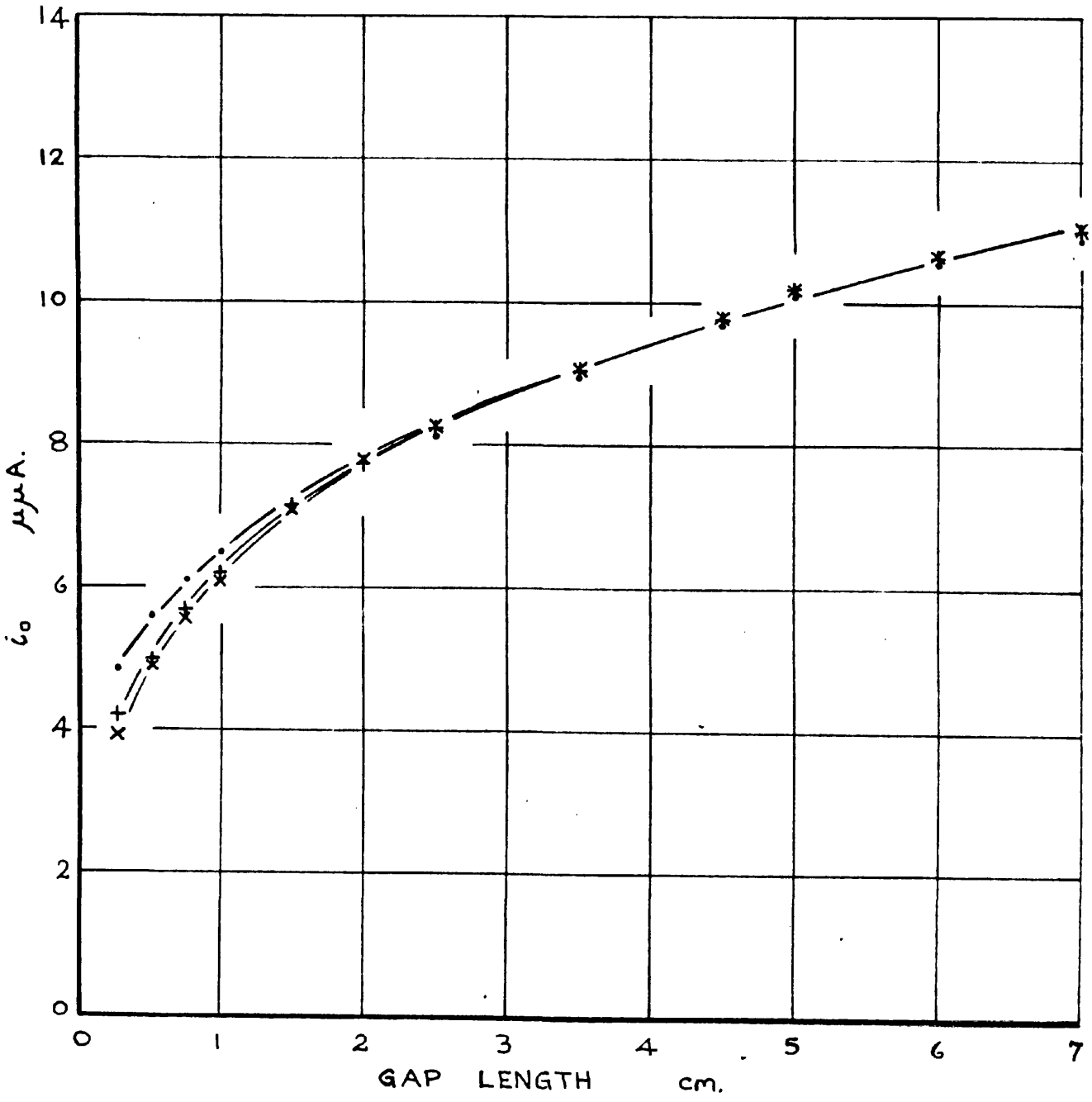

FIG. 53. MEASURED INITIAL IONIZATION CURRENTS i_0 FOR DIFFERENT CATHODE MATERIALS.

• Carbon
+ Magnesium
× Aluminium

0·46 mg. radium in brass anode.

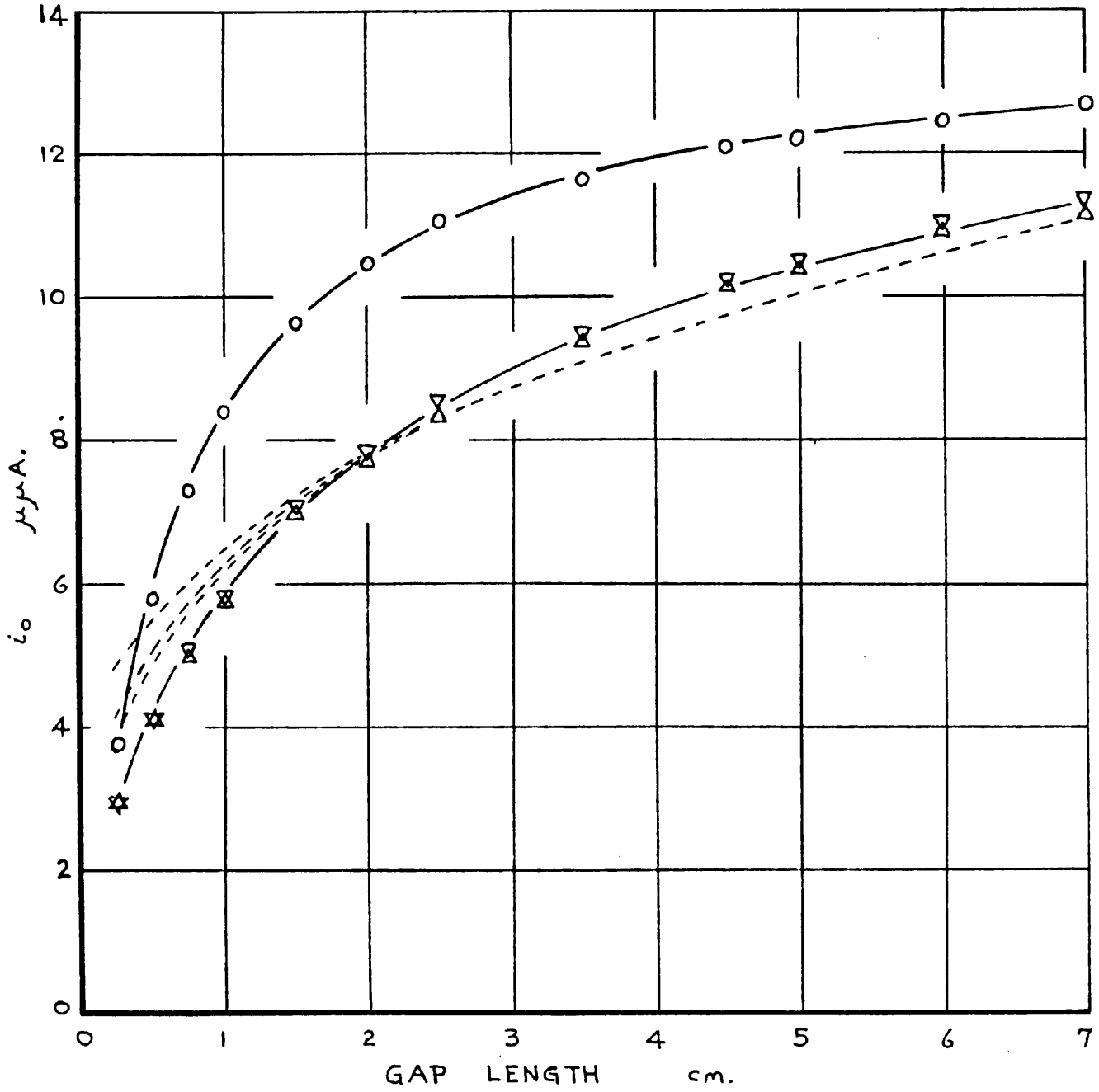

FIG. 54. MEASURED INITIAL IONIZATION CURRENTS i_o FOR DIFFERENT CATHODE MATERIALS.

△ Mild steel

▽ Copper

o Lead

---- Carbon, Magnesium, Aluminium (see FIG 53).

0·46 mg. radium in brass anode.

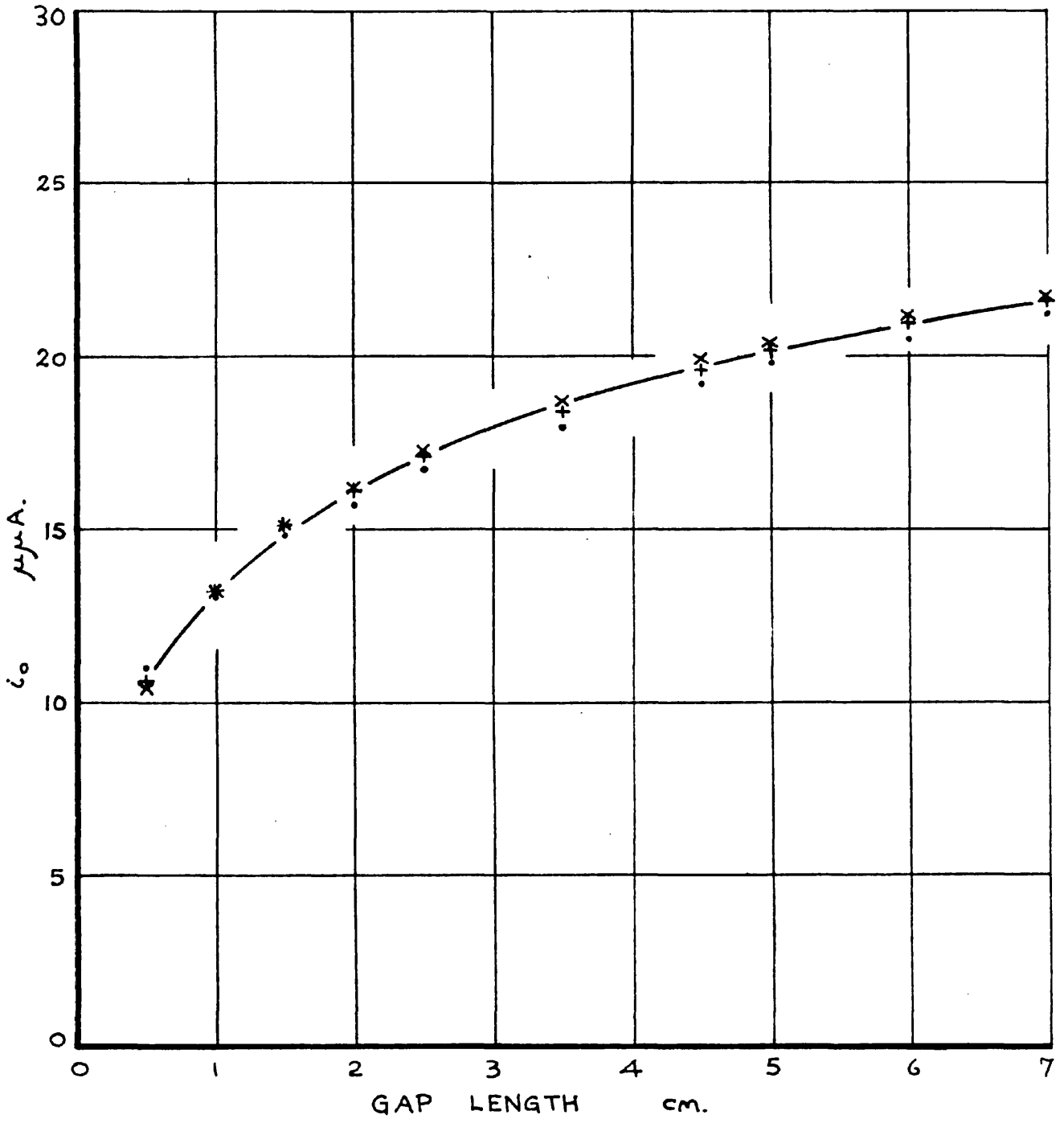

FIG. 55. MEASURED INITIAL IONIZATION CURRENTS i_o FOR DIFFERENT CATHODE MATERIALS.

• Carbon
+ Magnesium
× Aluminium

1·03 mg. radium in brass anode.

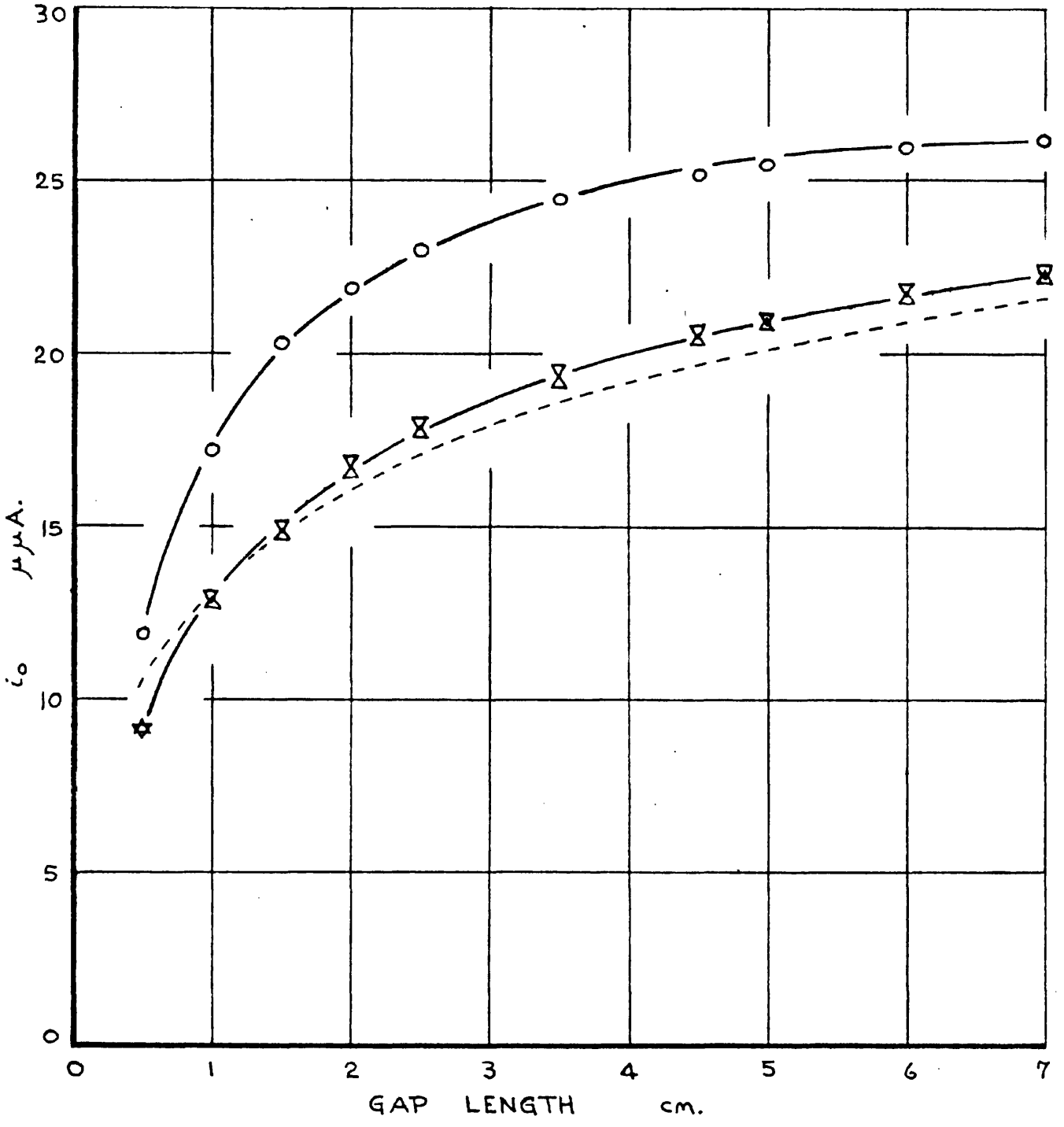

FIG. 56. MEASURED INITIAL IONIZATION CURRENTS i_o FOR DIFFERENT CATHODE MATERIALS.

△ Mild steel
▽ Copper
o Lead
---- Carbon, Magnesium, Aluminium (see FIG 55).

1·03 mg. radium in brass anode.